SPECTROSCOPY AND PHOTODYNAMICS
OF MOLECULES
AND VAN DER WAALS COMPLEXES

W.M. VAN HERPEN

SPECTROSCOPY AND PHOTODYNAMICS
OF MOLECULES
AND VAN DER WAALS COMPLEXES

SPECTROSCOPY AND PHOTODYNAMICS
OF MOLECULES
AND VAN DER WAALS COMPLEXES

EEN WETENSCHAPPELIJKE PROEVE OP HET GEBIED VAN
DE WISKUNDE EN NATUURWETENSCHAPPEN

PROEFSCHRIFT

TER VERKRIJGING VAN DE GRAAD VAN DOCTOR
AAN DE KATHOLIEKE UNIVERSITEIT TE NIJMEGEN,
VOLGENS BESLUIT VAN HET COLLEGE VAN DECANEN
IN HET OPENBAAR TE VERDEDIGEN
OP DONDERDAG 28 JANUARI 1988,
DES NAMIDDAGS TE 1.30 UUR PRECIES

door

WILHELMUS MARTINUS VAN HERPEN

geboren op 21 januari 1959
te Heesch

Krips repro Meppel
1988

Promotor   : Prof. Dr. A. Dymanus

Co-referent   : Dr. W.L. Meerts

Velen hebben een bijdrage geleverd aan het tot stand komen van dit proefschrift. Op deze plaats wil ik ieder daarvoor bedanken, en met name:

alle (oud) medewerkers van de afdeling Molecuul- en Laserfysica voor de prettige samenwerking;

Ruurd Taconis en Joop Konings, die gedurende hun afstudeerperiode bij het onderzoek betrokken waren;

Frans van Rijn en John Holtkamp voor hun onmisbare steun op electronisch gebied en Annet van der Heyden, Leo Hendriks, Eugene van Leeuwen en Cor Sikkens voor hun hulp en raad op velerlei terreinen;

de medewerkers van de dienstverlenende afdelingen: (service) instrumentmakerij, glasblazerij, vloeibare gassen en fotografie;

het Universitair Rekencentrum voor de geboden faciliteiten;

Paul Uijt de Haag en Lex Sewuster voor hun collegiale instelling en de vele opbouwende discussies;

en speciaal mijn ouders en Renita voor hun dagelijkse ondersteuning.

Aan mijn ouders
Aan Renita

CONTENTS

CHAPTER 1

INTRODUCTION AND OUTLINE OF THESIS

Molecular spectroscopy provides a powerfull tool to investigate geometric and dynamic properties of molecules. It provides information on the energy levels and transition properties between these levels. Molecular spectra reflect the electronic, vibrational and rotational degrees of freedom of molecules, the effects of nuclear properties and the response to electric or magnetic fields. In recent years the limits of spectroscopy have been extended in two different directions by developments in laser techniques. A very high resolution in frequency domain allows the study of small energy splittings and accurate determination of molecular constants. Detailed information may be derived for large molecules with very dense spectra. On the other hand application of very short laser pulses opens new possibilities in time domain to study fast dynamic effects in molecules. However, both area's are directly connected since they both reflect the molecular properties and they supply complimentary information. They may, however, also serve as a test for models derived from either time- or frequency domain work.

Most subjects described in this thesis are related to high resolution spectroscopy in frequency domain. One of the essential parts in this work is a narrow band radiation field, provided by a frequency stabilized single mode dye laser. To cover the entire optical spectral region different dyes have to be used. In the near ultraviolet region narrow band radiation was obtained by doubling the frequency of the laser in a medium with nonlinear properties [1]. Although the laser is optimized for frequency domain experiments, it proved also possible to obtain high quality time domain results. The continuous output of the laser can be modulated to form pulses with an adjustable duration and with a stable and narrow frequency band.

Another essential part in this study of high resolution spectra of large molecules is the molecular beam apparatus. Other high resolution techniques may be applied, such as Doppler free two photon spectroscopy [2], but application of a molecular beam allows an almost complete elimination of collisions, since all molecules travel at nearly the same speed and in the same direction. If the beam is crossed at right angles with the radiation field, also the Doppler effect is strongly suppressed and the observed linewidth is reduced.

9

Molecular beams are generally formed from an expansion through a nozzle into a vacuum tank. A reduction takes place in the expansion of the internal energy of the molecules. This cooling of rotational and vibrational degrees of freedom limits the population of energy levels to lower states and consequently simplifies the spectra. Cooling may be further enhanced by application of a seeding gas, mostly argon or helium. Due to the absence of collisions, molecular beams open possibilities of studying unstable species such as ions, radicals, metastable molecules and van der Waals (vdW) complexes

In recent years much attention was attributed to the study of vdW complexes of molecules with a number of inert gas atoms. These complexes form a well defined transition from a free molecule to a molecule in condensed phase. A study of the structure and intramolecular dynamics in ground as well as excited electronic state of these molecules provides insight of such phase transition from a microscopic point of view. Van der Waals complexes can also provide information on the parent molecule, since the intramolecular dynamics in this molecule may be slightly modified. In this way, comparison of parent molecule and vdW complex gives an indication of the origin of such dynamic effects

In chapter 3-A, 3-B and 4 an account is given of the study of vdW complexes of fluorene and tetracene with rare gas atoms. Laser induced fluorescence was detected emerging from the molecular beam. The vibronic spectra of such molecules are shifted with respect to related transitions in the parent molecule. The spectral shift and the determination of the effective structure of the complex yields information on the atom-molecule interaction potential. A small number of theoretical studies has been reported of such complexes. In case of tetracene a parametrisation of the potential was proposed as a sum of atom-atom Lennard-Jones pair potentials [3]. A more extended calculation of the fluorene-argon complex has recently been described by Brocks *et al.* [4].

For fluorene the rotational constants of the molecule and the vdW complex with argon were derived. This allows determination of an effective structure of the complex. Since from three moments of inertia one can not uniquely determine the molecular geometry, some basic assumptions have to be made. A rigid molecular frame is assumed with small zero point vibrational motions. A dualism remains about the sign of the derived coordinates of the argon atom within the complex. In chapter 3-B a comparison is made with the fully deuterated fluorene molecule in an attempt to determine the unique molecular structure. A check is made on contributions from zero point vibrations and on the validity of the rigid rotor model.

For the tetracene molecule a rotational assignment was made for the parent molecule. An identification of lines in the rovibronic spectra of the vdW complex with rare gas atoms was not possible due to spectral distortions. A nonradiative decay channel is opened for the complex, demonstrated by a reduction of the excited state lifetime [5]. This

channel is induced by intrastate coupling of the excited singlet state, most likely to isoenergetic vibrational levels of the lowest triplet state. The coupling increases with the mass of the attached rare gas atom.

Spectroscopy at rotational resolution allows derivation of molecular constants, directly connected to the molecular geometry and thus such spectroscopy gives insight in the structure of molecules. In chapter 5 a study is presented of rovibronic spectra of trans-stilbene. This molecule serves as a prototype in the study of trans-cis isomerization processes. The reaction is induced by vibronic excitation, followed by intramolecular vibrational redistribution of the energy to, among others, reactive modes. Special issues are the selectivity of certain vibrational modes in this proces and the structure of the molecule, both in ground and excited electronic state. It is demonstrated in chapter 5 that other intramolecular processes are present in the excited state of trans-stilbene, besides the isomerization effect. These processes hinder an accurate geometric analysis. Also spectra of stilbene-argon vdW complexes are presented. For these molecular complexes the spectral perturbances are reduced.

In chapter 6-A and 6-B a report is given on the spectroscopy and dynamics of the pyrazine molecule. The intramolecular dynamics of this molecule are attributed to the so-called limiting case of intermediate level structure [6]. The wealth of experimental data on the first excited singlet state of pyrazine is interpreted in terms of an excited singlet level $|S\rangle$, connected via intrastate coupling to a number of nearly isoenergetic triplet states $\{|T\rangle\}$. This results in a manifold of mixed states $|N\rangle$, the molecular eigenstates (ME),

$$|N\rangle = C_s |S\rangle + \sum_T C_t |T\rangle \qquad (1)$$

where the coefficients C_s and $\{C_t\}$ denote the singlet and triplet content of the ME-state. The ME-spectrum has been directly observed [7] and it was shown that the so-called zero order states $|S\rangle$ and $|T\rangle$ can be derived as well as the coupling matrix elements between them [8]. As is shown in chapter 6-A, one of the basic assumptions in this deconvolution procedure is not completely correct; the observed intensities in laser induced fluorescence spectra are not proportional to the absorption intensities. It is shown that this deviation is caused by a significant nonradiative decay of the triplet states. With the presented model a correction can be made for this deviation. An other problem in the deconvolution procedure is demonstrated in chapter 6-B. It is shown that the resolution in molecular beam spectroscpy can be even further extended with application of quantum beat spectroscopy. With this method it is shown that not all lines in the pyrazine ME-spectrum are completely resolved. On a spectral line quantum beats were observed following the

coherent excitation of this state. Thus spectral intensities do not always reflect the coefficients C_s of the singlet content of a single ME-state.

Chapter 7 is devoted to the experimental problem of obtaining high resolution absorption spectra of pyrazine. Recently much attention was attributed to the origin of intrastate coupling mechanisms in this prototype molecule [9,10]. A combination of absorption and laser induced fluorescence spectra allows derivation of the quantum yield for individual ME-states. This forms key information in the search of (J,K) dependence in the radiationless decay process. To obtain high resolution absorption spectra, a bolometer was inserted in the molecular beam. Since the quantum yield of pyrazine is low [11], the energy detected by the bolometer reflects the absorption spectrum. The resolution in these spectra is determined by the divergence of the molecular beam and is comparable to the resolution in the excitation spectra.

REFERENCES

[1]   W.A. Majewski, Opt. Commun. 45 (1983) 201.

[2]   E. Riedle, H,J, Neusser and E.W. Schlag, J. Chem. Phys. 86 (1982) 4847.

[3]   M.J. Ondrechen, Z.Berkovitch-Yellin and J. Jortner, J. Am. Chem. Soc. 102 (1981) 6568.

[4]   G. Brocks and D. van Koeven, submitted.

[5]   A. Amirav, U. Even and J. Jortner, J. Chem. Phys. 75 (1981) 2489.

[6]   F. Lahmani, A. Tramer and C. Tric, J. Chem. Phys. 60 (1974) 4431.

[7]   B.J. van der Meer, H.T. Jonkman, J. Kommandeur, W.L. Meerts and W.A. Majewski, J. Chem. Phys. 92 (1982) 565.

[8]   W.D. Lawrance and A.E.D. Knight, J. Phys. Chem. 89 (1985) 917.

[9]   P.J. de Lange, B.J. van der Meer, K.E. Drabe, J. Kommandeur, W.L. Meerts and W.A. Majewski, J. Chem. Phys. 86 (1987) 4004.

[10]   A. Amirav, Chem. Phys. 108 (1986) 403.

[11]   A. Frad, F. Lahmani, A. Tramer and C. Tric, J. Chem. Phys. 60 (1974) 4419.

DESCRIPTION OF THE SPECTROMETER

1. INTRODUCTION

The spectrometer contains four essential units for recording rovibronic spectra of molecules and van der Waals complexes; a molecular beam apparatus, a laser system, a detection unit and a unit for data recording and processing. The molecular beam machine is a modified version of a molecular beam electric resonance (MBER) apparatus, described elswhere [1,2]. The frequency range of the spectrometer has been extended to the optical and near uv region [3]. An arrangement was made to cross the molecular beam at various places with a laser beam. The laser induced fluorescence (LIF) from molecules in the beam is detected by collection optics and a photomultiplier. The topics described in this thesis do not involve the MBER configuration. Only the mass spectrometer proved very usefull in alignment of the beam and in monitoring the beam intensity during experiments. For one of the experiments a bolometer was used to detect the molecular beam.

In the following sections the essential parts of the spectrometer and its performance will be discussed. Topics that will succesively pass the attention are the molecular beam apparatus, the laser system with its peripheral equipment, the detection system and the recording and processing of data.

2. THE MOLECULAR BEAM MACHINE

An outline of the spectrometer is given in figure 1. The molecular beam is formed from a jet expansion. The source is made of quartz. It consists of a vessel which contains a supply of the sample in liquid or solid phase. A seeding gas (mostly argon or helium) is led through this chamber and mixes with vapour from the sample. The mixture is passed to the nozzle compartment, also made of quartz.
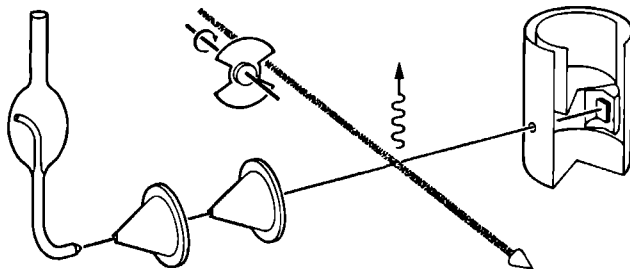
FIG. 1. Outline of the spectrometer. The molecular beam, formed from an expansion, is crossed by the laser and detected by a bolometer.

The diameter of the used nozzles varies from 75 till 125 μm The complete source is wrapped with heating wires, separated into a wires covering the supply vessel and the nozzle compartment. In this way the vapour pressure of the sample is controlled. A typical value is 1 mbar, in combination with a backing pressure of the seeding gas in the range from 0.3 to 4 bar. The use of quartz in construction of the source has the advantages that it is quite inert and that it allows heating up to 500 °C. To prevent flow of the sample in backward direction, where it might condense in colder areas, the entrance of the source is enclosed by a removable bulb A small hole is left open to allow the seeding gas to pass. It is possible to fill the source with the sample, while maintaining the vacuum in the beam apparatus.

The vacuum chamber is pumped by a diffusion pump in combination with a (500 m^3/h) Roots pump, keeping the pressure below 10^{-3} mbar. Two conical skimmers, of typically 1 mm diameter, form the molecular beam. They are positioned in a differential pumping system. In the area where the molecular beam crosses the laser beam, at 30 cm from the beam orifice, the pressure is reduced to 10^{-6} mbar, assuring collision free conditions. The molecular beam is detected by a mass spectrometer, allowing the beam intensity to be monitored during measurements. For experiments on pyrazine, when argon was used as seeding gas, the mass detector proved of little use, since the argon atom and the pyrazine molecule have the same mass. A mechanical chopper can be used to modulate the molecular beam. In this way phase sensitive detection may be applied to distinct for instance stray light from the laser.

14

3. LASER EQUIPMENT

Various laser systems have been used. Basicly they each of them contains an argon-ion pump laser, a dye laser system with its stabilization unit and a wavelength meter. The laser equipment is rigidly mounted to separate tables, mostly granite plates resting in sand, to damp resonances. Since the principles of dye laser operation are well known, only a brief description of the most relevant features is given here.

3.1 Standing wave laser

For the experiments on tetracene laser radiation was obtained from a standing wave dye laser system (Coherent 599-21), operating in a single frequency mode. The gain medium was formed by a solution of stilbene 3 in ethylene glycol. The optical resonator, consisting of a three-mirror folded cavity, contains a focus where the dye jet stream is applied. Pumping of the dye gain medium is performed by the uv lines (351-364 nm) of an argon-ion laser (Spectra Physics 171) at a typical power of 1.5 W. Selection of a single longitudinal mode is accomplished by a system of intracavity dispersive elements: a three-plate birefringent filter and two etalons with different free spectral ranges. Part of the output power is used to lock the frequency of the dye laser to the transmission of an external, pressure-tight temperature stabilized Fabry-Perot interferometer with a low finesse. Scanning of the laser is performed by adjusting the optical length of the reference cavity as well as the laser cavity. For this purpose a galvo driven plate is mounted in both cavities, at Brewster's angle. By controling the transmission frequency of the reference interferometer the laser frequency may be scanned. The short term frequency jitter of the laser is about 3 MHz, while the long term stability exhibits a frequency drift of less than 50 MHz/h. The output power varies over the tuning range of the gain medium but with 1.5 W pump power a typical output of single mode cw radiation of 50 mW is achieved at 450 nm. This power proved sufficient to cause severe saturation effects on the lowest vibronic transition in tetracene.

3.2 Travelling wave ring laser

The intracavity frequency doubling method was used in the Nijmegen laboratory [4] to generate tunable cw laser generation in the near uv (295-330 nm). The intracavity setup has the advantage of a high power of the fundamental wave. A modified ring laser

(Spectra Physics 380D) was used. The resonator of this laser contains two foci In one focus the dye jet stream is positioned, while in the other the $LiIO_3$ doubling crystal is placed. The gain medium, consisting of Rhodamine or DCM dyes dissolved in ethylene glycol, covers the range 580-670 nm. The ring laser is pumped by the visible lines (458-515 nm) of an argon-ion laser (Spectra Physics 171). In principle laser action occurs in two directions of the four-mirror cavity. By means of a Faraday rotator and a quartz plate, the polarization of a wave traveling in one direction is sligthly rotated, while the counter propagating wave is unaffected. The wave with a polarization mismatch after one round trip experiences a small loss, enough to assure laser action in one direction only. The intracavity power is enhanced in this travelling wave setup, compared to a standing wave configuration, because spatial hole burning effects are avoided Single mode operation is achieved by means of a single plate birefringent filter and two etalons with different free spectral ranges. Tuning of the laser is accomplished by adjusting the cavity length, while conserving single mode operation. Two galvo driven plates are inserted in the cavity for this purpose.

A small portion of the fundamental wave is coupled out of the resonator and used for stabilazation purposes. Two different units were applied to stabilize and tune the laser frequency: the Spectra Physics 389 Stabilok system, originally designed for this laser resonator, and a modified Coherent 599 stabilization system. Basically they both lock the laser frequency to the transmission of a sealed, temperature stabilized, low finesse interferometer. The laser is scanned by adjusting the optical length of this interferometer with an inserted galvo driven plate. Both systems allow a scaning range of about 50 GHz at the fundamental frequency. The bandwidth of the laser, due to frequency jitter, is 0.5 MHz with the Spectra Physics stabilization unit and 1.5 MHz with the modified Coherent apparatus. The long term frequency stability is about 10 and 40 MHz respectively and is due to the drift of the reference interferometer. These ratings are of course doubled when the second harmonic wave is considered.

The tunable cw ring laser, discussed in the foregoing was provided with a $LiIO_3$ crystal in the auxiliary beam waist of the resonator. The nonlinear behaviour of the response of this crystal to the high intensity intracavity fundamental wave allows the efficient generation of radiation at the second harmonic frequency. A general description of such effects of nonlinear optics was given by Bloembergen [5], while the specific application of the frequency doubling proces in $LiIO_3$ was described by Majewski [4] and Ubachs [6]. The intensity of the generated wave is proportional to the square of the fundamental intensity. The doubling proces is therefore much more efficient if it is carried out intracavity, or in an external resonator [7]. The present setup allows frequency doubling in the range 295-335 nm with a set of specially cut crystals. The crystals are

16

optimized for tuning in a narrow band around a certain value of the angle between the electromagnetic wave and the optical axis while its surface is at Brewsters angle. In the tuning range of the crystal a typical output power of the uv harmonic of 1 mW is obtained.

3.4 Frequency calibration

An important point in high resolution spectroscopy is the accurate calibration of the frequency scale in a spectrum. A distinction should be made wbetween the absolute and relative calibration. For relative purposes various sealed, temperature stabilized Fabry Perot interferometers were applied. A small portion of the output power of the dye laser is sent to this interferometer and its transmission is detected with a photodiode. The highly reflective, confocal mirrors provide a finesse of ca. 100 and a free spectral range of either 150 or 600 MHz for the different interferometers. The transmission frequency has a long term stability of typically 50 MHz/h. During a scan frequency markers are produced, which are recorded simultaneously with a spectrum. In processing the spectral data an interpolation is made between these markers to obtain a linear frequency scale.

The calibration of the free spectral range was performed against spectral splittings in the spectrum of the IO radical. The laser was scanned between two transitions, terminating in the same excited state, but starting from different levels in the ground electronic state. The ground state splitting is accurately known from microwave data [8]. For calibration in the red spectral region, where a different set of mirrors had to be applied, a similar technique was used with a splitting in the excited $A^2\Sigma^+$ state of the OH radical. This splitting was accurately determined in a microwave-optical double-resonance experiment [9].

Absolute frequency calibration was carried out in two different ways. In the red spectral region the frequency was determined with a monochromator in conjunction with the absorption spectrum of an iodine vapour cell. This reference spectrum was recorded simultaneously during a laser scan. The absorption lines have a width of 1.5 GHz and their frequencies are accurately documented [10]. The accuracy obtained is about 200 MHz.

For absolute wavelength calibration in the blue spectral region, no comparable reference spectra are available. Sometimes the less dense absorption spectrum of tellurium is used [11]. We applied a digital wavelength meter, described by Bekooy [3]. This Michelson interferometer type apparatus compares the unknown wavelength of the dye laser with the accurately calibrated wavelength of a stabilized reference laser. Its accuracy is mainly determined by the stability of the reference HeNe laser and amounts 1.2×10^{-7} throughout the visible region. Around 450 nm this implies an accuracy of about 70 MHz.
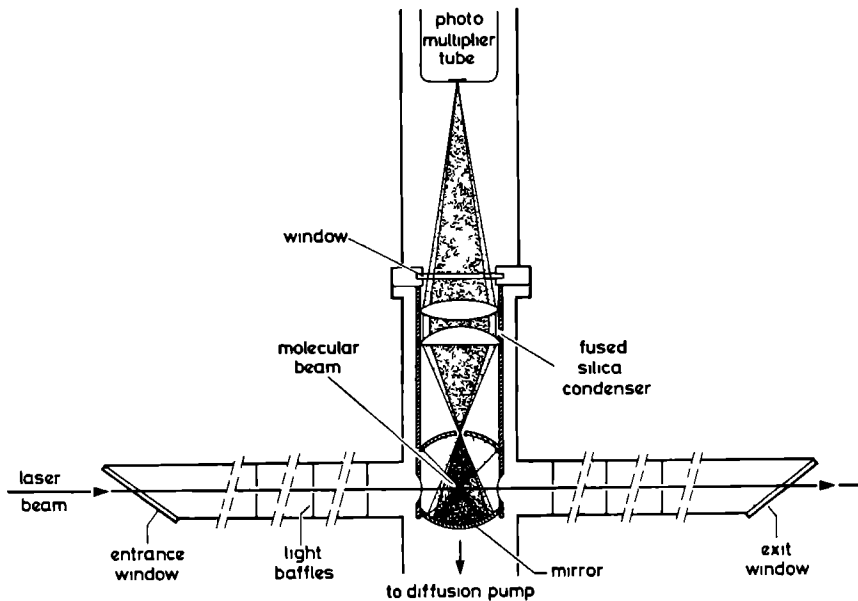
FIG. 2. The optical detection system. Laser induced fluorescence, emerging from the molecular beam is imaged to the photomultiplier. The hole in the upper collection mirror serves as a spatial filter.

4. DETECTION SYSTEMS

4.1 Optical detection

The optical detection system is outlined in figure 2. The entrance and exit windows of the laser excitation area are made of fused silica. They are positioned under Brewster angle at a distance of 60 cm from the molecular beam. Stray light is obstructed by black coated ligth baffles with diaphragms. The laser beam crosses the molecular beam perpendicularly. Laser induced fluorescence is collected by two sperical mirrors both with a 35 mm radius. The fluorescence is imaged through a 4 mm hole in the upper mirror (serving as a spatial filter) and a fused silica condensor to the cathode surface of a photomultiplier tube. The collection efficiency is estimated to be about 25%. No filters or other dispersive elements were used in the detection. All optics were enclosed in a black coated tube. The total amount of stray light is about 1000 counts per second when 1 mW of uv laser power is

applied The uv laser beam was focussed to typically 0.5 mm, so the usual laser intensity was in the order of 5 mW/mm^2. The photomultiplier (EMI 9863QA) has a sensitivity extending into the ultra violet, so that near resonant fluorescence could be detected. The tube is placed in a refrigerated housing, reducing the dark counts to about 10 per second The photomultiplier is connected to a photon counting system (Brookdeal 5CI) and phase sensitive detection is applied.

The spectral resolution in the molecular beam apparatus is affected by various contributions. The natural lifetime of the excited state gives rise to a homogeneously broadened line profile with a Lorenzian shape. Generally the instrumental limitations exceed this natural linewidth for the molecules considered. Contributions from laser frequency jitter, broadening due to curvature of the wavefront and transit time broadening effects, may be neglected compared to the residual Doppler broadening. The latter effect is caused by the divergence of the molecular beam. Molecules with a velocity component v_x along the laser beam, will experience an absorption frequency shifted from its value ω_0 by an amount $\delta\omega = v_x \omega_0 / c$. In case of a supersonic beam the density $n(v)dv$ of molecules with velocity v at a distance r from the nozzle, is given by [12]:

$$n(v)dv \propto \frac{\cos\theta}{r^2} v^2 \exp\left[-\left| \frac{v-u}{v_p} \right|^2 \right] dv .$$ (1)

Herein θ denotes the angle of $\underline{v}$ with the molecular beam axis, u is the stream velocity and $v_p = (2kT_t/m)^{1/2}$ with T_t the effective translational temperature. Equation (1) may be evaluated to a function $n(\omega',x) d\omega'$. of coordinate x along the direction of the laser beam and frequency $\omega' = \omega_0 + \delta\omega$ If we assume a constant detection efficiency in the interaction zone of laser and molecular beam, the inhomogenous absorption profile $d I(\omega)$ is found as a convolution of the density n and the homogenous natural lineshape $L(\omega,\omega')$, centered around a Doppler shifted frequency ω':

$$d I(\omega) = \int\limits_0^\infty \int\limits_{x_1}^{x_2} n(\omega',x) L(\omega,\omega') dx d\omega',$$ (2)

where the integration over x covers the entire cross section of laser and molecular beam. In the laser excitation area the diameter of the laser beam is about 0.5 mm, while the diameter of the molecular beam is, depending on the used skimmers, typically 3 mm. The spatial filtering of the dection system allows detection of a circular area with a 3 mm

diameter. It is expected that the detection efficiency is not constant along the entire interaction area of laser and molecular beam. The lineprofile in eq (2) therefore has to be convoluted with an unknown detection efficiency function. In cases where the homogeneous linewidth is small, the experimentally observed spectral lines have a nearly Gaussian form with a linewidth (FWHM) of typically 12 MHz in case of argon seeding and 24 MHz when helium is used as seeding gas. For molecules with a larger homogeneous linewidth, the observed profile becomes essentially Lorentzian.

4.2 Time resolved detection

The collection zone was also used for lifetime measurements of molecular eigenstates in the excited electronic state of pyrazine. In that case the spatial sensitivity is of particular interest. All observed lifetimes are below 600 ns. With argon as seeding gas the beam velocity is about 500 m/s. It is concluded that molecules travel a typical distance of less than 0.3 mm before emitting a photon. This distance is an order of magnitude below the size of the detected area and is sufficiently small to guarantee a constant detection efficiency during a preset time window.

A schematic overview of the experimental setup is given in figure 3. The polarized
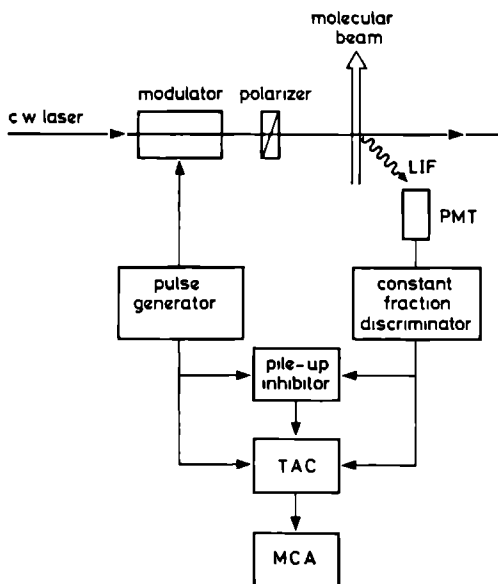

FIG. 3. Schematic view of the time resolved detection setup (TAC means time to amplitude converter, and MCA indicates the multi-channel analyzer).

20

cw laser beam is sent successively through an optical modulator (Coherent) and a polarizer. The transmission of this setup is regulated with electrical pulses from a pulse generator on the modulator. In this way a pulsed laser beam is formed with a contrast ratio of 150 and an adjustable pulse duration down to about 30 ns The laser beam crosses the molecular beam and LIF is detected by a photomultiplier. A constant fraction discriminator shapes the output pulses of the photomultiplier

The trigger pulse from the pulse generator starts a time to amplitude converter (TAC), while a detected photon is processed to a stop pulse Once the TAC is started, it generates a linearly increasing voltage. In case a stop pulse is detected within the preset time window, this voltage halts. Its final height is therefore proportional to the time elapsed after the start pulse. This voltages serves as input to a multi-channel pulse-height analyzer (MCA). With this method a photon counting histogram is obtained of counted photons versus time. The absolute time scale is calibrated using a pulse generator with known repetition frequency.

A problem may arise if a high counting rate is detected. An eventual second stop pulse in the same time window can not be detected by the TAC. This so called pile-up can be removed by suppressing those measurements in which multiple stop pulses occured. The laser power can be adjusted in such way that the probability for multiple occurences is far below the one for single photon events. A better way to suppres pile-up distortion is to count the number of occuring stop pulses during the preset time window and prohibit storage in the MCA if multiple events were detected. This latter approach was chosen in the experiment described.

4.3 Bolometer detection

Laser induced fluorescence data form essentially an exitation spectrum. That means that the spectral intensities depend on both the absorption and the emission probabilities of a transition. Since the quantum yield is not necessarily equal for all excited states, an absorption spectrum need not be proportional to an excitation spectrum. In a study of these photodynamic effects the molecular beam apparatus was modified. A bolometer was inserted in the molecular beam to detect the absorbed photons that do not give rise to fluorescence. The mechanical chopper was removed from the molecular beam and instead the laser beam was chopped at 90 Hz. Since the laser is chopped, phase sensitive detection of the LIF does not suppres the scattered laser light. However, the detection optics are designed as a spatial filter, strongly reducing stray light. Approximately 30 cm downstream of the crossing of the laser, the molecular beam reaches the bolometer. The doped germanium detector (Infrared Laboratories) with a size of 1x1 mm, is mounted on a

diamond substrate of 2x5 mm. The element is operated in the region 2.2-4.2 K by pumping a helium bath cryostat. At 4.2 K the noise equivalent power of the bolometer is 4.8×10^{-13} W/Hz$^{1/2}$ and the responsivity R is R=5x10 sup 4 ;V/W. The initial response time is 2.5 ms but during the measurements this value slowly increases due to the so-called cryofrost This effect is caused by the fact that molecules tend to condensate on the cold detector surface. Therefore the intensity of the molecular beam should be kept low and helium seeding is prefered. The pressure in the bolometer compartment of the apparatus is kept at 10^{-8} mbar. Nevertheless cryofrost imposes a limit on the operational time of the bolometer of about 4 hours. External sources of heat radiation were shielded by two screens at 4.2 K and 77 K. Laser stray light does not significantly reach the detector due to spatial filtering and the large distance.

The total beam signal is given by:

$$S_B = R N E, \tag{3}$$

where N is the number of particals per second and E the energy of the beam. Apart from the continuous translational and internal energy of the molecules, E contains contributions from the absorption energy. The latter one is separated by phase sensitive detection at a 1 s time constant. The signal to noise ratio in these experiments applied to the pyrazine molecule, was rather low (≈ 5). The main limiting factor is found to be the noise of the molecular beam.
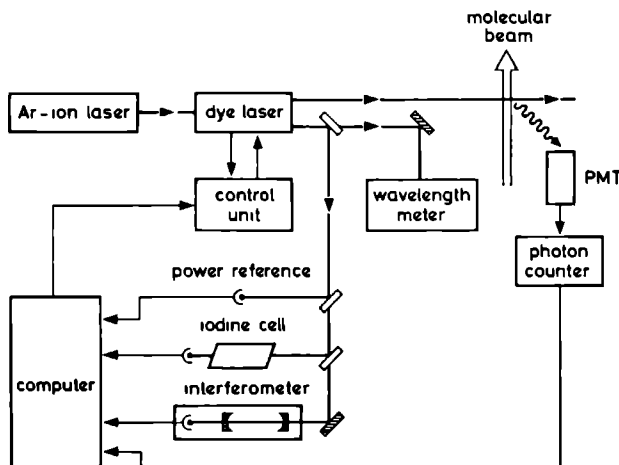

FIG. 4. Outline of the spectrometer and its peripheral equipment.

5. DATA RECORDING AND PROCESSING

The spectrometer is connected via various interfaces to a microcomputer (PDP 11/23). If desired, it is possible to scan the laser under computer control. All basic information, emerging from an experiment, can be stored by the computer. In fig. 4 an outline is given of the spectrometer and its peripheral equipment. The 8 digit dynamic range of the photon counter is converted to a binary form, before storage. The output voltage from various peripheral equipment is, after a 12 bit AD conversion, also recorded. In this way a relative frequency scale is obtained from the signal of a marking interferometer. Also the output power of the laser is recorded, as well as sometimes a reference spectrum of an iodine absorption cell. The number of samples to be taken of the various data channels need not be the same. The markers for instance have a width of about 5 MHz and samples are taken every 0.5 MHz. An iodine reference spectrum on the other hand has a 1.5 GHz linewidth and there such a high sampling rate would obviously be exaggerated. The linewidth of spectral lines in the molecular beam machine may differ for various molecules but always exceeds the residual Doppler linewidth of about 12 MHz. Therefore two different timing sequences are used. The sampling rate for the fast changing marker signal is controled by an internal clock of the computer. More slowly varying signals are sampled by a rate, determined from the internal clock of the photon counting system.

In processing the data, the position of the markers is accurately determined. By interpolation via a third order polynomial, the frequency scale is linearised for the molecular beam spectrum as well as the iodine reference spectrum. If needed the intensity may be normalized to the laser power. The computer allows easy handling of the obtained spectra by a graphic display. Full advantage is taken of the large dynamic range, which is much harder to do using a conventional pen recorder.

REFERENCES

[1]   F.H. de Leeuw and A. Dymanus, J. Mol. Spectrosc. 48 (1973) 427.

[2]   W.L. Meerts and A. Dymanus, Can. J. Phys. 53 (1975) 2123.

[3]   J.P. Bekooy, thesis, Katholieke Universiteit Nijmegen (1983).

[4]   W.A. Majewski, Opt. Comm. 45 (1983) 201.

[5]   N. Bloembergen, Nonlinear Optics, Benjamin/Cummings, London (1975).

[6]   W.M.G. Ubachs, thesis, Katholieke Universiteit Nijmegen (1986).

[7]   F. v. Moers, T. Hebert and A. Hese, Appl. Phys. B 40 (1986) 67.

[8]   S. Saito, J. Mol. Spectrosc. 48 (1973) 530.

[9]   J.J. ter Meulen, W. Ubachs and A. Dymanus, Chem. Phys. Lett. 129 (1986) 533.

[10]   S. Gerstenkorn and P. Luc, Atlas du spectroscopie d'absorption de la molecule d'iode, Centre National de la Recherche Scientifique, Paris, France, (1978);
       S. Gerstenkorn and P. Luc, Rev. Phys. Appl. 14 (1979) 791.

[11]   J. Cariou and P. Luc, Atlas du spectre d'absorption de la molecule de tellure, Centre National de la Recherche Scientifique II, Orsay, France, (1980).

[12]   W. Demtroder, Laser Spectroscopy, Springer, Berlin, 1981.

The structure of fluorene (C₁₃H₁₀) and the fluorene−argon van der Waals complex from a high-resolution near ultraviolet spectrum

W Leo Meerts, W A Majewski,[1] and W M van Herpen

Fysisch Laboratorium Katholieke Universiteit Toernooiveld 6525 ED Nijmegen The Netherlands

Received May 31 1984

The high resolution fluorescence excitation spectrum of the fluorene molecule and its van der Waals complex with argon has been studied Rotationally resolved spectra were obtained by combining a well collimated supersonic molecular beam with a single frequency tunable ultraviolet (uv) source The $S \leftarrow S_0$ O_0^0 vibronic transitions in fluorene and fluorene−argon were observed The rotational constants of both molecules were determined and from these the structure of the fluorene−argon complex has been deduced The argon atom is located above the middle five membered ring The coordinates of the position vector of the argon atom in the complex in the centre of mass system of fluorene are $r = (3\ 46 \pm 0\ 03)$ Å and $\vartheta = \pm (8\ 8 \pm 1\ 0)°$ A model calculation of the fluorene−Ar structure was found to be in quite good agreement with the experimental result The newly introduced inertial defect of the complex $\Delta I = -7(3)$ amu Å provided an experimental measure of the zero-point motion of argon in the complex

On a étudié à haute résolution le spectre d excitation de fluorescence de la molecule de fluorene et de son complexe de van der Waals avec l argon On a obtenu des spectres resolus rotationnellement en combinant un faisceau moleculaires super sonique à bonne collimation avec une source UV a fréquence unique ajustable Les transitions vibroniques $S \leftarrow S$ O_0 dans le fluorène et dans le complexe fluorène−argon ont ete observées On a determine les constantes rotationnelles des deux molécules et on en a deduit la structure du complexe fluorène−argon L atome d argon est situe audessus de l anneau central à cinq membres Les coordonnes du vecteur position de l atome d argon du complexe dans le systeme du centre de masse du fluorène sont $r = (3\ 46 \pm 0\ 03)$ Å et $\vartheta = \pm (8\ 8 \pm 1\ 0)°$ Un calcul de modèle de la structure fluorene−Ar a donne un tres bon accord avec le resultat expérimental Le defaut inertiel du complexe $\Delta I = -7(3)$ uma A introduit recemment a fourni une mesure experimentale du mouvement de point zéro de l argon dans le complexe

[Traduit par le journal]

1. Introduction

Laser spectroscopy in combination with molecular beams is a powerful tool in the investigation of the structure and dynamic behaviour of large molecules and their van der Waals complexes In most experiments the laser crosses the molecular beam close behind the nozzle In this 'free jet setup, high sensitivity and moderate resolution are achieved The line widths of the transitions are generally limited by the Doppler width which is, in a free jet experiment typically 600 MHz This resolution is high enough for single vibronic excitation and shows the rotational structure in smaller organic molecules and their complexes such as for example benzene−helium (1) For larger multi ring compounds, higher resolution is required to observe more than the rotational contour Rotational resolution not only facilitates structure determination of van der Waals complexes but becomes a necessity for studies of larger molecules and complexes

We achieved a considerable reduction of the Doppler width by increasing the distance between the source and the laser excitation region while strongly collimating

[1]Present address Herzberg Institute of Astrophysics National Research Council of Canada Ottawa Ont Canada K1A 0R6

the molecular beam (2 3) In this way line widths as narrow as 15 MHz were observed At such high resolution, not only could the rotational spectrum of naphthalene be studied (3), but also the molecular eigenstates in pyrazine (4) were revealed

Single vibronic excitation spectra of the fluorene (F) molecule (C₁₁H₁₀) and its complexes with argon (F−Ar) were reported before in several papers (5 6) In the present work we studied the $S_1 \leftarrow S_1$ O_0^0 vibronic transition in F and F−Ar We observed well-resolved rotational spectra in both molecules From the rotational analysis it has been concluded that the skeleton of the bare fluorene molecule is planar in accord with the crystalline work (7) The position of the out of plane hydrogens could also be determined From the difference in the moments of inertia of fluorene and fluorene−argon the structure of the complex has been deduced The argon atom is located above the five membered ring in the symmetry plane that bisects the molecule An intensity analysis has been performed yielding the rotational temperatures of F and F−Ar in the molecular beam Within experimental uncertainty a Boltzmann distribution was found with equal temperatures for the bare molecule and the complex

A calculation of the potential energy surface between the fluorene molecule and the argon atom using

atom–atom interactions has been carried out The result of this calculation is gratifying since it is in agreement with the experimentally determined structure of the complex

In analogy with the inertial defect for a planar molecule (8), we have introduced the inertial defect for the complex (ΔI^c) If the argon atom in the complex is located in the bisecting plane, ΔI^c should be zero for the equilibrium structure Deviations of ΔI^c from zero are a measure of the contributions due to the vibrational motion of the argon in the complex Experimentally, a significant value for ΔI^c has been determined

All observed lines in both F and F–Ar could be assigned as pure rovibronic transitions No perturbations such as in pyrazine (4) or pyrimidine (9) were found in the excited singlet S_1 states of F and F–Ar, which demonstrates the absence of any significant intersystem crossings in fluorene

2. Experimental

The experimental setup has been described in detail before (3), only the most relevant features will be discussed here The seeded beam technique has been used to reduce the internal temperature of the molecules in the beam This not only simplifies the rovibronic spectra considerably, but complexes are also readily formed in the ultracold beam A mixture of 1% fluorene and argon was expanded through a 100-μm nozzle The total backing pressure was 5 bar (1 bar = 100 kPa) and the reservoir was heated to 190°C In order to achieve rotational resolution, the molecular beam was strongly collimated by two diaphragms with a two-step differential pumping system The interaction zone, where the laser beam crossed the molecular beam, was 30 cm from the source This setup reduced the Doppler width to 15 MHz Fluorescence excitation spectra were obtained by collecting the undispersed total fluorescence The image of the fluorescing spot was focused on the photocathode of an EMI 9864/950 QA photomultiplier and measured by a standard photon counting system

The narrow band ultraviolet (uv) radiation has been obtained by our recently developed method of second-harmonic generation (SHG) (10) The SHG is achieved by placing a LiIO₃ angle-tuned crystal in a modified Spectra Physics ring dye laser Stabilized scans over 4 cm⁻¹ with a line width of less than 0 5 MHz could easily be made About 1 mW of continuous wave (cw) power has been applied at the interaction zone The absolute frequency calibration has been performed on the fundamental frequency by a 1-m monochromator and the calibration absorption spectrum of iodine (11) The relative frequency has been measured by a sealed off, temperature stabilized confocal Fabry–Perot interferometer with a 299 32-MHz free spectral range
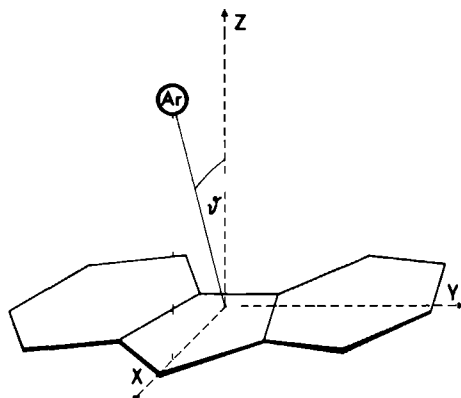

FIG 1 Definition of the coordinate system as used for fluorene and the fluorene–argon complex The origin of the coordinate system has been chosen at the centre of mass of the fluorene

3. Results and discussion

3 1 Fluorene

The low-resolution single vibronic spectrum has been studied before (5, 6) The strong transition at 296 nm has been assigned as the O_0^0 band of the $S_1(^1B_2) \leftarrow S_0(^1A_1)$ electronic transition We have investigated this transition under high resolution A completely rotationally resolved spectrum was obtained consisting of several hundreds of lines in a 100-GHz region Even most of the Q-branch transitions were resolved The typical count rate for a single line was 35 000 counts/s On basis of its structure (7), fluorene can be characterized as a near prolate asymmetric rotor with the a axis along the long axis (a axis in Fig 1) The rotational spectrum we observed was identified as an a type transition The electronic transition is therefore, long-axis polarized, in agreement with the conclusion from the crystal spectra (12) A region of 20 GHz around the pure vibronic transition frequency ν_0 was investigated in detail A total of 225 rotational transitions were assigned in this region All features, even the very weak ones with the rotational quantum number J as high as 19, were identified The transitions were fit to an asymmetric rotor model yielding the assignments of the lines, the rotational constants in the ground and excited electronic state and ν_0 An excellent fit was obtained with a standard deviation of 7 5 MHz for the lines The resulting molecular constants are given in Table I

Furthermore, it was carefully investigated whether any extra features due to intersystem crossings were observable In contrast to the situation in pyrazine (4)

TABLE 1 Molecular constants of fluorene and fluorene–argon in their S_0 and S_1 electronic states ($\Delta A = A' - A''$, $\Delta B - B' - B'$ $\Delta C = C' - C'$)

		Fluorene	Fluorene–argon
S_0	A''(MHz)	2 183 2(33)	811 1(29)
	B'(MHz)	586 520(69)	468 58(14)
	C'(MHz)	463 239(65)	401 58(13)
S_1	ΔA(MHz)	−73 387(14)	−1 402(27)
	ΔB(MHz)	6 716(38)	1 437(31)
	ΔC(MHz)	0 734(41)	4 961(26)
	ν_0(cm^{-1})'	33 775 547(5)	33 731 595(5)

The shift can be determined more accurately ν_1(F–Ar) – ν_0(F) = −43 952(3) cm^{-1}

and pyrimidine (9),[2] the spectra of fluorene and also the F–Ar complex were pure unperturbed rotational spectra Although it is expected that such a large molecule as fluorene would be in the range of the ' statistical limit" (13), the present result indicates that the interaction between the S_1 and the background states is very weak Furthermore, the lifetimes (23 ns) of the S_1 states (5) are so long that the natural line widths of these states (7 MHz) are still expected to be smaller than our Doppler limited line widths This is in accord with the experimental observations

The observation of single rotational transitions over a wide range of rotational states enabled us to determine the rotational (rot) temperature T_{rot} of the molecules in the beam For a Boltzmann population distribution, the intensity of a single rovibronic transition is given by

$$[1] \quad I = I_0(2J'' + 1)g_n A_{J''K''_{-1}K''_{+1}}$$
$$\times \exp\left[-E(J'', K''_{-1}, K''_{+1})/kT_{rot}\right]$$

where J'', K''_{-1}, and K''_{+1} are the rotational quantum numbers of the ground electronic state with rotational energy $E(J'', K''_{-1}, K''_{+1})$ and I_0 is a constant For a near prolate asymmetric top, $A_{J''K''_{-1}K''_{+1}}$ can be approximated by the Honl–London factors for the prolate symmetric top limit (14) The coefficient g_n denotes the statistical weight due to the nuclear spins The fluorene molecule can be characterized by the C_{2v} molecular symmetry group The molecule has five pairs of equivalent hydrogens, four pairs in the plane of the skeleton and one pair out of this plane The values for g_n are (e = even, o = odd)

$$g_n = 496 \text{ for } (K''_{-1}, K''_{+1}) = \text{(ee) or (oo)}$$
$$g_n = 528 \text{ for } (K''_{-1}, K''_{+1}) = \text{(eo) or (oe)}$$

These two numbers differ by only 6% The observed intensities have typical uncertainties of up to 5–10%

---

[2]As an example, this can easily be verified for the alkalicyanides using the results from ref 17

Therefore, the effects due to the nuclear spin statistics are negligible within experimental errors The reason that the two values for g_n are so close is that a large number of hydrogens in fluorene are only pairwise at equivalent positions

The relative intensities from the rotational spectrum were fitted to [1] with T_{rot} as the only parameter A single rotational temperature could be assigned, $T_{rot} = 2$ 3(3) K

Although a structure determination is impossible for fluorene with only the rotational constants from Table 1, these data contain direct information about the position of the two out-of-plane hydrogens It has been shown from crystalline work (7) that the carbon skeleton of the fluorene molecule is planar Furthermore, it is obvious that the hydrogens on the six-membered rings are in the same plane The two remaining hydrogens bound to the carbon in the bisecting plane are located in the xz plane symmetrically around the xy plane (see Fig 1) Let us separate the contributions to the moments of inertia along the principal axes I_g ($g = x, y, z$) into a part containing the contributions from the atoms in the xy plane (I_g^0) and a part arising from the out-of-plane hydrogens (ΔI_g)

$$[2] \quad I_g = I_g^0 + \Delta I_g$$

Let

$$[3] \quad \Delta = I - I_c - I_s = (I^0 - I_c^0 - I_s^0)$$
$$+ (\Delta I - \Delta I_c - \Delta I_s)$$

Neglecting zero-point motions, the planarity conditions for I_g^0 impose

$$[4] \quad I^0 - I_c^0 - I_s^0 = 0$$

The accuracy of this equation is determined by the contributions to I_g^0 from the zero-point motions We estimate that a value of 0 2 amu Å^2 is a good upper limit for these contributions It can easily be seen that

$$[5] \quad \Delta = -2 \sum_i m_i z_i^2$$

where i represents the out-of-plane atoms with mass m_i and position z For fluorene, the sum simply reduces to $-4m_H z_H^2$, $|z_H|$ is the distance to the xy plane The values for I_g are readily obtained from the rotational constants given in Table 1 by using $I_a = h/8\pi^2 A$, $I_b = h/8\pi^2 B$, and $I_c = h/8\pi^2 C$, and the correlation $(a, b, c) \rightarrow (y, x, z)$ Substitution yields $\Delta = -2$ 18(40) amu Å^2 and $|z_H| = 0$ 74(5) Å By defining θ_H as the angle between the CH bond of the out-of-plane hydrogens and the xy plane, and r_{CH} as the length of this bond, it follows that $z_H = r_{CH} \sin \theta_H$ Within the present accuracy of z_H, the CH bond length may be assumed to be $r_{CH} = 1$ 08 Å, as in many methyl groups, therefore,
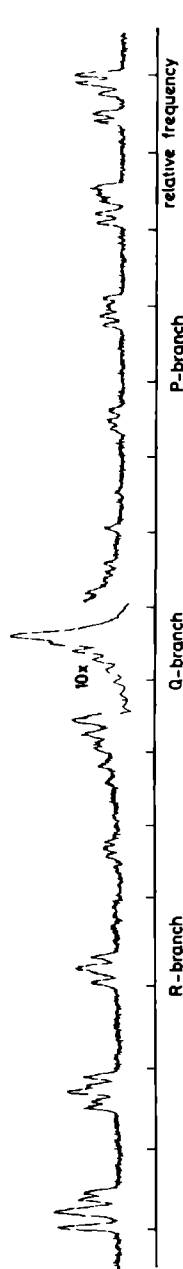
FIG. 2 Rotationally resolved spectrum of the fluorene argon complex near the electronic origin of the O_0^0 transition at 33 731 595 cm^{-1} The frequency markers are at every 598 64 MHz

TABLE 2 Calculated and observed moments of inertia for fluorene (in units of amu Å^2)

	Calculated value	Experimental value
$I(I_a)$	231 1	231 5(3)
$I(I_b)$	866 71	861 66(10)
$I(I_c)$	1095 63	1090 97(15)

$\theta_H = (43 \pm 4)°$ This determines the position of the out-of-plane hydrogens

The moments of inertia of the fluorene molecule can be calculated from the structure of the C skeleton (7) and the assumption that the CH distances from the in plane hydrogens equal 1 08 Å, while the CH bonds point along the line between the centre of the six-membered ring and the connecting carbon atom The result of this calculation is given in Table 2 The calculated and experimental values agree to within 0 6%, which is very satisfactory This demonstrates that the structures of the free fluorene molecule and the fluorene in the crystalline state do not differ significantly

3 2 Fluorene–argon

Shifted about 44 cm^{-1} to the red side of the fluorene O_0^0 transition, a spectrum has been observed that was identified as that of the F–Ar complex The transition was about a factor of 100 weaker than that of the bare fluorene molecule The central 9 GHz part of the F–Ar spectrum is shown in Fig 2 It shows a typical a-type spectrum with an unresolved Q branch and well-resolved P- and R-branches A total of 151 rotational transitions in a region of 23 GHz around ν_0 were iden tified and fitted to an asymmetric rotor Hamiltonian Again an excellent fit was obtained, with a standard deviation for the lines of 7 6 MHz The best fit rotational constants and ν_0 for F–Ar are presented in Table 1

For the F–Ar complex, we were also able to derive a rotational temperature from the intensity measurements of the assigned rotational transitions In the complex, the effects of the nuclear spin statistics on the intensities are even smaller than for fluorene itself, because of the lower symmetry of the complex (see below) Again a Boltzmann distribution was found with $T_{rot} = 2$ 1(4) K The rotational temperature of the F–Ar complex in the beam is, to within the experimental accuracy, equal to that of the bare fluorene molecule This result demonstrates that internal heating by com plex formation is probably lost in the full expansion of the molecular beam

We shall now show that the position of the argon in the complex can be determined from only the change in the moments of inertia from the bare molecule to the complex This allows a structure determination of the

complex even without accurate knowledge of the structure of the bare molecule In the following, we assume that in the complex the structure of the molecule is unaltered We take I_x, I , and I as the moments of inertia of the bare molecule along its principal axes, x,

y, and z respectively In Fig I these axes are indicated for fluorene Let (x_0, y_0, z_0) be the position of the argon atom in the complex defined in the principal axis system of the molecule, then some simple mechanics yields the moment of inertia tensor of the complex $(I^c_{\alpha\beta})$

$$[6]\quad (I^c_{\alpha\beta}) = \begin{bmatrix} I_x + \mu(y_0^2 + z_0^2) & -\mu x_0 y_0 & -\mu x_0 z_0 \\ -\mu x_0 y_0 & I_x + \mu(x_0^2 + z_0^2) & -\mu y_0 z_0 \\ -\mu y_0 z_0 & -\mu y_0 z_0 & I + \mu(x_0^2 + y_0^2) \end{bmatrix}$$

with μ the reduced mass $M_{Ar}M_F/(M_{Ar} + M_F)$ A diagonalization of $(I^c_{\alpha\beta})$ gives the moments of inertia of the complex $(I^c_\xi, I^c_\eta, I^c_\zeta)$ along its principal axes (ξ, η, ζ) as a function of (x_0, y_0, z_0) By fitting $(I^c_\xi, I^c_\eta, I^c_\zeta)$ to the experimental values from Table 1, we determine $|x_0| = 0\ 53(7)$ Å, $y_0 = 0$, and $|z_0| = 3\ 42(3)$ Å The argon atom is, therefore, located in the bisecting plane of the molecule at a distance from the centre of mass of fluorene of $r = (3\ 46 \pm 0\ 03)$ Å with $\vartheta = \pm(8\ 8 \pm 1\ 0)°$ (see Fig 1) To within these uncertainties, the structure in the ground and excited electronic states are found to be equal The ambiguity in the sign of ϑ originates in the fact that the diagonalization of $(I^c_{\alpha\beta})$ yields a quadratic function in x_0, y_0, and z_0 Because of the symmetry of fluorene, it follows that the Ar atom in F−Ar is located above either the positive or negative x axis Intuitively it might be expected that the argon atom is "pushed" towards the negative x direction by the steric effect of carbon and hydrogen atoms in the xz plane

In an attempt to remove the ambiguity of the F−Ar structure, we carried out a model calculation of the potential surface of the F−Ar complex using the method described by Ondrechen et al (15) The structure of fluorene discussed in Sect 3 1 has been adopted An absolute minimum in the energy was found for argon at the coordinates (in angstroms) $(x_0, y_0, z_0) = (0\ 13, 0, 3\ 48)$ with respect to the centre-of-mass coordinate system of fluorene (Fig 1) Figure 3 shows three cuts through the coordinates of the potential minimum The absolute potential minimum is above the central five-membered ring In Fig $3a$ we have indicated the two possible experimental positions Because of the large anharmonicity of the potential surface in the x direction, the expectation value of the x coordinate in the ground vibrational state of the complex will be shifted considerably, with respect to the equilibrium distance, towards the negative x direction The magnitude of this shift, although hard to estimate, can be as large as 0 5 Å A molecular dynamics calculation such as discussed by Brocks et al (16) is needed to get a

more accurate value for this shift Work in this direction is in preparation, however, at the present stage we might conclude that the potential anharmonicity will favour the experimental structure labelled as 1 in Fig $3a$, i e , a negative x value The large maximum in the potential energy for positive x values is dominated by the contributions of the out-of-plane hydrogen A better picture of the fluorene−argon potential along the x axis is obtained by plotting the minimum of the potential relaxing the z coordinate The result of this calculation is depicted in Fig 4 The effect of the out-of-plane hydrogens clearly shows up in the fact that the minimum in the potential energy is found for larger values of z near these hydrogens The large maximum from Fig $3a$ is now removed However, the large anharmonicity in the x direction is still present, thus favouring structure 1 from Fig $3a$ A gratifying quantitative agreement is, therefore, obtained between the rather simplified model calculations and the experimental structure of the F−Ar complex

The potential surface, especially in the x direction, is very flat This will allow for large amplitude motions of the argon atom in the complex, which gives rise to large zero-point motion effects In the case of F−Ar, an experimental measure can be obtained for these effects In analogy with the inertial defect for a planar molecule (8), we shall call this the inertial defect of the complex (ΔI^c) For $y_0 = 0$ $(\eta \| y)$ it can easily be shown from [6] that

$$[7]\quad \Delta I^c = [I^c_\xi + I^c_\zeta - I^c_\eta] - [I_x + I - I]$$

must be equal to zero if the zero-point motion contributions are neglected With the results from Table 1, we find $\Delta I^c = -7(3)$ amu Å^2 for both the ground and the excited electronic states The accuracy of the experimental structure is mainly limited by the value of ΔI^c This also prevents observation, within the experimental accuracy, of a change in the structure of the complex upon electronic excitation The inertial defect is not equal to zero, because only for the equilibrium
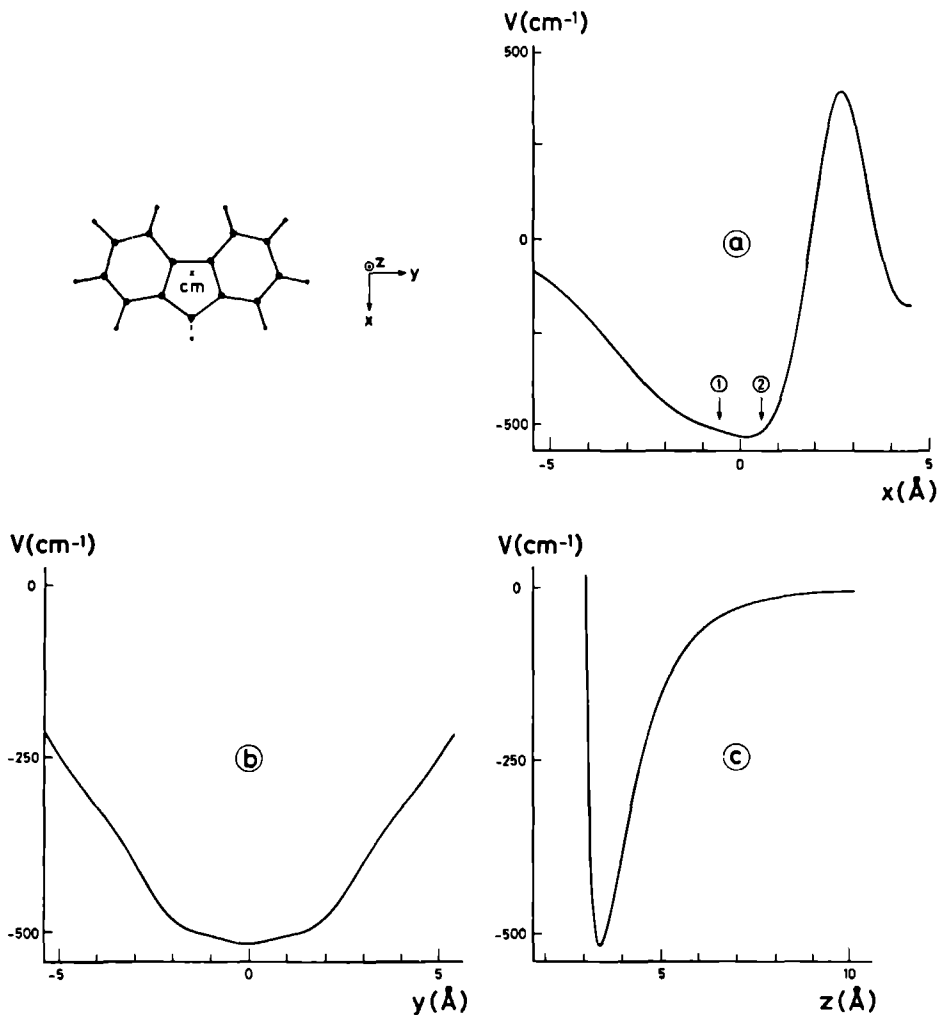
FIG. 3 Potential energy curves for a single argon with fluorene The energy is drawn vs the position (in angstroms) of the argon atom in the centre of mass coordinate system of fluorene (see insert) (a) Energy as a function of x along the line (y – 0 z = 3 48) The two arrows indicate the two possible experimental positions (b) Energy as a function of y along the line (x = 0 13 z = 3 48) (c) Energy as a function of z along the line (x = 0 13 y = 0)

configuration does I_x exactly equal $h/8\pi^2 A_x$ In a given vibrational state, the vibrational averaging gives rise to deviations, since $\langle 1/r^2 \rangle \neq 1/\langle r^2 \rangle$ It is expected that similar to the inertial defect for a planar molecule, a molecular dynamics calculation (16) of the complex will yield quite an accurate prediction for ΔI^r, which

directly measures the contributions to the vibrationally averaging process This will provide an excellent test of the shape of the potential

In conclusion, we have shown that rotationally resolved electronic spectra can be obtained for complexes with organic molecules even as large as fluorene At
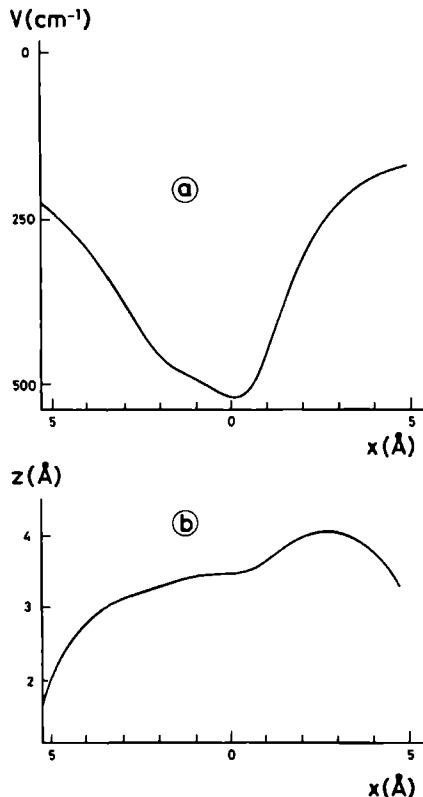
Fig 4 The minimal potential interaction energy between fluorene and argon in the xz plane ($v = 0$) (a) Minimal potential energy vs the x coordinate (z adjusted) (b) The z coordinate corresponding to minimum energy

present there remains some ambiguity in the sign of the positional angle ϑ of the argon atom in the complex This problem can be solved by studying the rovibronic spectrum of a deuterated fluorene − argon complex Such an experiment is currently underway

Acknowledgements

1 S M BECK M G LIVERMAN D L MONTS and R E SMALLEY J Chem Phys 70 232 (1979)
2 W L MEERTS and W A MAJEWSKI Laser spec troscopy VI Edited by H P Weber and W Luthy Springer Verlag Berlin F R G 1983 p 147
3 W A MAJEWSKI and W L MEERTS J Mol Spectrosc 104 271 (1984)
4 B J v D MEER H TH JONKMAN J KOMMANDEUR W L MEERTS and W A MAJEWSKI Chem Phys Lett 92 565 (1982)
5 A AMIRAV U EVEN and J JORTNER Chem Phys 67 1 (1982)
6 S LEUTWYLER W EVEN and J JORTNER J Chem Phys 79 5769 (1983)
7 D M BURNS and J IBALD Proc R Soc London Ser A 227 200 (1954)
8 W GORDY and R L COOK Microwave molecular spec tra Interscience Publishers Inc New York NY 1970
9 W L MEERTS W A MAJEWSKI B J v D MEER and J KOMMANDEUR J Chem Phys To be published W L MEERTS W A MAJEWSKI B J v D MEER and K DRABE Symp Mol Spectrosc Proc 39th Columbus OH 1984
10 W A MAJEWSKI Opt Commun 45 201 (1983)
11 S GERSTENKORN and P LUC Atlas du spectroscopie d absorption de la molecule d iode Centre National de la Recherche Scientifique Paris France 1978 S GERSTENKORN and P LUC Rev Phys Appl 14 791 (1979)
12 A BREE and R ZWARICK J Chem Phys 51 903 (1969)
13 M BIXON and J JORTNER J Chem Phys 48 715 (1968)
14 G HERZBERG Molecular spectra and molecular struc ture Vol 2 D Van Nostrand Company Inc Princeton NJ 1966
15 M J ONDRECHEN A BERKOVITCH YELLIN and J JORTNER J Am Chem Soc 103 6586 (1981)
16 G BROCKS A v D AVOIRD B SUTCLIFFE and J TENNYSON Mol Phys 50 1025 (1983)
17 J TENNYSON and B T SUTCLIFFE Mol Phys 46 97 (1982)

ROTATIONALLY RESOLVED SPECTROSCOPY OF DEUTERATED FLUORENE AND THE FLUORENE-ARGON VAN DER WAALS COMPLEX

W.M. van Herpen and W. Leo Meerts

Fysisch Laboratorium, Katholieke Universiteit

Toernooiveld, 6525 ED Nijmegen, The Netherlands

ABSTRACT

With a single frequency tunable uv source in combination with a collimated molecular beam, rovibronic fluorescence spectra were obtained of fully deuterated fluorene and its van der Waals complex with argon. The O_0^0 vibronic band in both molecules was assigned and molecular constants were derived. The position of the argon atom in the complex is determined above the middle ring of the fluorene molecule. It is shown that substantial zero-point motions are present in the complex, hindering a precise determination of the effective structure.

1. INTRODUCTION

In recent years several studies have been reported on spectroscopic investigations of large aromatic molecules and their van der Waals (vdW) complexes. In order to limit the population of numerous energy levels at room temperature in these large molecules, most work has been performed using molecular jet techniques. The reduction of internal degrees of freedom in the expansion facilitates the interpretation of the otherwise congested spectra. The spectral resolution is generally sufficient to observe rovibronic bands in relatively small molecules as the benzene-helium complex [1]. For larger molecules like fluorene (FL) only vibronic resolution is achieved in a jet. The electronic shift of some

bands of FL-argon vdW complexes has been reported as well as the lifetime of the first electronic excited singlet S_1 state [2]. This shift is caused by the difference in interaction between FL and argon in the ground and excited state of the complex. The assignment of various vibronic bands of FL-R (R=Ne, Ar, Kr, Xe) complexes by a mass resolved technique was reported by Leutwyler *et al.* [3].

To obtain information regarding the structure of the molecule or its complexes, rotational resolution is needed. Previous work showed that this can be achieved by using a strongly collimated molecular beam in combination with a narrow band radiation source [4]. The position of the out of plane hydrogen atoms in the FL molecule was determined from the rotational constants. The effective structure of the FL-Ar complex was also obtained. Yet, such conclusions rest on some basic assumptions.

First, the frame of the parent molecule is considered a rigid rotor. The rotational constants however reflect the effective structure of the molecule, which may be different. For the determination of the position of the out of plane hydrogen atoms the 'inertia defect' of the molecule is used [4]. This defect is affected by the zero-point vibrations. These contributions were neglected in the previous work. A check on the validity of this approximation is given by comparing different isotopic species of the molecule. In case the rigid rotor approach is applicable, data from various isotopic species should yield the same effective structure.

A second problem concerns the derivation of an effective structure of the complex. The diagonalization of the inertia tensor results in a quadratic function in the coordinates of the argon atom in the centre of mass frame of FL. It is therefore not possible to distinguish between positive and negative signs of these coordinates. By isotope substitution the centre of mass of FL is shifted and the problem is transformed to a different axis system. In combining data from different isotopic species it is, therefore, in principle possible to derive an unique solution for the effective structure.

A third problem originates from the interpretation of the effective structure as derived from the rovibronic spectra. Recent theoretical work of Brocks *et al.* [5] has shown that the argon atom experiences a large amplitude motion in the complex. This molecule can not be considered to be a rigid rotor. An experimental indication that such motions are present may be found in spectroscopic work on different isotopes. A rigid rotor molecule will yield the same effective structure for all isotopes. In a more floppy molecule these isotopes may exhibit differences.

With these problems in mind we have measured the rovibronic O_0^0 band of the fully deuterated fluorene molecule FL-d_{10} and its vdW complex with argon. A comparison is made with data from FL-h_{10} as reported in a previous paper [4].

2. EXPERIMENTAL

The measurements were performed using laser induced fluorescence detection in a seeded molecular beam. The experimental setup has been described elswhere [6] FL-d_{10} with a 98 9 % deuterium abundancy (MSD Isotopes) was heated in a quartz source to about 110 °C. With argon as seeding gas, a jet expansion was made from a 125 μm diameter nozzle. The typical backing pressure was 0.5 bar. Two diaphragms in a differential pumping system strongly collimated the molecular beam, which resulted in a residual Doppler linewidth of about 15 MHz. The molecular beam is crossed by a laser beam at a distance of 30 cm from the beam orifice. The total, undispersed fluorescence is collected and imaged to a photomultiplier tube. Data recording is performed by a standard photon counting system, interfaced with a microcomputer. The narrow band laser radiation is generated by intracavity frequency doubling of a cw single mode ring dye laser [7]. The O_0^0 transition of FL-d_{10} around 294.9 nm is at the edge of the tuning range of the $LiIO_3$ doubling crystal, but still a typical uv power of 0.2 mW was obtained. This proved sufficient to record the spectrum at a 0.1 s time constant. Relative frequency calibration was carried out using a sealed temperature stabilized Fabry-Perot interferometer, while absolute frequency measurements were performed using an iodine reference absorption spectrum [8].

3. RESULTS AND DISCUSSION

3.1 fluorene

The FL molecule can be characterized by C_{2v} symmetry. The molecule has a planar structure, apart from two out of plane hydrogen atoms protruding from the five membered ring. It is a near prolate asymmetric rotor with an asymmetry parameter $\kappa=-0.857$. The (a,b,c) principal axes are identified as (y,x,z) in fig. 1. The O_0^0 band of FL-h_{10} has been studied before [2,3,4]. It was shown to be a $S_1 (^1B_2) \leftarrow S_0 (^1A_1)$ singlet-singlet transition with a parallel type rotational structure. The electronic transition dipole moment is along the a-axis in agreement with earlier conclusions from crystal spectra [9]. We measured the O_0^0 band of the deuterated FL-d_{10} molecule under rotational resolution.
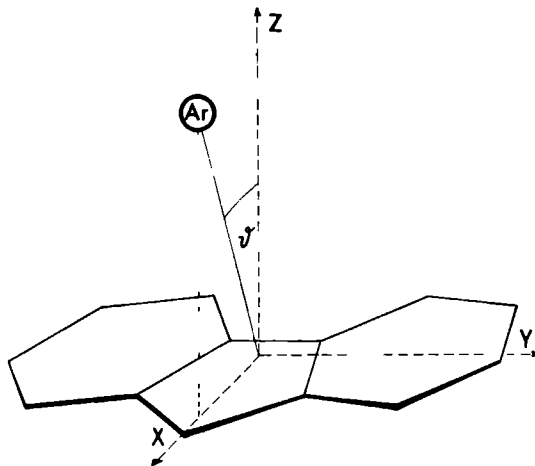
FIG. 1. Orientation of the coordinate system as used for fluorene and the fluorene-argon complex. The origin is taken at the centre of mass of fluorene.

The spectrum is very well resolved; also its Q branch. The observed linewidth is 15 MHz and is determined by the experimental limitations. We therefore conclude that the natural linewidth is smaller than 15 MHz and thus the lifetime of the FL-d_{10} excited S_1 state has a lower limit of 10 ns. The lifetime of the FL-h_{10} species has been reported as 23 ns [2]. The observed band was identified as an a-type rotational band. A total number of 450 lines was assigned in a 30 GHz region, with the selection rules for (K_{-1},K_{+1}): (ee) - (eo) and (oe) - (oo); where e means even and o odd. Lines with J up to 20 were fitted to an asymmetric rotor model [10] with an excellent fit. A standard deviation of 3.4 MHz was obtained in the lines. From the fit we obtained the rotational constants as listed in table 1 and the rotationless transition frequency ν_0, given in table 2 The shift of ν_0 with respect to the FL-h_{10} species is determined as 129.128(3) cm^{-1}.

The observed band contains a number of isolated single rotational lines. From the observed intensities we deduce the rotational temperature T_{rot} in the molecular beam. The intensity of a transition is given by:

$$1 = I_0 (2J''+1) g_n A(J'',K''_{-1},K''_{+1}) \exp\left[\frac{-E(J'',K''_{-1},K''_{+1})}{kT_{rot}}\right] \qquad (1)$$

Here $A(J'',K''_{-1},K''_{+1})$ can be approximated by the Honl-London factors for a symmetric top molecule. The various pairs of equivalent nuclear spins in FL-d_{10} give rise to different spin statistical weights g_n.

TABLE 1. Molecular constants (MHz) of the fluorene and fluorene-argon molecule in their S_0 and S_1 electronic states. ($\Delta A=A'-A''$ etc.)

		FL-d_{10}	FL-d_{10}Ar
S_0	A"	1826.2(25)	754.4(38)
	B"	531.694(73)	416.74(13)
	C"	414.064(70)	370.54(13)
S_1	ΔA	-57.300(11)	-1.743(20)
	ΔB	5.735(13)	1.417(26)
	ΔC	0.459(12)	4.246(27)

TABLE 2. Rotationless $S_1 \leftarrow S_0$ O_0^0 transition frequencies (cm^{-1}) for fluorene [4] and the relative frequency shift $\Delta\nu=\nu-\nu_0$(FL) of deuterated fluorene and the vdW complexes with argon.

	ν_0	$\Delta\nu$
FL-h_{10}	33775.547(12)	
FL-h_{10}Ar		-43.952(3)
FL-d_{10} a)	33904.675(12)	
FL-d_{10}Ar		-44.504(3)

a) The absolute isotope shift can be determined more accurately:

ν_0(FL-d_{10}) - ν_0(FL-h_{10}) = 129.128(3) cm^{-1}.

The values for g_n are: 29646 for (K_{-1},K_{+1}) is (ee) or (oo) and 29403 in case (K_{-1},K_{+1}) is (eo) or (oe). These small differences in intensity are negligible in comparison with our experimental accuracy of about 5%. A fit of 100 line intensities to equation (1) yielded a rotational temperature of $T_{rot} = 3.7(4)$ K. This temperature is somewhat higher than obtained in previous experiments because we used a rather low argon pressure to manage our supply of deuterated fluorene economically.

By simulation of the spectrum, using the obtained molecular constants and the derived rotational temperature, it appeared that all spectral features, even the weak ones, could be reproduced. There is no indication for any perturbations in the spectrum due to, for example, intersystem crossings or internal conversion [11,12].

As shown in ref. [4] it is possible to obtain information on the effective structure of the FL molecule. The carbon skeleton of the molecule is planar, as derived from crystalline data [13]. If it is assumed that the hydrogen atoms connected to the two six membered rings are located in the same plane, there are only two out of plane atoms. Both hydrogens protruding from the five membered ring are located in the xz plane, symmetrically around the xy plane. The moments of inertia along the principal axis I_g (g=x,y,z) can be separated into contributions from the in plane atoms I_g^0 and a part arising from the out of plane atoms ΔI_g :

$$I_g = I_g^0 + \Delta I_g \tag{2}$$

By definition of the quantity Δ analogous to the inertia defect of a planar molecule as:

$$\Delta = I_z - I_x - I_y \tag{3}$$

it can be shown that:

$$\Delta = \delta - 2\sum_i m_i z_i, \tag{4}$$

with:

$$\delta = I_z^0 - I_x^0 - I_y^0. \tag{5}$$

In eq. (4) i indicates the out of plane atoms with mass m_i and position z_i. In case of FL

this equation reduces to:

$$\Delta = \delta - 4m_h z_h^2 \tag{6}$$

where $|z_h|$ is the effective distance to the xy plane. The hydrogen mass m_h has to be replaced by the mass m_d of the deuterium atom for the deuterated fluorene. The planarity condition for I_g^0 imposes $\delta = 0$ if the zero-point motions are neglected. In that case we would expect that $\Delta(FL-d_{10}) \approx 2\Delta(FL-h_{10})$. For $FL-h_{10}$ it was derived that $\Delta = -2.18(40)$ amuÅ^2. From table 1 it can easily be shown that $\Delta = -6.71(45)$ amuÅ^2 for the $FL-d_{10}$ molecule. There is apparently not a simple factor of two difference in the value of Δ for both fluorene isotopes. To account for the deviation a contribution from zero-point motions of $\delta \approx 1$ amuÅ^2 would be necessary. This seems a resonable value. For comparison: the inertia defect in the naphthalene molecule amounts $\delta = -1.4$ amuÅ^2 and $\delta = -0.2$ amuÅ^2 for the fully deuterated naphtalene [6].

We conclude from the observed values of Δ for $FL-h_{10}$ and $FL-d_{10}$ that zero-point contributions can not be entirely neglected in eq. (6). The derivation of an effective coordinate z_h for the out of plane hydrogen atoms suffers therefore from a substantial inaccuracy, due to the deficiency of the rigid rotor model.

fluorene-argon

The O_0^0 band in the FL-Ar vdW complex is red shifted with respect to the corresponding band in the FL molecule. It also exhibits a parallel a-type structure. The Q branch is only partially resolved. Part of the $FL-d_{10}Ar$ O_0^0 band is shown in fig. 2. A total of 216 lines in the spectrum was assigned and fitted to the asymmetric rotor Hamiltonian. From the fit we obtain the molecular constants as shown in table 1 and the rotationless transition frequency ν_0 as indicated in table 2. The fit yields a standard deviation in the lines of 4 MHz. The linewidth in the spectrum is again determined by the residual Doppler width and amounts 15 MHz. Within the spectral accuracy there is no background signal in the spectrum as was observed in case of the tetracene-argon vdW complex [12].
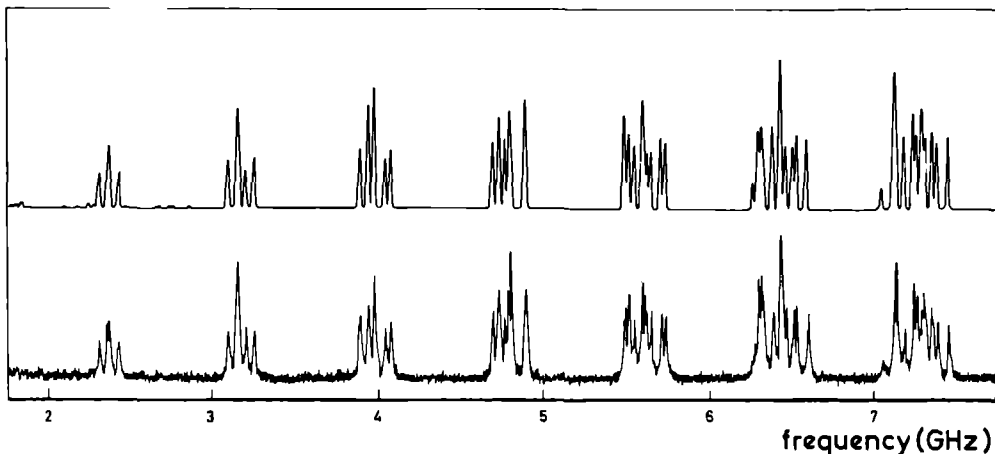
FIG. 2. Part of the R branch of the O_0^0 band of the deuterated fluorene-argon vdW complex. The calculated spectrum (top trace) is also shown. The indicated frequency scale is relative to the electronic origin of the band.

A number of single rotational lines was observed in the spectrum. From their relative intensities a rotational temperature T_{rot} was derived, using eq. (1). It appears that under the same expansion conditions, the rotational temperature of FL and FL-Ar are equal. With the use of eq. (1) and the derived constants the spectrum was simulated, as shown in fig. 2. All observed spectral lines could be accounted for within the experimental accuracy. The frequency shift ν_0(FL-Ar)-ν_0(FL) of the complex with respect to the parent molecule is determined as -44.504(3) cm^{-1}. This is comparable with the value for the FL-h_{10} species: -43.952(3) cm^{-1}.

As was shown in ref. [4], it is possible to derive an effective structure of the vdW complex, assuming the FL parent molecule has a rigid structure. The moment of inertia tensor of the complex $(I_{\alpha\beta}^c)$ can be expressed as a function of the moments of inertia along the principal axis (I_x, I_y, I_z) of the bare molecule and the position (x_0, y_0, z_0) of the argon atom in this axis system. By diagonalizing $(I_{\alpha\beta}^c)$ one obtains the moments of inertia of the complex along its principal axis (ξ, η, ζ) as a function of (I_x, I_y, I_z). These moments of inertia are fitted to the experimental values. The value for y_0 is zero within the obtained accuracy. Obviously this could be expected because of the symmetry plane of the molecule. In the final fit we therefore keep the coordinate fixed at $y_0=0$. In that case the

inertia tensor is simplified. By diagonalizing one obtains (I_ξ, I_η, I_ζ). It can be shown that if ΔI^c is defined as:

$$\Delta I^c = I_\xi + I_\eta - I_\zeta - (I_x + I_z - I_y), \qquad (7)$$

it follows $\Delta I^c = 0$. With the molecular constants from table 1 we derive $\Delta I^c = -12.(5)$ amuÅ^2 in ground state as well as excited state, thus deviating from zero. The difference can be accounted for by zero-point vibrations in the parent molecule as well as the complex. These contributions can apparently not entirely be neglected, indicating that both molecules are not ideal rigid rotors.

By fixing the value of y_0 the degrees of freedom are reduced and only two moments of inertia of the complex are needed to solve x_0 and z_0. Since ΔI^c in eq. (7) is not exactly equal zero, we obtain slightly different solutions, depending on which pairs of constants are used. This gives a good indication of the obtained accuracy. In the centre of mass frame of FL-d$_{10}$ we find $|x_0|=0.31(10)$ Å, $y_0=0.$, $|z_0|=3.46(3)$ Å, or by defining r_0 and θ as indicated in fig. 1: $r_0=3.46(3)$ Å, $|\theta|=8.8(1.0)°$. The obtained accuracy is not limited by the experimental uncertainty in the molecular constants but by the fact that the molecules do not behave as ideal rigid rotors.

The derived coordinates can not directly be compared with those from FL-h$_{10}$ as given in ref. [4]. One has to transform between the different centre of mass frames. This centre of mass can be calculated from the structure of the carbon skeleton [13] and the assumption that all CH bonds point along the line connecting the carbon atom and the centre of the six membered ring. The bond length is taken as 1.08 Å. For the two out of plane hydrogens the bond angle with the molecular plane is taken as $\theta=43°$. This structure reproduces the molecular constants for FL-d$_{10}$ and FL-h$_{10}$ within 0.6% and seems therefore reliable. The centres of mass are positioned on the intersecting line of the xz and xy plane. Their x coordinates differ only 0.01 Å. In the centre of mass frame of FL-d$_{10}$ the argon position as derived in ref. [4] would be $x_0=0.52(7)$ Å or $x_0=-0.54(7)$ Å, $y_0=0.$ and $|z_0|=3.42(3)$ Å. We note that the agreement between both the two obtained possible structures is marginal and also that therefore a distinction between the two possible values of x_0 can not clearly be made. The uncertainty in x_0 exceeds the small displacement (0.01 Å) of the centre of mass by almost an order of magnitude. The small shift is caused by the fact that most deuterium atoms are positioned symmetrically around the centre of mass. A maximum shift would be reached by substituting only hydrogen and carbon atoms with positive x coordinates, by their heavier isotopes. In this way a

theoretical shift of the centre of mass of 0.06 Å may be expected. Still this is rather small compared to the obtained uncertainty in x_0.

We conclude that a distinction between two possible effective structures of the complex cannot be made. This is not caused by the fact that the accuracy in the obtained molecular constants is insufficient but by the fact that the parent molecule and its vdW complex form no ideal rigid rotor molecules. Contributions from zero-point vibrations are clearly present. The data confirm calculations of Brocks *et al.* [5], stating that the argon atom in the complex experiences large amplitude motions (with amplitudes $\approx$ 0.3 Å).

ACKNOWLEDGMENTS

REFERENCES

[1] S.M. Beck, M.G. Liverman, D.L. Monts and R.E. Smalley, J. Chem. Phys. 70 (1979) 232.

[2] A. Amirav, U. Even and J. Jortner, Chem. Phys. 67 (1982) 1.

[3] S. Leutwyler, U. Even and J. Jortner, J. Chem. Phys. 79 (1983) 5769.

[4] W.L. Meerts, W.A. Majewski and W.M. van Herpen, Can. J. Phys. 62 (1984) 1293.

[5] G. Brocks and D. van Koeven, submitted.

[6] W.A. Majewski and W.L. Meerts, J. Mol. Spectrosc. 104 (1984) 271.

[7] W.A. Majewski, Opt. Comm. 45 (1983) 201.

[8] S. Gerstenkorn and P. Luc, Atlas du spectroscopie d'absorption de la molecule d'iode. Centre National de la Recherche Scientifique, Paris, France, (1978);
S. Gerstenkorn and P. Luc, Rev. Phys. Appl. 14 (1979) 791.

[9] A. Bree and R. Zwarick, J. Chem. Phys. 51 (1969) 903.

[10] J.K.G. Watson, J. Chem. Phys. 46 (1967) 1935.
J.K.G. Watson, J. Chem. Phys. 48 (1968) 4517.

[11] E. Riedle, H.J. Neusser, and E.W. Schlag, J. Phys. Chem. 86 (1982) 4847.

[12] W.M. van Herpen, W.L. Meerts and A. Dymanus, J. Chem. Phys. 87 (1987) 182.

[13] D.M. Burns and J. Ibald, Proc. R. Soc. London Ser. A 227 (1954) 200.

Rotationally resolved laser spectroscopy of tetracene and its van der Waals complexes with inert gas atoms

W M van Herpen, W Leo Meerts, and A Dymanus

Fysisch Laboratorium, Katholieke Universiteit Nijmegen, Toernooiveld 6525 ED Nijmegen
The Netherlands

By using a molecular beam apparatus in combination with a single frequency dye laser we were able to resolve several rovibronic bands in the S_1 electronic state of tetracene ($C_{18}H_{12}$) and its van der Waals complexes with inert gas atoms The spectra of tetracene have been assigned and rotational constants were derived for the S_0 and S_1 electronic state The existence of perturbations in the rotational spectra of the van der Waals complexes is demonstrated

I. INTRODUCTION

The study of the structure, binding energies and dynamic behavior of large (e g , aromatic) molecules and their van der Waals (vdW) complexes is hindered by complicated spectra One can try to use Doppler-free techniques in cell experiments[1] but then the relatively high temperature gives rise to an enormous amount of spectral lines in the rotational bands An experimental setup with a free jet expansion of the molecules in a seeding gas is more convenient In this way, a cooling of the internal degrees of freedom of the molecules is accomplished, resulting in a considerable reduction of the number of spectral lines Moreover, vdW complexes are readily formed in the expansion If laser excitation occurs directly behind the nozzle the spectral resolution is sufficient to study rotational bands of smaller molecules like the benzene–helium vdW complex,[2] but for larger molecules like anthracene,[3] tetracene,[4] and pentacene,[5] only vibrational resolution is achieved By enlarging the distance between the nozzle and excitation area of the crossing laser beam and by strongly collimating the molecular beam, one can reduce the residual Doppler width With the latter setup and using a single frequency laser, we were able to resolve rotational spectra of naphthalene,[6] the fluorene–argon vdW complex,[7] and even the molecular eigenstates of pyrazine [8]

We report the study of rovibronic bands of tetracene (T) and its vdW complexes with rare gas (R) atoms, argon, krypton, and xenon, in the regime of low vibrational energy ($< 500 \, \mathrm{cm}^{-1}$) A preliminary report of some of these results has already been presented [9] In the present paper, a full account of the available information is given The tetracene molecule consists of four benzene rings in line The S_1 state of T has only been studied with vibrational resolution [4] It is therefore necessary to study rotational resolved spectra of the molecule before proceeding to vdW complexes The rotational bands give insight in the structure of the free molecule and they also serve as a check for the vibrational assignment It was found before[4] that vibrational excitation in the S_1 state, 1600 cm^{-1} above the ground vibrational level, shows a shortening of the decay lifetime This effect has been attributed either to the S_1–T intersystem crossing or to the S_1–S_0 internal conversion A study at rotational resolution allows one to investigate such electronic interactions, even near the electronic origin of the S_1 state It will be shown in this paper that such interstate couplings, although weak, show up in

the regime of low vibrational energies These effects are enhanced in the vdW complexes of T with noble gas atoms and are clearly observed in the present study The increased interstate coupling is found to be in agreement with lifetime measurements at vibrational resolution,[11] where it is shown that the decay lifetime of the T–R complexes decreases rapidly in the order argon, krypton and xenon

Model calculations[10] of the T–R vdW complexes predict a possibility of tunneling effects by a large amplitude motion of the rare gas atom An experimental determination of the complex structure may serve as a test of the potential energy surface For the T–R_2 molecules the existence of chemical isomers is theoretically unlikely An experimental unambiguous determination of the structure is a worthwhile undertaking It was found, however, that no rotationally resolved spectra for the higher clusters were observable This lead to the conclusion that the interstate interactions with the S_1 state are increased in the larger clusters

II. EXPERIMENTAL SETUP

In order to obtain much simpler (less congested) spectra we used the seeded beam technique In this way considerable reduction of the internal temperature of molecules emerging in an expansion is acheived Moreover, this expansion has the advantage of an efficient production of vdW complexes of T with the seeding gas in the molecular beam The spectrometer has been described before [6 12] We used a quartz source, in which a sample of T (Aldrich) was heated to approximately 210 °C The vapor, mixed with the seeding gas, was expanded through a 100 μm nozzle into a vacuum chamber The molecular beam was doubly skimmed, reducing the Doppler linewidth to about 15 MHz The interaction zone with the laser was at 30 cm from the beam orifice The undispersed laser-induced fluorescence was imaged onto the photocathode of a photomultiplier tube (EMI 9863/350) We used a standard photon counting system (Ortec Brookdeal 5C1) The molecular beam was chopped and phase sensitive detection was applied to suppress scattered laser light The typical preset counting time was 0 1 s

Narrow band radiation was obtained from a single frequency cw dye laser system (Coherent Radiation 599-21) A solution of stilbene 3 in ethylene glycol was used as a gain medium The dye laser was pumped by the UV lines (351–364 nm) from an Ar-ion laser (Spectra Physics 171-UV)
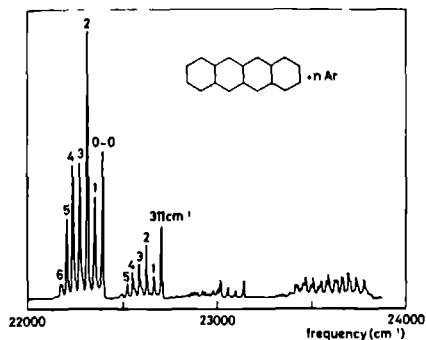
43

FIG 1 Low resolution vibronic spectrum of tetracene seeded in argon (backing pressure 4 bar) The T-Ar$_n$ ($n = 1 2$) vdW complexes are indi cated The spectrum has not been normalized to the laser intensity

The bandwidth of the dye laser was about 3 MHz and the typical output power 50 mW For relative frequency marking, we applied a sealed off temperature stabilized Fabry-Perot interferometer with a 150 MHz free spectral range For absolute frequency measurements a home-built wavelength meter was used [12] Its principle is based on a Michelson interferometer which compares the dye laser wavelength with the accurately known wavelength of a reference HeNe laser By removing the intracavity étalons of the dye laser, the bandwidth could be increased to 30 GHz In that case, the laser could be continuously scanned by a Lyot filter over the whole region of the gain medium

The spectrometer is interfaced with a microcomputer (PDP11/23 plus) Data recording by the computer provides a large dynamic range in the spectra The computer scans the laser and stores simultanously data from the spectrum and the frequency markers In processing the data it becomes possible to make accurate corrections for nonlinearity in the scan Moreover, the computer facilitates the tedious determination of the spectral positions and intensities

III. THE $S_1 \leftarrow S_0$ TRANSITION OF TETRACENE

Excitation spectra at vibrational resolution in a seeded molecular beam are obscured by spectra of vdW complexes of T with seeding gas atoms Distinction between the various transitions is based on the use of different seeding gases, the pressure dependence of the spectral intensities and the order

of appearance of various bands belonging to the vdW complexes [11][13][14] In Fig 1, a typical low resolution spectrum of T expanded in argon is shown Effective cooling of the internal temperature of the molecule is accomplished at lower pressures than formation of vdW complexes These complexes appear at relatively high pressures and increase rapidly with the backing pressure All vibronic transitions in our experiments arise from the vibrational ground state due to the effective vibrational cooling in the expansion To identify the various complexes and vibrational states, it proved to be very helpful to operate our laser at low (1 cm^{-1}) resolution This also allowed an easy optimalization of the backing pressure for the formation of different complexes

Tetracene belongs to the D_{2h} point group and the ground and singly excited electronic states are characterized by A_g and B_{2u} symmetry (with the axis chosen as $\{x,y,z\} = \{c,b,a\}$) Several vibrational states of the $S_1 \cdot S_0$ transition of tetracene have been assigned by Amirav et al [4] The vibrational structure of the S_1 state can be divided into three regimes Below a vibrational energy (E_v) of $E_v = 1000$ cm^{-1} there is a sparse level structure Above this level, Fermi resonances appear, fading into a quasicontinuum at about $E_v = 1800$ cm^{-1} We studied three vibrational states in the low energy regime under rotational resolution Two of these states belong to an a_g-type totally symmetric vibrational mode, which is active for the S_1 ($^1B_{2u}$) $\leftarrow S_0$ (^1A_g) symmetry-allowed electronic transition The nontotally symmetric b_{1g}-type mode, which has also been studied, gains its intensity from a coupling with the higher energy $^1B_{1u}$ electronic state and is much weaker than the symmetry allowed transitions The observed transition frequencies to the excited state vibrational modes are listed in Table I

The spectrum around 22 396 53(2) cm^{-1} was identified as the 0–0 electronic transition Small differences in spectral positions do exist between different investigations [11][14][15] We observed no spectral features at lower frequencies which were independent of the type of seeding gas The spectrum appeared to be very strong To avoid strong saturation effects, reduction of the cw laser power to a few mW was necessary at a focus of about 0 5 mm diam in the interaction region The transition around 22 708 cm^{-1} belongs to a totally symmetric (311 cm^{-1}) vibrational mode in the excited electronic state As expected, the spectrum thus proved to be of the same transition type as the 0–0 transition

Within experimental accuracy, we did not observe any differences between the 0–0 and 311 cm^{-1} vibronic transition The linewidth in the spectra is 15 MHz and is determined by the residual Doppler width of the spectrometer

TABLE I Experimental rotation-free S_1 ($^1B_{2u}$) $\leftarrow S_0$ (^1A_g) vibronic transition frequencies v_0 of tetracene and the relative shifts[a] ($\Delta v = v - v_0$) of the corresponding transitions of the vdW complexes

Assignment	T v_0 (cm^{-1})	T-Ar Δv (cm^{-1})	T Ar$_2$	T-Kr	T-Kr$_2$	T-Xe
(0–0)	22 396 53(2)	− 41 67(5)	− 80 6(1)	− 66 9(1)	− 124(1)	− 110 0(1)
(311 cm^{-1})	22 707 84(2)	− 41 42(5)	− 79 9(1)	− 66 5(1)	− 123 4(1)	
(471 cm^{-1})	22 867 62(2)	− 41 52(5)	− 80 0(1)	− 66 9(1)		

[a] The accuracy for the complexes is limited by the lack of a complete rotational assignment
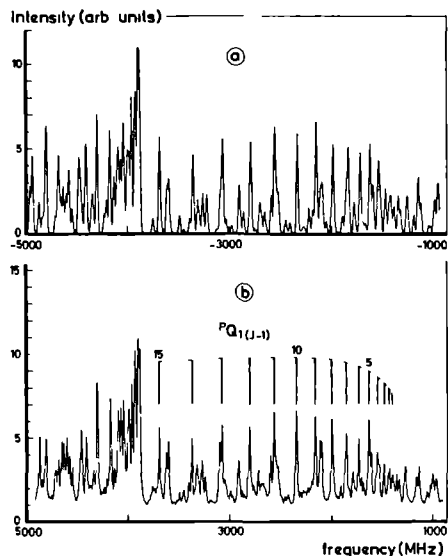
Intensity (arb units) ———

FIG 2 Part of the 0–0 perpendicular band around $\nu_0 = 22\,396\,53(2)$ cm^{-1} of tetracene In the experimental spectrum (b) a Q branch with $K''_{-1} = 1$ is indicated Band (a) is calculated from the obtained rotational constants, using rotational temperature of 2 3 K

This is in agreement with decay lifetime measurements of the excited state [4] The spectra were uniquely identified as a b-type perpendicular transition This corresponds to a transition dipole moment along the short molecular axis The b-type transitions follow the selection rules ee↔oo and eo↔oe for $K''_{-1}, K''_1 \leftrightarrow K'_{-1}, K'_1$ Such a spectrum shows hardly any characteristic features and it consists of complicated subbands Part of the 0–0 transition is depicted in Fig 2 A Q band with $K''_{-1} = 1$ is indicated As a starting point for the assignment, we used rotational constants derived for the 471 cm^{-1} vibronic transition which will be discussed below A total of 65 lines of this spectrum in a 10 GHz region around the origin was fitted to an asymmetric rotor model [16–18] All strong spectral lines in this region were included, containing rotational states up to $J = 15$ From the fit we obtain the rotation free transition frequency ν_0 and the A, B, and C rotational constants in the excited state as well as the ground electronic state In the final fit, all parameters were varied simultaneously with an excellent result A standard deviation of 2 2 MHz was obtained None of the observed frequencies deviated more than 5 MHz from the calculated value The spectral intensities were considered separately and will be discussed below As will be shown, not only the frequencies, but also the intensities of the spectral lines could be accounted for The molecular constants are given in Table II These constants are in good agreement with those derived from crystallographic data [19 20] All data could be fitted very well within experimental accuracy without taking distortion effects into account Also, it can be easily deduced from the

TABLE II Rotational constants of the tetracene molecule in the S_0 (^1A_g) and S_1 ($^1B_{2u}$) electronic states ($\Delta A = A - A''$, $\Delta B = B - B''$, $\Delta C = C - C''$) The data is derived from the 0–0 vibrationless and the 471 cm^{-1} vibrational transition

	S_0		S_1	
Constant	(MHz)		Constant	(MHz)
A	1630 (1)		ΔA	17 4(1 2)
B	213 4(2)		ΔB	− 1 81(8)
C	188 8(2)		ΔC	− 1 19(8)

rotational constants that there is no significant inertial defect ΔI in the T molecule in neither the ground state nor the studied excited states

The observed 471 cm^{-1} vibrational mode (Fig 3) corresponds to a nontotally symmetric b_{3g}-type vibration The rovibronic spectrum was identified as an a-type parallel band with selection rules ee↔eo and oo↔oe for $K''_{-1}, K''_1 \leftrightarrow K'_{-1}, K'_1$ This spectrum shows a characteristic P, Q, and R branch Moreover, the density of lines is less than in the perpendicular bands, so the identification of the spectrum is much simplified As a starting point for the assignment, we used estimated rotational constants, derived from the crystal structure We assigned a total of 160 lines in an 8 GHz region around the band origin and fitted them to the asymmetric rotor model Even part of the Q branch was resolved and could be included in the fit All parameters were varied simultaneously and this fit also proved very satisfactory with a standard deviation of 4 0 MHz All data could be fitted within experimental accuracy The rotational constants derived conformed to the 0–0 transition within statistical uncertainty The values listed in Table II stem from combined data of both spectra

For the parallel-type spectrum, we observed a number of single rotational transitions which allowed us to determine the rotational temperature of molecules in the beam The intensity of separate rovibronic lines is given by

$$I = I_0(2J + 1)g_n A(J'', K''_{-1}, K''_1)$$
$$\times \exp\left[-\frac{E(J'', K''_{-1}, K''_1)}{kT_{rot}} \right] \quad (1)$$

Herein, I_0 is a constant and $E(J'', K''_{-1}, K''_1)$ the rotational energy of the ground state level As T is a near prolate asymmetric top $A(J'', K''_{-1}, K''_1)$ can be approximated by the Honl–London factors for the limiting case of a symmetric top molecule The factor g_n is the statistical weight of the nuclear spin, determined by the number of allowed spin configurations The T molecule can be characterized by D_{2h} molecular symmetry It contains three groups of four equivalent hydrogen nuclear spins each The value for g_n is 1072 for $(K''_{-1}, K''_1) = (e,e)$ and 1008 in all other cases The statistical weights are very close for the different rotational symmetries because of the large number of hydrogen atoms in the molecule Such a small difference is below our detection limit and can be neglected Relative intensities from the 471 cm^{-1} parallel band were fitted to Eq (1) The spectrum was taken at a typical backing pressure of 2 bar, using argon
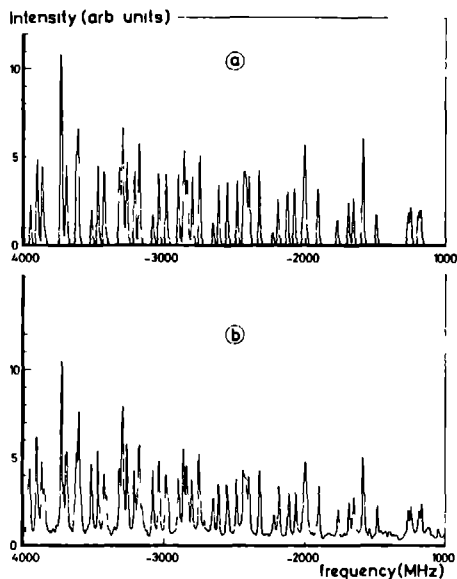
Intensity (arb units)

(a)

4000   -3000   -2000   1000

(b)

4000   -3000   -2000   1000
frequency(MHz)

FIG 3 Part of the P branch of the 471 cm   parallel band of tetracene around ι , $- 22\ 867\ 62(2)$ cm $^{-1}$ The experimental (b) as well as the calculated (a) spectrum is reproduced

for a seeding gas A single rotational temperature T_{rot} = 2 3(3) K could be assigned

By simulation of the spectra using Eq (1) and the constants derived (Figs 2 and 3) it appeared that there were no strong unidentified spectral features in either the parallel or the perpendicular bands The lack of significant inertia defect and distortion effects, indicates the planar rigid structure of this molecule in the ground state, as well as the lower vibrational modes of the S_1 electronic state The vibrational states of T considered in this work all showed clear unperturbed rotational spectra Similar data in the low energy regime of benzene[1] and naphthalene[6] also show that these molecules exhibit no observable centrifugal distortion and have a small inertial defect in the ground state as well as the first excited electronic state At higher vibrational energy, the rotational spectra experience perturbations from e g , Coriolis couplings between vibrational states[21] or Fermi resonances For the anthracene molecule, no rotational resolved spectra are available Rotational contour analysis[1] tend to the conclusion that, in the low energy regime, perturbations are not very large These spectra of aromatic molecules are thus different from those of e g , azabenzenes as pyrazine,[8] pyrimidine,[22] and triazine,[23] which show perturbations due to intramolecular couplings, also at low vibrational modes

The linewidth in the spectra does not exceed the residual Doppler width in the spectrometer The experimental error in the intensities is at least 5% and shows no significant deviation from the expected values according to Eq (1) As can be seen from Figs 2 and 3, we observed a significant back-

ground in the spectra of T in the order of 20% of the intensity of single lines This constant level cannot be caused by laser stray light, because the molecular beam was chopped and phase sensitive detection was applied Such a background was absent in earlier measurements on the IO radical[12] where the same apparatus was used and is apparently not due to some machine effect The overlap of spectral lines is limited certainly in the parallel band, and thus cannot account for the background signal As possible explanations for this signal, we will discuss the contribution from isotopic species and interstate couplings

The natural abundance of the ^{13}C isotope is about 1% Since there are 18 carbon atoms in tetracene about 19% of the T molecules will contain one or more ^{13}C atom Not all carbon atoms are at equivalent positions and consequently not all isotope bands will coincide Nevertheless, we did not observe separate transitions due to isotropic species of T The many different isotopic species might give rise to an almost constant background in the spectra due to overlap of lines The intensity of this level depends on the size of the relative shift of the different isotope bands and is hard to estimate However, the contributions from isotopic species might in part explain the background

Although we assign a "clean" rotational spectrum in T, in contrast to observations in pyrazine[8] and pyrimidine,[22] it is not excluded that weak couplings between the S_1 state and other states in the molecule give rise to the observed background signal Our observations in azabenzenes justify the assumption that a sizable fraction of the rotational lines in T is accompanied by weak satellite transitions due to either intersystem crossings, i e , singlet–triplet interactions, or internal conversion, S_1–S couplings Because of the very high density of rotational lines in T, we might expect a complete overlap of these weak transitions, resulting in a smooth background This speculation is supported by the experimental results on the tetracene–noble gas complexes presented in the next section In that case, the spectra indicate a strong increase in coupling between the S_1 and other states in conjuction with a strong increase of the smooth background signal

IV. TETRACENE–RARE GAS VAN DER WAALS COMPLEXES

A. Formation and identification

We studied T–R_n (R = Ar,Kr,Xe, n = 1,2) vdW complexes in the molecular beam under rotational resolution These complexes are effectively formed in the expansion of T with the rare gas The production of T–He$_n$ and T Ne$_n$ complexes in this way proved unsuccessful Even at the maximum backing pressure of 4 bar the cooling in the expansion was insufficient At this pressure, the cooling with neon is much better than with helium as carrier gas Amirav et al[11] claimed the observation of the weak 0–0 band of the T–Ne complex, using a high backing pressure This band is shifted $- 5$ cm^{-1} with respect to the 0–0 transition in T Due to the vibrational congestion in our spectra, we were unable to probe this region under rotational resolution Mixtures of a small amount of helium or neon in argon improved the cooling conditions but were too inefficient in formation of the T–
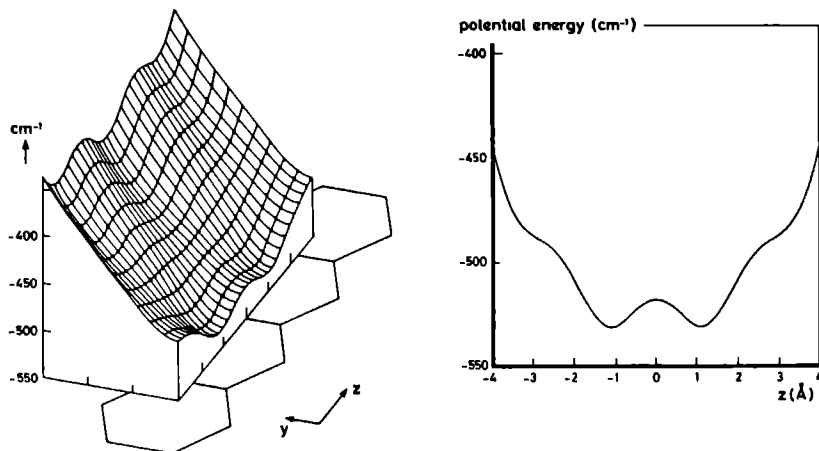
FIG 4 Calculated energy surface of the tetracene–argon interaction   The skeleton of the tetracene molecule is shown on the same scale and with the same orientation as used for the surface   The potential along the z axis at $y = 0$ clearly shows a double well structure

He or T–Ne vdW complexes   On the basis of former experience[7] we expect the rotational temperature of the T–R_n complexes in the argon beam to be comparable to that of the host molecule   Internal heating in complex formation is effectively cooled in the molecular expansion using argon, krypton, or xenon

The vibrational assignment of various T–R_n transitions has been reported by Amirav et al[11]   The accuracy in their absolute frequencies is limited[14 15] by nonlinearity in the scans   We studied transitions in the T–R_n complexes corresponding to the transitions in the T molecule mentioned before (i e , the 0–0 vibrationless, 311 and 471 cm^{-1} vibrational transitions)   In Fig 1, a low resolution spectrum is depicted of T expanded in argon at a backing pressure of 4 bar   The various bands are well separated   Transitions in the various complexes are more or less regularly shifted with respect to corresponding bands in the parent molecule   The vibrational excitations of the T–R_n molecules are very close but not identical to those of T, indicating that the vibrational mode of the complex is based in large part upon the vibration of the T host molecule   The spectra are red shifted with respect to the analogous transitions in the parent molecule   There is no spectral overlap between the various transitions of T and the different complexes in the regime of low vibrational energy   For the T–Kr_n and T–Xe_n complexes, we observed spectra similar to that of Fig 1 but with some extra weak spectral features which were assigned as vdW vibrational modes of the complexes   This structure is well resolved but of such low intensity that it was not further explored

B. Theoretical considerations

Model calculations of T–R_n complexes have been performed by Ondrechen et al[10]   A Lennard-Jones 6-12 potential was used with pairwise interactions between the R atom and atoms in the T molecule   Higher order terms and three-body interactions were neglected   We repeated the model calculations with a slight modification but extended the calculated area of the potential surface over the entire molecule   The main goal was to thoroughly examine the possible existence of chemical isomers   Although these calculations provide only a rough indication of the geometry of the complexes, we found similar calculations very satisfactory for the fluorene–argon vdW complex[7]   In Fig 4, part of the T–Ar potential surface is shown   We used for the interaction energy

$$V_{\text{T R}} = - \sum_{\alpha} \frac{A_{R\alpha}}{r_{R\alpha}^6}\left(1 - \frac{r_0^6}{r_{R\alpha}^6}\right), \qquad (2)$$

where the coefficients $A_{R\alpha}$ and r_0 are obtained from Ref 10   The summation is over all atoms in the T host molecule at a distance $r_{R\alpha}$ of the rare gas atom   We varied the distance of the R atom to the molecular plane for minimum energy   This modification to Ref 10 was certainly necessary in the case of nonplanar molecules like fluorene although it does not affect the results for T very much   A favorable position of a single R atom is predicted above the T molecular plane, near the center of an inner ring of the molecule   The calculated distance between the inert gas atom and the molecular plane is 3 43, 3 50, and 3 72 Å for argon, krypton, and xenon, respectively   In spite of the simplicity of the model, the calculations rule out the existence of any other configuration of the T–R complex   The unique equilibrium structure of the complexes in principal can be determined from rotationally resolved spectra of the T–R complex and the T parent molecule   This provides direct information on the potential surface

The T–R theoretical potential surface has a kind of double well shape along the long molecular axis, which becomes more pronounced for smaller noble gas atoms   Depending
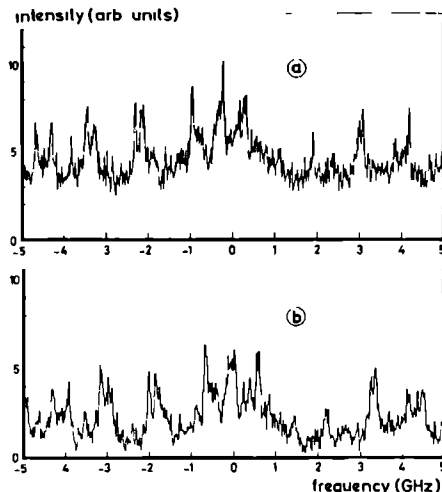
47

intensity (arb units)

intensity (arb units) —

FIG 6 Part of the *P* branch of the 471 cm⁻¹ parallel band of the tetracene–argon vdW complex The onset of the *Q* branch is at the right hand side of the figure

FIG 5 Comparison between the 0–0 (b) and 311 cm⁻¹ (a) rovibronic bands of the tetracene–argon vdW complex

on the height of the barrier (estimated 14 cm⁻¹ for T–Ar), this will give rise to tunneling splitting, resulting in doubling of the rotational spectra Calculations of such vdW vibrational modes have been reported for the pentacene R complexes [24] As is clear from Fig 4, the potential surface is rather flat along the long molecular axis A large amplitude motion of the R atom along this axis might thus be possible Let us consider such a large amplitude motion (contortion) [25] of the R atom along the T long molecular axis If the separation of this motion and rotation is assumed, the zero-order roconvibronic wave functions are of the form

$$\Phi_{\text{reve}} = \Phi_{\text{rot}} \Phi_{\text{con}} \Phi_{\text{vib}} \Phi_{\text{el}} \qquad (3)$$

We describe the T R complex by C_{2v} symmetry and assume that the symmetries of the wave functions of the T parent molecule are more or less conserved in the T–R complex It then follows that allowed electronic–contortional transitions are determined by the condition for the irreducible representations

$$\Gamma(\Phi'_{\text{con}} \Phi'_{\text{el}}) \otimes [\Gamma(\Phi''_{\text{con}} \Phi''_{\text{el}})] \supset \Gamma(\mu_a), \qquad (4)$$

where μ_a is a molecule fixed component of the dipole moment This μ_a can be expanded in the vibrational normal coordinates For allowed electronic transitions, the first term in this expansion is the leading term The contortional wave functions can be symmetric (s) or antisymmetric (a) with respect to reflection in a plane through the short molecular axis of T so they can be of a_1 or b_2 symmetry For the selection rules of the contortional transitions follows s↔s, a↔a, s↔a So if the approximations made are valid, we may expect a spectrum with two rotational bands The distance between these bands is determined by the difference between contortional splittings in the ground and excited vibronic levels
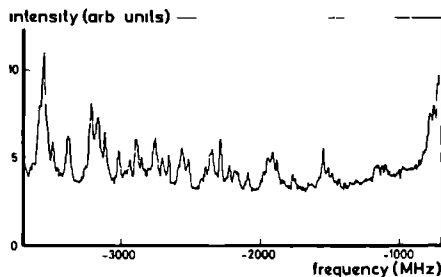
C. The T–Ar vdW complex

The 0–0 and 311 cm⁻¹ vibronic transitions in T both involve an a_g-type totally symmetric vibration in the S_1 electronic state For the T parent molecule, the rotational bands proved to be identical In the T–Ar vdW complex, again both states behave in the same way The rotation-free transition frequencies are almost equally shifted (Table I) and the rotational band contours are nearly the same This strongly suports the identification of the bands The spectra show a characteristic perpendicular shape with pronounced *Q* branches (Fig 5) It should be noted that this structure seems to be on a broad background Such background was also found in the T molecule (Sec III), but it looks larger in the T–Ar complex Comparing the details of both transitions, it appears that small differences do exist Because of the high density of states no single spectral lines are observed and it is difficult to estimate the exact linewidth We assume that it is still Doppler limited The 471 cm⁻¹ nontotally symmetric b_{1g} vibrational mode of T gave rise to a weak parallel band The corresponding transition in the T–Ar complex (Fig 6) is shifted − 41 52(5) cm⁻¹ but still has a clear parallel (*a* type) shape As the transition dipole moment conserves its orientation with respect to the parent molecule, we may conclude that the orientation of the *a* axis in the parent molecule and the complex is very much alike This is in agreement with rotational constants derived from the model calculations The observed spectral linewidth in the band is 15 MHz and thus still due to the experimental limitations The expected natural linewidth on basis of lifetime measurements [11] is about 8 MHz

All these rotational bands were single vibronic transitions We did not find any evidence for a splitting of the vibrational states due to a potential barrier for movements along the long molecular axis It is thus concluded that such barriers must either be small or the splittings in ground and excited vibronic states must be almost identical It seems very unlikely that these equal splitting are the case for all three vibrational modes that have been studied

Unfortunately, we did not succeed in assigning the rotational spectra of the T–Ar vdW complex As this molecule has very small rotational constants, the spectra are extremely dense, even at a 15 MHz linewidth and a rotational tem-
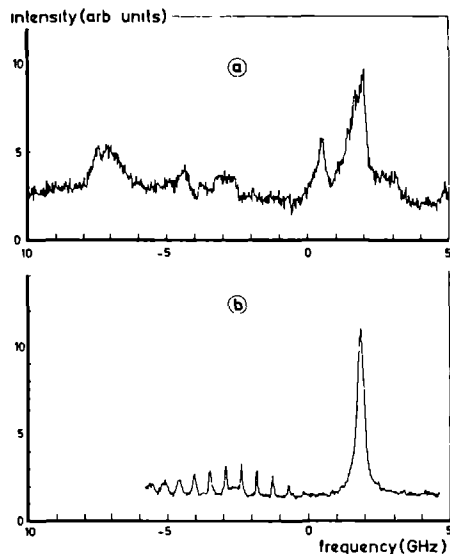
FIG 7 Comparison between the 0–0 (b) and 311 cm⁻¹ (a) rovibronic bands of the tetracene krypton vdW complex

perature of less than 3 K Only in the case of the parallel band a limited number of single rotational lines was observed (Fig 6) On the basis of the experimental resolution it should be possible to resolve and assign the rotational bands of a molecule as large as the T–Ar complex Despite much effort such an assignment could not be found For example, the clear sequence of Q branches in the perpendicular bands looks distorted In the parallel band there seems to be an excess of lines which is most clearly demonstrated by a rather broad Q branch Although there is no incontestable proof, we are convinced that this appearance of extra lines is due to perturbations in the rotational spectra for the following reasons It is very unlikely that the unexpectedly high spectral density is caused by a large asymmetry of the complex On basis of the calculated geometry we expect an asymmetry parameter $\kappa = -0.97$ This is comparable with the value for the parent molecule ($\kappa = -0.966$) Both molecules are thus near prolate rotors Geometrical changes in the complex structure hardly affect the asymmetry We consider the calculated potential surface to be sufficiently reliable to rule out large deviations from the determined geometry A change of geometry upon excitation might complicate the assignment of the spectrum However, since the number of rotational states does not change, the number of rotational transitions should not be affected A clear indication for the existence of a surplus of transitions in the T–Ar bands is given by the spectra of the T–Kr and T–Xe complexes were the effects are much more evident

The parallel band (Fig 6) of the T–Ar complex shows a structureless background signal This background level is significantly stronger than observed in the parent molecule

For the perpendicular bands, the spectra are too dense to draw an unambiguous conclusion From comparison of both spectra (Fig 5) it is clear that there exists a difference in background level and that it is much higher for the 311 cm⁻¹ band The isotope effect of the carbon atoms, mentioned in Sec III, is too small to account for the entire level in the 311 and 471 cm⁻¹ bands Another contribution may arise from a weak combination band The transition dipole moment for the parallel band in the parent molecule is along the a axis, which is slightly rotated in the complex Consequently the dipole moment has a component perpendicular to the a axis, which allows a weak perpendicular band The transition dipole moment for the 311 cm⁻¹ band, however, is along the b axis The orientation of this axis in the complex is the same as in the parent molecule and so this will not give rise to hybrid bands However, a substantial background is observed It is felt that only the combination of transitions in isotopic species and combination bands cannot fully account for the observed backgrounds The remaining part must be ascribed to a strong S_1 background state interaction The nature of this effect has been discussed for T in Sec III Due to the increase in interstate coupling in the complex, as concluded from the spectroscopy, an increase in background signal might also be expected As a speculative suggestion, we would also like to mention two other possible sources of the broad structureless background (i) hot bands in the spectra of the complexes and/or (ii) effects of predissociation There are, however, no clear indications in this direction and we will not further discuss them

D. The T–Kr vdW complex

The observed red shift of the T–Kr vibronic transitions with respect to the T parent molecule is much larger than for the T–Ar complex as can be seen from Table I The influence of the krypton atom on the vibrational levels in the ground and excited state of T is thus different from the influence of an argon atom An indication of some large effects is also given by a shortening of the fluorescent lifetime of the complex to 7 ns[11], and a reduction of the excitation intensity The rotational spectra of the T–Kr complex also clearly display the existence of strong perturbations in the excited electronic state

The 0–0 transition and the transition related to the 311 cm⁻¹ vibration in T have hardly any resemblance, as may be seen from Fig 7 The 0–0 spectrum extends over a broad region of more than 100 GHz and suggests the presence of two transitions There is a pronounced Q-like branch, typical for a parallel band, and at a distance of about 4 GHz, a number of smaller Q branches, characteristic for a perpendicular transition Individual spectral lines are no longer observed The 311 cm⁻¹ vibronic transition shows an unrecognizable structure of some broad shallow patterns The 471 cm⁻¹ vibration involves a symmetry forbidden transition in T In the T–Kr complex, the excitation intensity is further decreased and the spectrum becomes very weak It consists of a small hump on a broad background, without any further structure

In none of the studied transitions in T–Kr we observed individual spectral lines The expected linewidth on basis of

the measured lifetime is about 25 MHz and exceeds the residual Doppler width Therefore the line profile will become almost Lorentzian with tails which extend some way from the region of the peak Combined with the high density of states, this causes spectral overlap

The krypton atom in its natural occurrence is mainly found in four isotopes, with a relative abundance of about 12%, 12%, 57%, and 17% for ^{83}Kr, ^{84}Kr ^{83}Kr, and ^{86}Kr, respectively Of course this slightly affects the rotational spectra and gives rise to a smeared out structure The observed large effects though of the T–Kr spectra will be affected, but certainly not caused by the existence of the various isotopes

Assuming the 0–0 vibronic transition consists of two rotational bands, the question arises if this could be caused by a contortional motion However, this is very unlikely for the following three reasons First, the model calculations show that the potential barrier for krypton should be smaller than for argon and no effects were found for the T–Ar complex Second, if coupling to the vibration is neglected, the rotational transitions to both contortional states should exist of the same type i e both spectra should be either parallel or perpendicular bands Third, no evidence was found for a similar splitting in the 311, and 471 cm⁻¹ T–Kr spectra, which involve low vibrational modes of the T parent molecule On basis of model calculations mentioned before, we may rule out the existence of chemical isomers Also, the possibility of a vdW vibrational mode causing an additional band, is rejected The splitting between the two bands is too small for such a vibrational energy

It is remarkable that, in spite of the differences in degree of perturbations in the rotational spectra, the redshift with respect to the T parent molecule is almost equal (Table I) for the different vibronic transitions The relative increase in constant background in the I–Kr spectra should be noted The increasing perturbation with excited state energy and the large linewidth point in the direction of a coupling of the S_1 electronic state with one or more other states

E The T–Xe vdW complex

The 0–0 rovibronic band of the T–Xe complex experiences the largest red shift [110 0(1) cm⁻¹] of all studied T–R molecules It shows even less structure than the T–Kr spectra Now there also exists a broad (> 100 GHz) background with only some small humps as structure in a 30 GHz region No traces of individual lines have been observed so the natural linewidth in the spectrum must be of considerable size The decay lifetime has been estimated[11] to be 1 5 ns, corresponding to a linewidth of 100 MHz It should be noted also that the abundant quantity of isotopic species present in a natural amount of xenon will obscure the spectrum

The 0–0 band is quite weak, suggesting that the decay of the excited state is mainly of nonradiative character We did not study other even weaker, T–Xe rovibronic bands The observed spectrum supports our conclusion about the existence of a coupling between the S_1 electronic state and dark background states in the complex It is clear that this interaction is enhanced for heavier rare gases

F. T–R₂ vdW complexes

As can be seen from Table I, a number of transitions of the T–R₂(R = Ar, Kr) vdW complexes have been studied The shift of these rotational bands with respect to the corresponding transition in the host molecule is close but not equal to twice the shift of a T–R complex From this the conclusion, it may be drawn that the second R atom occupies a position on the surface of the host molecule, which is geometrically inequivalent with the position of the first atom From model calculations,[10] it is found that in the most favorable case, both R atoms are on the same side of the T molecular plane The benefit of this geometry arises from the R–R interaction

All transitions in the T–R₂ complex, mentioned in Table I, qualitatively behave in the same way They show no individual lines, due to a large linewidth[11] The spectra have hardly any structure and merely consist of a broad flat band There are no indications that the spectra consist of a multiple of bands, due to, for example, chemical isomers

V. CONCLUSION

It was shown that rotationally resolved spectra can be obtained from large organic molecules like tetracene and even its vdW complexes We considerably improved the accuracy of several vibronic transitions in the host molecule as well as the T–R$_n$ complexes Rotational spectra of T have been assigned and molecular constants of the free molecule were obtained The rigid planar structure of the parent molecule was deduced It was also shown that there are no clear perturbations in the rotational spectra of the lower vibrational modes in the S_1 electronic state

The spectral data of the T–R$_n$ ($n = 1$ 2) complexes confirm lifetime measurements No clear effects of tunneling splittings were observed Perturbations in the excited electronic singlet state are demonstrated These effects are very small in the T–Ar molecule, more pronounced in T–Kr, and very large in T–Xe and T–R₂ complexes It was observed that these perturbations increase with excited state energy, with the size of the complex, and with the mass of the inert gas atoms It may then be connected to e g , the different polarizabilities of these atoms The spectral perturbations may be induced by S–T intersystem crossings, S_1–S_0 state mixing, or even by a coupling of the S_1 state with higher energy levels The presence of such interaction is clearly demonstrated by the 471 cm⁻¹ a-type transition This band is symmetry forbidden but becomes allowed by coupling with the S_2 ($^1B_{1u}$) state As the anomalous effects occur for different vibrational levels, Fermi resonances will not be its cause Testing of available model calculations on the complex structure was not possible due to a lack of complete assignment of the rotational bands However, the existence of chemical isomers for these small complexes is shown to be very unlikely

A significant background level in the spectra of T as well as T–R$_n$ molecules was observed Part of this background can be attributed to isotopic species and hybrid bands However, it is felt that there is strong evidence to ascribe a certain fraction of the background signals in the spectra to the above discussed interaction between the S_1 and other states

50

ACKNOWLEDGMENTS

[1] F Riedle, H J Neusser, and E W Schlag, J Chem Phys 75, 4231 (1981)

[2] S M Beck, M G Liverman, D L Monts and R E Smalley, J Chem Phys 70 232 (1979)

[3] B W Keelan and A Zewail, J Chem Phys 82, 3011 (1985)

[4] A Amirav, U Even, and J Jortner, J Chem, Phys 75, 3770 (1981)

[5] A Amirav, U Even, and J Jortner Chem Phys Lett 72, 21 (1980)

[6] W Majewski and W L Meerts, J Mol Spectrosc 104, 271 (1981)

[7] W L Meerts, W A Majewski and W M van Herpen, Can J Phys 62, 1293 (1984)

[8] B J van der Meer, H T Jonkman J Kommandeur, W L Meerts, and W A Majewski, Chem Phys Lett 92, 565 (1982)

[9] W M van Herpen, W L Meerts, and A Dymanus, Laser Chem 6, 37 (1986)

[10] M J Ondrechen, Z Berkovitch-Yellin, and J Jortner, J Am Chem Soc 103, 6586 (1981)

[11] A Amirav, U Even, and J Jortner, J Chem Phys 75, 2489 (1981)

[12] J P Bekooy, W L Meerts, and A Dymanus, J Mol Spectrosc 102, 320 (1983)

[13] U Even, A Amirav, S Leutwyler, M J Ondrechen, Z Berkovitch-Yellin, and J Jortner, Faraday Discuss Chem Soc 73, 153 (1982)

[14] I Raitt, A M Griffiths, and P A Freedman, Chem Phys Lett 80, 225 (1981)

[15] A Amirav and J Jortner, Chem Phys 85, 19 (1984)

[16] J K G Watson J Chem Phys 46, 1935 (1967)

[17] J K G Watson, J Chem Phys 48, 4517 (1968)

[18] T Torring J P Bekooy, W L Meerts, J Hoeft, E Tieman, and A Dymanus, J Chem Phys 73, 4875 (1980)

[19] J Monteath Robertson, V C Sinclair, and J Trotter, Acta Crystallogr 14, 697 (1961)

[20] R B Campbell and J M Robertson, Acta Crystallogr 15, 289 (1962)

[21] E Riedle, H J Neusser, and E W Schlag, J Phys Chem 86, 4847 (1982)

[22] W L Meerts and W A Majewski, Laser Chem 5, 339 (1986)

[23] H Saigusa and E Lim, J Chem Phys 78, 91 (1983)

[24] S Leutwyler and A Schmelzer, J Chem Phys 79, 4385 (1983)

[25] P R Bunker, *Molecular Symmetry and Spectroscopy* (Academic, New York, 1979), pp 344–351

51

A SPECTROSCOPIC STUDY OF TRANS-STILBENE AND
ITS VAN DER WAALS COMPLEX WITH ARGON
IN A SUPERSONIC MOLECULAR BEAM

1. INTRODUCTION

The dynamics and spectroscopy of trans-stilbene (1,2-diphenylethylene, fig. 1) has been an issue in recent years in the context of the trans-cis isomerization mechanism in the first excited singlet state of this molecule. The photoisomerization involves a reaction coordinate which is close to a well defined spatial coordinate: the rotation about the ethylenic double bond. Therefore such substituted ethylenes like trans-stilbene (tS) are especially interesting and tS has become one of the prototype molecules in studies concerning photoisomerization. The reaction is induced by vibronic excitation, followed by an intramolecular vibrational redistribution (IVR) of the energy, among others, to reactive modes. One of the subjects of interest in the dynamics of photoisomerization is the question of vibrational mode selectivity in this proces. During the past years, tS has been studied extensively. Most studies were carried out in solid phase or in solution [1,2,3]. Both, infrared and Raman studies were reported [4,5,6]. It was concluded that in the ground electronic state tS is planar if imbedded in a crystal [6], but in solution or vapor phase the molecule may be distorted by a twist of the phenyl groups (ϕ) [4]. It was shown from a gas diffraction study that the molecule is probably non-planar and that the phenyl groups are rotated by approximately 30° about the C-ϕ bonds [7]. A more precise experimental determination of the ground state structure of the isolated tS molecule may be accomplished from rotational resolved spectroscopy of the free molecule. Such attempt is described in this work.

Most attention has been attributed to the first excited singlet electronic state. If rotation about the ethylenic bond over an angle θ is considered, different minima in the potential energy are present as a function of θ [8]. The potential energy is expected to depict minima at the trans- $(\theta=0°)$, the cis- $(\theta=180°)$ and also at a perpendicular $(\theta=90°)$ geometry, where the latter forms the absolute minimum. Calculations of the vibronic
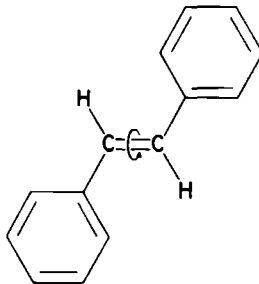
FIG. 1. The molecular frame of the trans-stilbene molecule.

structure of trans- and cis-stilbene were carried out by Warshel [9]. Recently detailed experimental data has become available of the vibronic structure of tS from molecular jet studies [10,11,12] and very low vibrational modes were demonstrated. Time-resolved measurements indicate that the lifetime of the excited vibronic states is nearly constant at a value of 2.7 ns [13,14] for vibrational energies below 1000 cm^{-1}. Above this energy the lifetime decreases, marking the onset of a nonradiative decay channel. The quantum yield in the regime of low vibrational energy is near unity [10,15,16] and consequently there is no significant S_1-T_1 intersystem crossing. No mode selectivity was found in this region and it is concluded that vibrational relaxation within the trans-geometry is much faster than isomerization to the perpendicular configuration.

A special subject of interest is the formation of van der Waals (vdW) complexes of stilbene. Under jet expansion conditions the cooling of internal energy of tS is sufficient to form a high density of vdW complexes of stilbene with carrier gas atoms, mostly argon or helium. Such complexes have been reported recently with vibronic resolution [10,17]. In the study of the tS photoisomerization process, spectroscopy at rotational resolution may provide important information regarding the molecular structure in the ground electronic state as well as different vibrational levels in the excited state. A study of the vdW complexes may form a severe test for models presented in the study of the tS parent molecule since complexation will affect the isomerization process.

No spectroscopy at rotational resolution of tS has been reported so far. From band contour studies [18] it was concluded that there are no evident structure changes between various excited state vibrations, including torsional motions. Recently Felker *et al.* [19] reported a time-resolved polarization technique to study the rotational constants and geometries of large molecules. This technique was applied to tS and rotational constants were derived [20]. In the present work we report on the direct observation of rotational resolved spectra of tS. They form a direct test of the time-domain data and give insight

in the molecular geometry and dynamics of this molecule. Also rovibronic spectra of tS-argon vdW complexes were observed. Approximate rotational constants were derived and an assignment is proposed, different from the one given in ref. [10].

2. EXPERIMENTAL SETUP

The spectrometer is described in chapter 2 and we will only briefly discuss some points specific for the experiments on tS. High resolution spectra of rovibronic transitions were obtained by detection of laser induced fluorescence (LIF) emerging from a molecular beam. An expansion was made of tS vapor and argon carrier gas in vacuum through a 100 μm nozzle. A quartz source was used where a supply of tS (Merck) was heated to 140 °C to raise its vapor pressure. Argon was added to a total pressure in the range 0.25-1 bar. Two skimmers with a 2 mm diameter in a differential pumping system collimated the molecular beam. The molecular beam was chopped and phase sensitive detection was applied at a 0.2 s time constant to suppress stray light. The typical output power of the uv laser was 0.7 mW with a bandwidth below 1 MHz. The combination of laser, collection optics, seeding gas and collimation of the molecular beam allows observation of spectral lines with a residual Doppler width of 12 MHz. However, this value is exceeded by the natural linewidth of tS, which amounts to 70 MHz for the O_0^0 electronic band. For absolute frequency measurements the reference absorption spectrum of an iodine vapor cell was used [21]. The spectrometer is interfaced with a microcomputer and all relevant spectral data is stored. This provides a high dynamic range in the spectra and in processing the data a linear frequency scale is obtained.

3. RESULTS AND DISCUSSION

A. Trans-stilbene

As was mentioned above, the structure of tS differs for different phases. If the molecule is planar, it may be described by C_{2h} symmetry but if the phenyl groups are rotated out of plane in opposite senses [7] C_2 symmetry has to be adopted. Most convenient is to use C_{2h} symmetry, since results can be easily converted to C_2 symmetry by dropping subscripts u and g for the various irreducible representations. An axis system is chosen

54

such that the z-axis is the out of plane axis and the x-axis is parallel to the long in plane axis. The electronic transition $S_1(B_u) \leftarrow S_0(A_g)$ is induced by a transition dipole moment along the long molecular axis [22,23] and is dipole allowed. The moments of inertia depend on the orientation of the phenyl groups but it is clear that tS is a near prolate symmetric top molecule with the principal axis identified as (x,y,z)-(a,b,c), respectively. Vibronic transitions in this molecular beam study start from the ground vibrational state due to the effective vibrational cooling in the expansion. Therefore allowed vibronic transitions will end in an a_g vibrational mode, but if C_2 symmetry is adopted also modes with a_u symmetry become allowed. The spectral intensities within a rotational band are affected by different nuclear spin statistical weights of the initial levels. In tS there are six pairs of equivalent hydrogen nuclear spins. Due to the large number of spin states, the statistical weights are almost equal for the different irreducible representations and may be neglected in the purpose of this work.

We studied five vibronic transitions of tS with rotational resolution. The expansion conditions were varied to study the effects of rotational and vibrational cooling. At a backing pressure of 1 bar vibrational relaxation is complete since no traces of hot bands were observed and we are convinced that all studied transitions start from the vibrational ground state level. From comparison with former experiments with similar molecules and expansion conditions [24,25] we expect a rotational temperature near 2.5 K for molecules in the beam. In figure 2 the O_0^0 vibrationless spectrum is depicted. The band extends over a broad region of about 60 GHz and displays a dense spectrum, even at this low rotational temperature. The observed linewidth is 70 MHz in agreement with lifetime measurements of the excited state [13,14]. With the origin of the band chosen as in fig. 2, different regions can be distinguished within the spectrum. Near the origin a sharp structure with a sudden frequency step is identified as a Q-branch. On the left and right of this branch a dense manifold of lines form the accompanying P- and R-branches. The transition shows the characteristics of a parallel band, in agreement with the transition dipole moment along the a-axis. However, an other peculiar spectral structure is present at the low frequency side of this band. An unexpected, relatively weak but clear sequence of groups of lines is observed. Before turning to a more precise analysis of the band, the question arises if this is not an accidental disturbance in the spectrum for this particular transition, (for example due to a hot band).

We observed however, that other observed rovibronic bands exhibit an almost identical structure. As an example in fig. 3 the 198 cm[1] band is shown. Table 1 lists the transition frequencies of the studied bands. The assignment is according to ref [11].
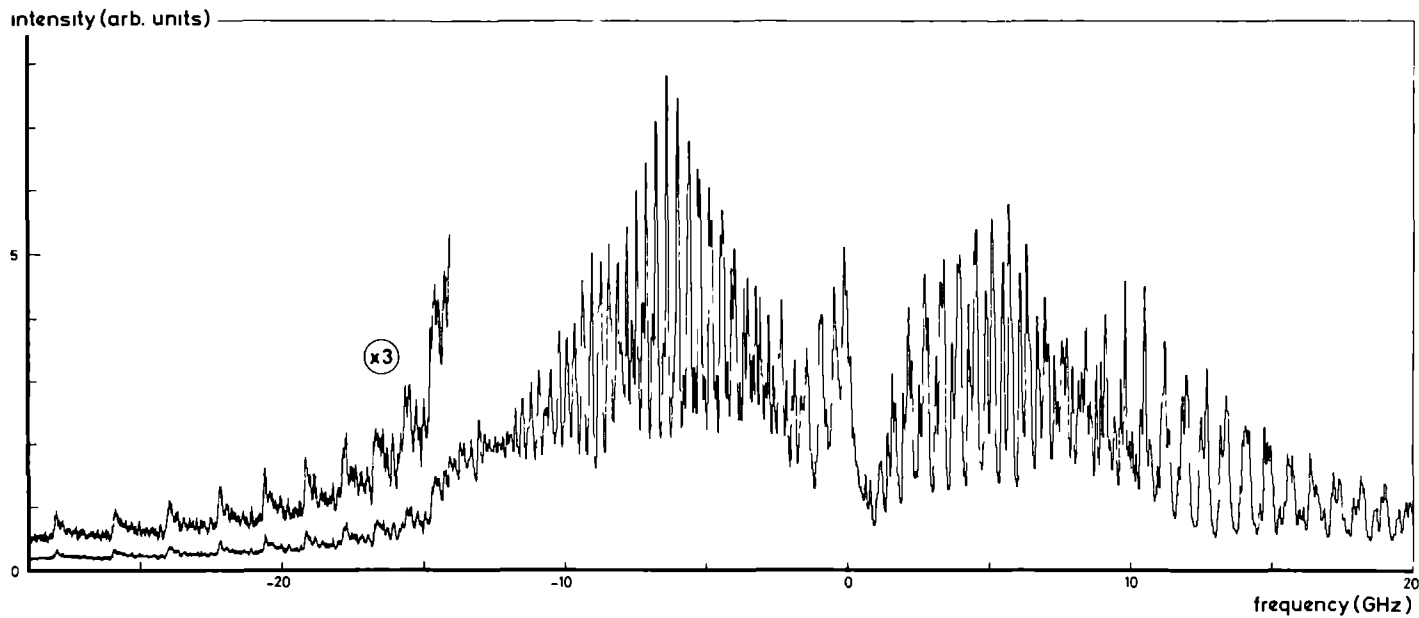
FIG. 2. The O_0^0 vibrationless transition of trans-stilbene. The origin of the band is at $32234.06(5)$ cm^{-1} is chosen at the centre of the transition.
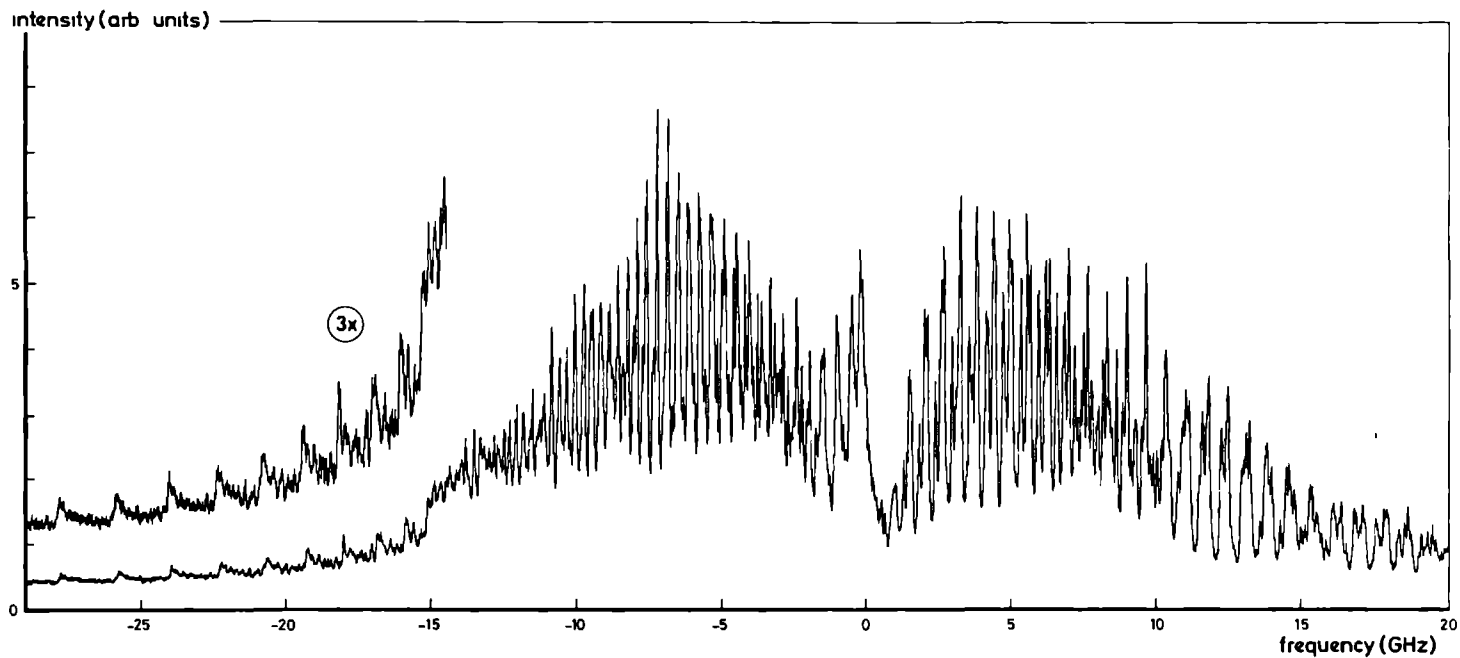
FIG. 3. The 25_0^1 rovibronic band of trans-stilbene. This transition is shifted 197.92(5) cm^{-1} with respect to the electronic origin.

TABLE 1. Observed transition frequencies (cm^{-1}) of rovibronic bands of trans-stilbene and the stilbene-argon van der Waals complex.

	$\nu-\nu_0$	assignment [a]
tS	0 [b]	0
	82.21(5)	36^1_0
	95.15(5)	37^1_0
	197.92(5)	25^1_0
	788.14(5)	25^4_0
	1247.10(10)	13^1_0
	1330.89(10)	12^1_0
	1451.54(10)	$12^1_0 + 25^1_0$
S-Ar	-40.04(5)	
	-63.07(5)	

The accuracy is determined by the lack of a complete rotational assignment.

a) The vibrational assignments are according to ref. [11].

b) The absolute transition frequency of the electronic origin is determined as 32234.06(5) cm^{-1}.

The low frequency vibrations at 82 and 95 cm^{-1} are assigned as torsional motions about the ethylenic bond. The ν_{25} mode involves an in-plane vibration at 198 cm^{-1}. The assignment of the 788 cm^{-1} is uncertain. It may be attributed to the 25^4_0 mode but also a combination band of a 591 cm^{-1} fundamental and ν_{25} is possible. All these bands with a vibrational energy below 1000 cm^{-1} show an almost identical structure. The sequence at the low frequency side is present in all bands and is therefore not due to an accidental occurance such as a Fermi resonance. The possibility of a hot band is also excluded. It is very unlikely that all observed vibrations display an identical vibrational splitting in the ground and excited electronic state. The observed linewidth in these transitions is 70 MHz

in accordance with the excited state lifetime [13,14]. As can be seen from figs. 2 and 3, there is a small but significant broad background in the spectra. Its relative magnitude differs slightly for the different bands and there is a tendancy that the background increases with excited state vibrational energy. A similar background was observed in the rovibronis spectra of tetracene [25] but it was absent in the spectra of fluorene [26]. In these experiments the same spectrometer was used and we conclude that apparently no machine effect is involved.

The bands at energies above 1000 cm^{-1} display a sudden increase in spectral linewidth and in relative magnitude of the background signal. The excitation intensities of these bands decreases, but it is clear that at the 1451 cm^{-1} band no individual lines are observed. The transition consists of a very broad (several wavenumbers) band without any structure. The 1247 and 1331 cm^{-1} bands display a weak contour similar to the vibronic origin, with no resolved structure, on a broad bacground. This increase in linewidth is reflected by a decrease in the excited state lifetime [11,14]. However, the lifetime for the 1451 cm^{-1} band has decreased with a factor of two with respect to the electronic origin while the increase in linewidth suggests a much faster lifetime decrease.

We concluded that in the regime of low vibrational energy the observed bands do not contain accidental spectral features. As was mentioned above, tS is an almost symmetric top prolate rotor. The rotational bands as displayed in figs. 2 and 3 do not resemble a symmetric top band. We have tried to assign the band with an asymmetric rotor model but despite much effort such assignment could not be found. The analysis of the band is hindered by the high density of lines, combined with the substantial natural linewidth. However, we feel convinced that the lack of an rotational assignment is due to a perturbation in the spectra. This perturbation is present in the entire spectrum but a clear indication is found at the low frequency side of the band. The frequency of the bandheads in the spectra of figs. 2 and 3 can be described by:

$$\nu = \nu_1 + \alpha K_0 + \beta K_0^2 \tag{1}$$

with $\nu_1 = -13.8(2)$ GHz, $\alpha = 10.(2)$ MHz, and $\beta = -86.(2)$ MHz. To understand the outlines of the observed regular sequence of groups of lines, we assume for the moment a symmetric top model. In that case the rotational energy levels are given by:

$$E_{rot} = B J(J+1) + (A-B) K^2 \tag{2}$$

59

The mentioned sequence in the spectrum can be interpreted as a sequence of Q-branches. If we consider the possibility of a parallel ($\Delta K=0$) or a perpendicular ($\Delta K=\pm 1$) band it follows that in case of a perpendicular transition the splitting of these groups of lines would be of order $2(A-B)$. For tS this value is estimated as 4.9 GHz. The observed splittings are much smaller and consequently the lines belong to the Q-branch of a parallel band. Such possible perpendicular band has to be taken in consideration since, although the transition moment is basically along the a principal axis, also a transition dipole moment along the b axis is symmetry allowed if C_2 or C_{2h} symmetry is assumed.

The appearance of combination bands, centered around the same electronic origin thus can not be excluded. If the assignment of a parallel band Q-branch is adopted, the origin of this band is calculated near -14 GHz in figs. 2 and 3. Two important conclusions may be drawn Firstly, the origin of this band is clearly different from the apparent origin of the remaining part of the spectrum. Secondly, the accompanying P-branch is missing. The R-branch could be hidden in the spectral congestion at the high frequency side of this origin.

On basis of the above analysis we conclude that the vibronic bands of tS consist of various (parallel) rotational bands with unusual selection rules. Recently Zewail and co-workers [19,20] reported a time-resolved polarization method to derive rotational constants. The technique was applied to tS, which was assumed to behave as a (near) symmetric rotor. With the derived rotational constants [20] we simulated the rotational spectrum and concluded that no agreement was found with our experimental data. This does not imply that the model presented by Zewail and co-workers lacks accuracy but it indicates that the interpretation of its experimental data has to be addressed very carefully in cases where deviations may occur from the ordinary behaviour of rotational bands.

A question remains on the origin of the spectral perturbances in tS. Since the quantum yield is near unity [10,15,16] neither significant effects of intersystem crossing with the lowest triplet state nor effects of internal conversion to high vibrational levels of the ground electronic state can be expected. Internal rotation of the phenyl groups about the C-ϕ bond will cause additional splittings of energy levels and could result in extra spectral lines. This might very well be the origin of the observed effects. However, the experimental data show no dependence on vibrational energy in the regime 0-1000 cm^{-1} while it would be expected that internal rotation will be sensitive for vibrational excitation. An extensive theoretical treatment of effects of internal motions in tS will be presented elswhere [27]. Preliminary results indicate that effects of internal rotation in the ground electronic state give rise to very small splittings of energy levels, which will not show up in the spectra.
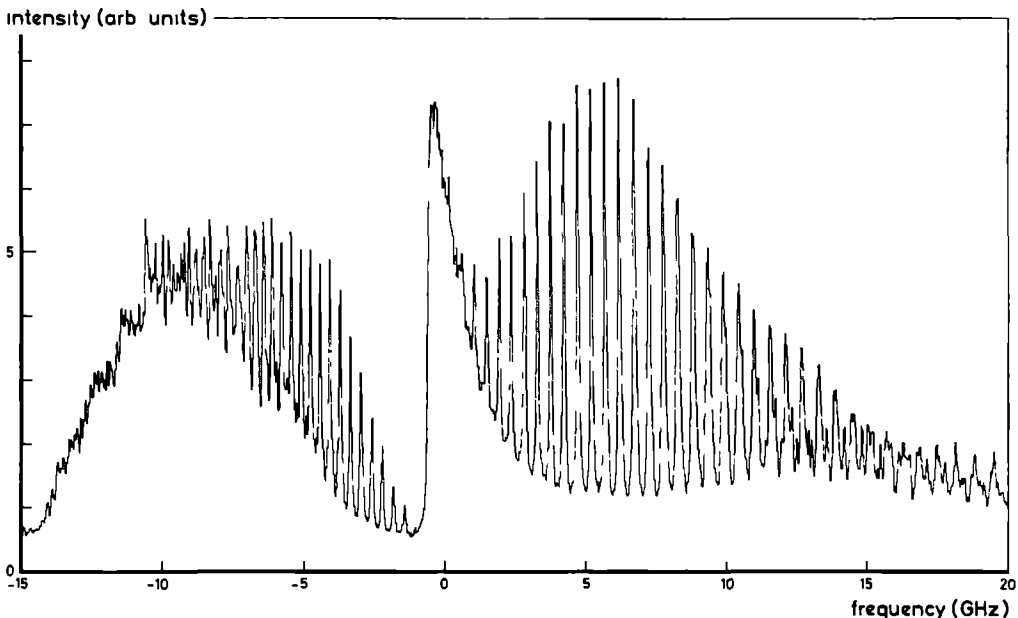
FIG. 4. The O_0^0 vibrationless transition of the stilbene-argon van der Waals complex. The origin of the band is shifted -63 07(5) cm^{-1} with respect to the electronic origin of trans-stilbene.

B. Stilbene-argon van der Waals complexes

The cooling of internal energy in the molecular beam expansion allows the effective formation of vdW complexes of stilbene with the carrier gas. Such complexes have been observed [10,17] with helium and argon under vibrational resolution. The origin of bands of S-R (R=He,Ar, n=1,2,..) is red-shifted with respect to the frequency of the related transition in the tS parent molecule. This is caused by an increased binding energy of the excited state, compared with the ground state. We have concentrated in this work on transitions in S-Ar vdW complexes near the electronic origin. It was shown [10] that the S-He$_n$ (n=1-4) complexes exhibit a regularly spaced splitting of 5.8 cm^{-1} and it was suggested that the helium atoms occupy equivalent sites on the parent molecule. The most likely place for such attached atoms is above and below each of the two phenyl groups. For the S-Ar$_n$ vdW complexes a similar behavior is expected. Zwier et al. observed some weak bands and made an assignment, based on the order of appearance. We propose a

different assignment, based on rotational resolved structure.

A relatively strong band, shifted -63 cm^{-1} with respect to the electronic origin of tS is assigned as the O_0^0 band of the S-Ar vdW complex. This is in accord with mass resolved photon ionization spectroscopy [17]. At a relative shift of -41 cm^{-1} another, very similar band is observed. This transition is assigned as an excited vibrational mode of the S-Ar complex. It is not clear wether this 23 cm^{-1} vibration is originates from a low frequency mode of stilbene or from an argon-molecule vibration. Zwier *et al.* observed a weak feature around -20 cm^{-1} and with the present assignment this would match very well to the v=2 vibration. If a similar sequence of appearance is present like in case of S-He$_n$ complexes, the S-Ar$_2$ complex would be expected around -130 cm^{-1} and indeed a very weak spectral feature is observed [10].

The transition frequencies of the observed rovibronic bands of the S-Ar complex are listed in table 1. Both bands exist of resolved but very dense spectra. No single lines were observed but the linewidth is estimated as 80 MHz, in accord with lifetime measurements. The transitions depict a clear P-Q-R-branch structure (fig. 4). The density of lines in the -40 cm^{-1} band is somewhat higher, probably due to a larger splitting in the K-structure. We conclude that the spectra seem less complicated than related bands of the tS parent molecule. This supports the vision that for tS the complex spectral structure is connected with internal motions, which are hindered in the S-Ar complex. Both observed bands of S-Ar show a weak, continuous background as was also observed in the parent molecule. We made a rotational assignment of the O_0^0 band of S-Ar with a symmetric rotor model. This was very satisfactory for states up to J=25. The derived rotational constants are B"=C"=203(1) MHz and $\Delta A \approx \Delta B$=3.5 MHz, where $\Delta A = A'-A"$ and $\Delta B = B'-B"$. These constants match very well with a planar geometry of the stilbene frame [9] with a single argon atom at a distance of 3.4 Å above one of the phenyl groups. This clearly supports our assignment. A simulation of the spectrum with a rotational temperature of 3 K and the constants derived above reproduced the spectrum but clearly showed that intensity mismatches exist. The intensity distribution of a rotational band is given by:

$$I = I_0 (2J"+1) g_n A(J",K"_{-1},K"_{+1}) \exp\left[\frac{-E(J",K"_{-1},K"_{+1})}{kT_{rot}}\right] \tag{3}$$

where g_n denotes the nuclear spin statistical weigth and $A(J",K"_{-1},K"_{+1})$ the Honl-London factors. If this distribution is applied to the S-Ar band of fig. 4, the relative weights of the P, Q, and R-branches are not reproduced. For example the Q-branch is much broader

than expected on basis of eq. 2. It seems as if higher J-states obtain a relatively more favourable transition probability.

A more accurate assignment of the spectra should make use of an asymmetric rotor Hamiltonian. This encounters difficulties since no or little resolved K-structure is observed and is to be expected in the branches. The S-Ar complex forms a very near symmetric top rotor and it is not excluded that the identification of the principal axis changes upon excitation. Consequently the (K_{-1}, K_{+1}) selection rules of the rotational transitions will change. Combined with the anomalous intensity distribution, we feel that there are too many unknown parameters to make an unique assignment in terms of an asymmetric rotor model

ACKNOWLEDGEMENTS

REFERENCES

[1] G. Rothenberger, D.K. Negus and R.M. Hochstrasser, J. Chem. Phys. 79 (1983) 5360.

[2] M. Sumitani, N. Nakashima and K. Yoshihara, Chem. Phys. Lett. 68 (1979) 255.

[3] F. Heisel, J.A. Miehe and B. Sipp, Chem. Phys. Lett. 61 (1979) 115.

[4] A. Bree and M. Edelson, Chem. Phys. Lett. 51 (1980) 77.

[5] M. Edelson and A. Bree, Chem. Phys. Lett. 41 (1976) 562.

[6] Z. Meic' and H. Güsten, Spectrochim. Acta. Part A 34 (1978) 101.

[7] M. Traetteberg, E.B. Frantsen, F.C. Mijlhoff and A. Hoekstra, J. Mol. Struc. 26 (1975) 57.

[8] G. Orlandi and W. Siebrand, Chem. Phys. Lett 30 (1975) 352.

[9] A. Warshel, J. Chem. Phys. 62 (1975) 214.

[10] T.S. Zwier, E. Carrasquillo and D.H. Levy, J. Chem. Phys. 78 (1983) 5493.

[11] J.A. Syage, P.M. Felker and A.H. Zewail J. Chem. Phys. 81 (1984) 4685.

[12] T. Urano, H. Hamaguchi, M. Tasumi, K. Yamanouchi and S. Tsuchiga, Chem. Phys. Lett. 137 (1987) 559.

[13] J.A. Syage, P.M. Felker and A.H. Zewail, J. Chem. Phys. 81 (1984) 4706.

[14] T.J. Majors, U. Even and J. Jortner, J. Chem. Phys. 81 (1984) 2330.

[15] A. Amirav and J. Jortner, Chem. Phys. Lett. 95 (1983) 295.

[16] M. Sonnenschein, A. Amirav and J. Jortner, J. Phys. Chem. 88 (1984) 4214.

[17] D. Bahatt, U. Even and J. Jortner, Chem. Phys. Lett. 117 (1985) 527.

[18] B.W. Keelan and A.H. Zewail, J. Phys. Chem. 89 (1985) 4939.

[19] P.M. Felker and A.H. Zewail, J. Chem. Phys. 86 (1987) 2461.

[20] J.S. Baskin, P.M. Felker and A.H. Zewail, J. Chem. Phys. 86 (1987) 2483.

[21] S. Gerstenkorn and P. Luc, Atlas du spectroscopie d'absorption de la molecule d'iode. Centre National de la Recherche Scientifique, Paris, France, (1978);
S. Gerstenkorn and P. Luc, Rev. Phys. Appl. 14 (1979) 791.

[22] R.H. Dyck and D.S. McClure, J. Chem. Phys. 36 (1962) 2326.

[23] G. Hohlneicher and B. Dick, J. Photochem. 27 (1984) 215.

[24] W.A. Majewski and W.L. Meerts, J. Mol. Spectrosc. 104 (1984) 271.

[25] W.M. van Herpen, W.L. Meerts and A. Dymanus, J. Chem. Phys. 87 (1987) 182.

[26] W.L. Meerts, W.A. Majewski and W.M. van Herpen, Can. J. Phys. 62 (1984) 1293

[27] J.W.I. van Bladel, internal report department of Molecuul- en Laserfysica, Nijmegen, (1987).

High resolution lifetime measurements of the perturbed $J'=0$ levels of the $^1B_{3u}$ state of pyrazine

Willy M. van Herpen and W. Leo Meerts
Fysisch laboratorium, Katholieke Universiteit, Toernooiveld, 6525 ED Nijmegen, The Netherlands

Karel E. Drabe[a] and Jan Kommandeur
Laboratory for Physical Chemistry, University of Groningen, Nijenborgh 16, 9747 AG Groningen, The Netherlands

The lowest excited singlet $^1B_{3u}$ state of pyrazine is known to be coupled to a number of triplet $^3B_{3u}$ states. Using a strongly collimated molecular beam and a single frequency laser it is shown that the $J' = 0$ of the 0_0^0 transition contains at least 36 states. We have individually excited eight of these states and studied its decay. The lifetimes found (typically 450 ns) do not scale with the intensities of the excitation spectrum. This deviation is caused by a nonradiative decay of the zero order $^1B_{3u}$ states. With a simple model it was possible to reconstruct the absorption spectrum, the energies of the zero order states and its coupling strengths. The zero order decay rates of the singlet and triplet states have been determined. The value obtained for the zero order singlet state is 5 MHz, the values for the triplet states range from 0 6 to about 5 MHz

I. INTRODUCTION

Van der Meer *et al*[1] have recently shown that the $^1B_{3u} \leftarrow {}^1A_g 0_0^0$ band of pyrazine contains many more lines than expected for an ordinary allowed electronic transition. This additional structure originates from a coupling between the electronic S_1 state and isoenergetic levels of the lowest triplet (T) state. It was found that the $S_1 \leftarrow S_0$ transition has the characteristics of a c type spectrum of a near oblate symmetric top. Transitions corresponding to different values of the total quantum number J were well separated. Different $J' \leftarrow J''$ transitions in the P and R branch of the band could therefore easily be assigned. However, the K-rotational structure turned out to be of the same order of magnitude as the splittings due to the S_1–T coupling. Consequently no complete rotational assignment was possible with the exception of $P(1)$ and $R(0)$ transition. These transitions only connect states with $K_c = 0$. In the absence of S_1–T interactions these transitions should appear as a single line. In studying the $P(1)$ transition we solely probe the $J' = 0$, $K_c = 0$ state of the S_1 excited level. It is therefore that we have investigated the $P(1)$ transition in more detail in this work. The spectrum first observed in Ref. 1 has presently been recorded with a larger dynamical range and is shown in Fig 1. The original spectrum from Ref. 1 was interpreted in terms of a coupling between the S_1 and a number of triplet states. From the spectrum Van der Meer *et al*[2] determined the relative energies of and the couplings strengths between the zero order states. The procedure used a dediagonalization of the energy matrix to a bases of the zero order states. In order to be successful, relative energy positions and steady state absorption intensities of the lines in the $P(1)$ transition are needed. Unfortunately experimentally we observe a laser *excitation* spectrum. The relation between the two different

spectra and the validity of the dediagonalization method will be discussed.

Recently Amirav *et al*[3] studied the absolute fluorescence quantum yield from photoselected rotational states. Their interpretation of the rotational dependence of the quantum yield is based on the radiative and nonradiative decay width of each molecular eigenstate (ME). De Lange *et al*[4] also investigated the rotational dependence of the quantum yield. They showed that the radiationless decay of the $^1B_{3u}$ electronic state for $J' < 4$ is due to Coriolis coupling. If this were the only radiationless process, the excitation spectrum should be proportional to the absorption spectrum. The magnitude of a possible nonradiative width of the zero order triplet states will determine whether the assumption of proportionality between the excitation spectrum and the absorption spectrum is correct. Since this assumption plays an important role in the understanding of the radiationless decay of the S_1 state of pyrazine[1-6] an attempt was undertaken in this paper to derive the absorption spectrum of the $J' = 0$ states. We therefore studied the lifetimes of individual molecular eigenstates in the $P(1)$ transition. This allowed us to extract the absorption spectrum from the excitation spectrum and to determine the decay rates of the zero order states

II. EXPERIMENTAL

In order to resolve the molecular eigenstates of the 0_0^0 transition of pyrazine we have used a molecular beam setup in combination with a single frequency dye laser. The apparatus situated at Nijmegen, was described in detail before[7,8] and only a brief description of the most relevant features is given here. Pyrazine was seeded with argon and expanded by a continuous nozzle (100 μm diameter) at a backing pressure of 0 5 atm in a vacuum chamber. The source was kept at room temperature and the rotational temperature obtained is estimated to be about 3 K. The molecular beam was strongly collimated by two conical skimmers. In the interac-

[a] Present address Physical Chemical Laboratory, Vrije Universiteit, de Boelenlaan 1083, 1081 HV Amsterdam The Netherlands

tion zone with the radiation field, 30 cm from the beam ori-
fice, the residual Doppler width was 15 MHz The undis-
persed laser induced fluorescence was imaged to the
photocathode of a photomultiplier tube (EMI 9863/350
QA)

The narrow band radiation field was obtained by second
harmonic generation[9] in a modified ring dye laser (Spectra
Physics) For this purpose a LiIO₃ angle tuned crystal was
placed inside the laser cavity About 2 mW of cw UV power
was produced with a bandwidth of less than 0 5 MHz Rela-
tive frequencies have been measured by a sealed off tempera-
ture stabilized Fabry–Perot interferometer

For recording the $P(1)$ spectrum of Fig 1 the spectrom-
eter was computer controlled by a PDP11/23plus The laser
induced fluorescence collected was detected by a standard
photon counting system interfaced with the microcomputer
The molecular beam was chopped and phase sensitive detec-
tion was applied to suppress background radiation

For the lifetime measurements the laser was held on the
peak of a transition to a ME while the laser radiation was
modulated with an electro-optic modulator (Coherent Ra-
diation) in conjunction with a polarizer This resulted in
single frequency pulses of 40 ns duration with a light on and
off ratio of about 150 The repetition rate was 12 kHz The
photons emitted upon excitation of pyrazine were detected
using a single photon counting technique Pile up was prohi-
bited by a pile-up inhibitor For the two strongest lines in the
spectrum about 0 1 photon per shot was detected

III RESULTS FOR P(1)

Since the first data on pyrazine were taken[1] considerable
improvements on the spectrometer allowed us to obtain
more detailed spectra of the $^1S_1 \leftarrow {}^1S_0$ transition in this mole-
cule Figure 1 shows the present results The improvements
were found in a stronger and better cooled molecular beam,
reduction of the residual Doppler width to 15 MHz and opti-
mization of the optical system Furthermore the dynamic
detection range was increased with the help of digital data
recording The spectrum of Fig 1 is taken with a preset
counting time of the photon counter of 0 1 s and has a signal-
to noise ratio of 10³ This spectrum shows many more details
of weak well resolved transitions The 12 previously ob-
served features[1] in the $P(1)$ transition are, of course, also
reproduced A total of 36 lines has been counted from the
spectrum of Fig 1 Table I lists the relative frequencies and
intensities The accuracy in the frequency scale is limited by
thermal drift of the marking interferometer and is estimated
to be about 1 5% while the intensities have an uncertainty of
5% For eight of the stronger lines in the $P(1)$ spectrum we
could study the decay after excitation with a 40 ns pulse
Figure 2 shows the decay of the strongest line of the $P(1)$
spectrum It was found that all observed decays showed
within experimental accuracy single exponential behavior
The lifetimes τ of the excited state levels were determined by
a least-square fit of each of the decay curves over a period of
at least 4τ The results are listed in Table I We estimate an
accuracy of about 50 ns in τ This is mainly due to limitations
in the detection system and the background caused by the
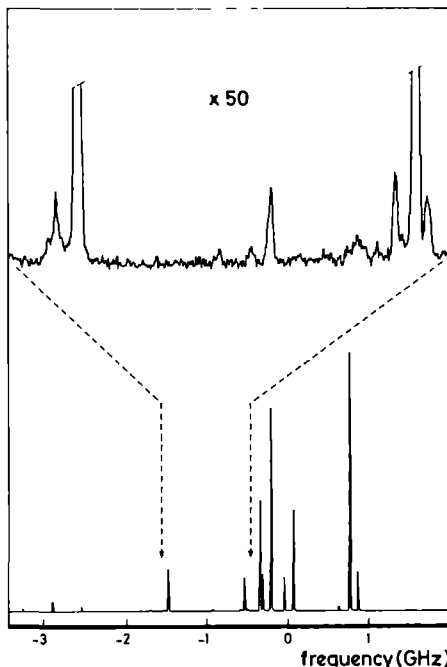finite contrast ratio of the optic modulator

The $^1S_1$ $({}^1B_{3u}) \leftarrow {}^1S_0({}^1A_g)$ optical transition in pyra-
zine dictates a c-type rotational spectrum Since the mole-
cule is a near symmetric top molecule, the only features in
the spectrum are transitions of the type $\Delta K_c = 0$, where K_c
represents projection of the rotational quantum number J on
the c axis Therefore, all transitions in the $P(1)$ spectrum
arise from one single $|J,K_c\rangle$ ground state Consequently, the
integrated steady state excitation intensities all contain the
same Boltzmann population factor This situation is unique
in the $P(1)$ and $R(0)$ transitions in contrast to the other
branches, e g, $P(2)$ Figure 3 shows the rate constants
($\gamma_{ME} = 1/\tau$) vs the excitation intensity for the studied levels
in the $P(1)$ perturbed transition This figure clearly demon-
strates that, primarily for the weaker lines, the decay rates
are not proportional to the steady state intensities In Sec IV
we will discuss the consequence of this observation

IV. THEORY

A molecular eigenstate in the excited electronic state
can formally be expanded in the zero order singlet state $|S\rangle$
and a set of triplet states $\{|T\rangle\}$ by

$$\Phi_{ME_i} = C_{S_i}|S\rangle + \sum_T C_{T_i}|T\rangle \tag{1}$$

The zero order states have their own independent decay
channels with rates γ_S and $\{\gamma_T\}$, respectively We assume

TABLE I Energies,[a] excitation intensities, and lifetimes belonging to the $P(1)$ member of the $^1B_{1u}$ 0^0_0 transition of pyrazine Also the calculated relative absorption intensities are given

Energy (MHz)	Excitation intensity	Lifetime (ns)	Absorption intensity
– 4725	18		
– 4337	42		
– 3849	20		
– 3686	21		
– 3245	81		
– 2884	376		
– 2530	179		
– 2438	33		
– 2341	22		
– 1881	21		
– 1770	28		
– 1694	39		
– 1536	28		
– 1515	58		
– 1456	1 666	200 (50)	0 118
– 1071	19		
– 984	20		
– 929	58		
– 689	30		
– 637	25		
– 589	66		
– 535	1 278	512	0 065
– 502	55		
– 353	3 891	443	0 122
– 318	1 441		
– 221	8 168	342	0 200
– 44	1 305	437	0 071
62	4 031	560	0 110
593	21		
631	199		
765	10 000	280	0 245
867	1 503	529	0 069
1443	28		
1867	55		
2722	28		
2781	29		

[a] The ME energies are referred to the center of gravity of the excitation spectrum which is at $\nu =$ 12 192 MHz relative to the electronic origin ν_0 of the $^1B_{1u} - {}^1A_g$ 0^0_0 transition
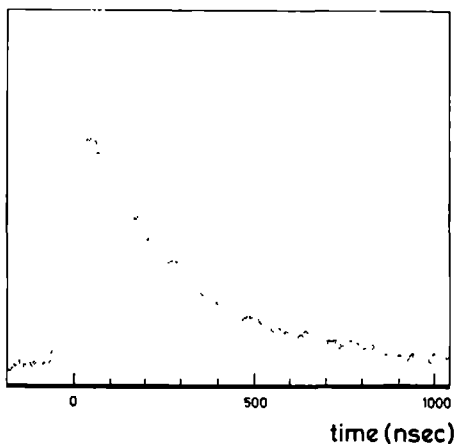

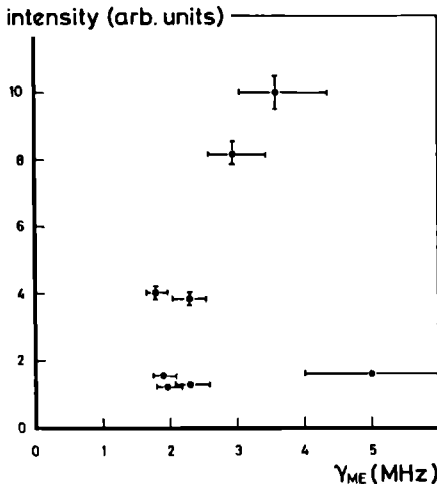FIG 2 Decay curve of the strongest line of the $P(1)$ transition

time (nsec)

intensity (arb. units)

FIG 3. Relation between the decay rates and the excitation intensity for $P(1)$ lines of pyrazine

γ_{ME} (MHz)

that there is no decay within the triplet states involved in the sum of Eq (1) In that case the decay rate of the ith molecular eigenstate is given by

$$\gamma_{ME_i} = |C_{Si}|^2\gamma_S + \sum_T |C_{Ti}|^2\gamma_T. \tag{2}$$

It is thus supposed that there is no significant decay within the zero order state manifold. The zero order width γ_S can be split in a radiative γ_S^r and nonradiative γ_S^{nr} contribution with

$$\gamma_S = \gamma_S^r + \gamma_S^{nr}. \tag{3}$$

The nature of γ_T may also be radiative or nonradiative. We can safely assume it to be of nonradiative character, since the phosphorescence rate of pyrazine is small.

The steady-state absorption intensity A_i of the ith ME is

$$A_i \propto |\mu_{ME_i}|^2 I_i = |\mu_S|^2 |C_{Si}|^2 I_i, \tag{4}$$

where μ_{ME_i} and I_i are the ith transition dipole moment of the zero order singlet state and the laser intensity, respectively A linear laser intensity response is assumed since no saturation effects were observed at a 2 mW laser power level.

Experimentally we observe in the frequency spectrum the steady-state excitation intensity E_i integrated over its inhomogeneous line profile, which is given by

$$E_i \propto \frac{A_i \gamma_{ME_i}}{\gamma_{ME_i}}$$

$$\propto \frac{\gamma_S^r |\mu_S|^2 I_i |C_{Si}|^4}{\gamma_{ME_i}} \tag{5}$$

or

$$E_i = \frac{\alpha |C_{S_i}|^4}{\gamma_{MF_i}} \qquad (6)$$

Here α is a constant (independent of the ME's) and γ_{MF_i}, the radiative decay rate of the ith ME If the decay rates of the molecular eigenstates are dominated by the singlet decay ($\gamma_S \gg \gamma_T$, or $\gamma_T \approx 0$), Eq (2) can be rewritten as

$$\gamma_{ME_i} = |C_{S_i}|^2 \gamma_S \qquad (7)$$

and the excitation intensity becomes

$$E_i = \frac{\alpha |C_{S_i}|^2}{\gamma_S} \qquad (8)$$

In this case the absorption and excitation intensities both scale with the singlet intensity $|C_{S_i}|^2$ It also follows that E_i is proportional to its corresponding decay rate γ_{ME_i}

V. RECONSTRUCTION OF THE ZERO ORDER SITUATION

The reconstruction of the zero order states is beset by the problem that one measures excitation spectra rather than absorption spectra In an earlier publication[2] it was assumed that the excitation spectrum was directly proportional to the absorption spectrum, which implied that the zero order triplet states did not decay on their own This then implies that the decay rates of the ME's would be proportional to their excitation intensity Looking at Table I at the intensities of the strongest lines and their decay, it is clear that deviations exist, as is also shown in Fig 3 The line with the highest relative excitation intensity (10 000) has approximately the same decay rate as the one with an excitation intensity six times lower (1 666)! This clearly demonstrates the existence of a nonzero nonradiative decay (γ_T) of the zero order triplet states Therefore, the absorption and excitation spectra differ in relative intensities

In principle we can derive the absorption spectrum from the excitation spectrum and reconstruct the zero order energies, coupling matrix elements and lifetimes of the states $|S\rangle$ and $\{|T\rangle\}$ in three steps

(i) Experimentally we determine the excitation intensities and lifetimes of the ME's in the $P(1)$ transition We can then derive the absorption spectrum by utilizing Eq (6)

$$|C_{S_i}|^2 = (E_i \gamma_{ME_i}/\alpha)^{1/2} \qquad (9)$$

Here the constant α is determined by experimental conditions such as sensitivity of the detection system In principle α can be calculated using $\Sigma_i |C_{S_i}|^2 = 1$ and Eq (9) if γ_{ME_i} is measured for all ME's However, in order to find the absorption spectrum only the relative values for $|C_{S_i}|^2$ are needed [2,10]

(ii) The exact and unique dediagonalization procedure of Lawrance and Knight[10] can now be applied to the absorption spectrum obtained in step (i) The method described in Ref 10 gives an elaborate procedure, involving a Green's function inversion approach, to compute the zero order energies of the states $|S\rangle$ and $\{|T\rangle\}$, together with the coupling elements V_{s_i} In this procedure the steady state absorption

intensities and relative energy positions of the lines in the $P(1)$ transition are needed An essential condition is the fact that only one state component ($|S\rangle$) carries oscillator strength with respect to the initial state The solution for the zero order states and coupling strengths is unique and its accuracy is limited only by the uncertainties in the experimental data

(iii) The dediagonalization from step (ii) also provides the composition of the projection of the ME states on the zero order singlet and triplet states ($C_{S_i}, \{C_i\}$) Equation (2) yields a set of linear equations with the same number of decay rates ($\gamma_S, \{\gamma_{T_i}\}$) The solution of these equations thus gives the decay rates of the zero order states

Unfortunately not all γ_{MF}'s could be measured because of the low excitation intensities of some ME's Therefore, let us first assume that the widths of the ME's of which the

TABLE II Relative energies[a] singlet–triplet coupling matrix elements and rate constants[b] of the zero order triplet states The reconstruction of the $P(1)$ absorption spectrum of pyrazine has been performed for the eight strongest lines and for all 36 lines separately All values are in MHz

	8 States			16 States		
	Energy	V_{s_i}	γ	Energy	V_{ST}	γ
Singlet	− 43		5(4)	− 362		7 3
Triplet				− 4705	270	2 0
				− 4307	327	2 0
				− 3832	220	2 0
				− 3666	250	2 0
				− 3216	267	1 9
				− 2823	370	1 9
				− 2496	236	1 9
				− 2414	249	2 0
				− 2319	265	2 0
				− 1872	110	2 0
				− 1761	103	1 9
				− 1683	114	1 9
				− 1533	39	1 9
				− 1509	54	1 8
	− 1286	462	5(1)	− 1291	479	5 6
				− 1062	122	1 9
				− 976	99	1 9
				− 913	158	1 9
				− 684	59	1 9
				− 633	49	2 0
				− 584	50	1 9
	− 502	119	1 6(0 5)	− 513	74	1 0
				− 486	120	2 6
	308	105	1 6(0 5)	− 334	47	1 4
				− 282	102	1 8
	− 98	150	2 7(0 5)	− 89	160	2 4
	13	117	0 6(0 5)	17	133	0 7
	463	457	3(2)	459	474	3 9
				598	66	1 8
				650	120	1 5
	848	67	1(0 5)	849	76	1 4
				1433	116	2 0
				1849	184	2 0
				2702	245	2 0
				2962	234	2 0

[a] The energies are relative to the center of gravity of the complete excitation spectrum The position of the singlet level is at the center of gravity of the absorption spectrum and therefore is not necessary at 0 MHz

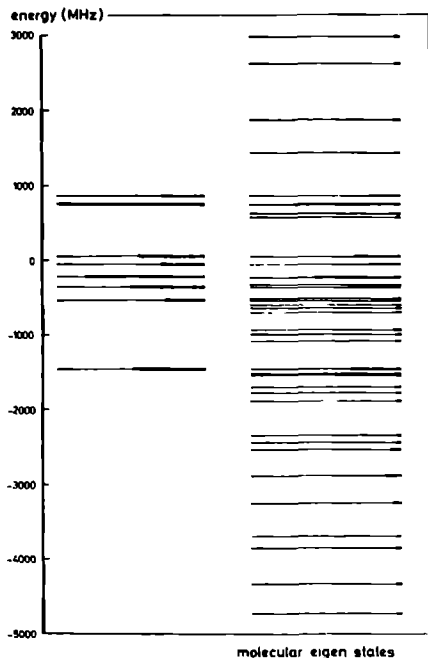[b] The indicated error ranges are introduced by experimental uncertainties in lifetimes and intensities

68

energy (MHz)

lifetimes were not measured are zero (This is obviously wrong, since we do measure an excitation intensity at their position) The eight states of which the lifetimes have been determined contain the major part (91%) of the total excitation intensity Applying the procedure described above, we can then derive the absorption spectrum, which will now consist of only eight lines The relative absorption intensities are given in Table I, while the zero order energies of the states $|S\rangle$ and $\{|T\rangle\}$, together with their widths and the coupling elements V_{sI} are given in Table II The uncertainties indicated include the experimental errors in the lifetime and intensity measurements and the correlations between the parameters introduced by the described procedure The width of the zero order singlet state has a lower limit of 3 3 MHz, which is imparted to it by the pure radiative lifetime of 290 ns, determined independently[11–13] from the absorption intensity Our solution indeed satisfies this constraint

Neglecting those ME's for which no lifetime measurements are available, will introduce an extra uncertainty in the final numbers As we will show this will not substantially affect the conclusion given below We can investigate the case in which we give all ME's without a measured lifetime an assumed lifetime under the condition that the width of the singlet state exceeds 3 3 MHz Using the dediagonalization procedure we find that the assumed lifetimes must then ex-

ceed 450 ns It also apears that these lifetimes have an upper limit of about 700 ns in order to give valid solutions for the zero order decay rates In Table II the calculated results are given for the zero order states, their couplings and their widths in case we assume a lifetime of 500 ns for the unknown values The energy of the singlet state is shifted considerably, but the triplet states, their widths and the coupling elements are not very much affected

The purpose of the foregoing was mainly to compare the singlet character of the ME's, i e, their relative absorption intensities, in case we use the eight strongest lines and in case of the full set of 36 states Figure 4 displays the result for both calculations It will be clear that including the full set just leads to a slight redistribution of the singlet amplitudes This gives an *a posteriori* justification of our procedure

VI. CONCLUSION

It was unambiguously shown that excitation to a single ME state in the $P(1)$ transition gives rise to a single exponential decay of such a ME The present study is the first to demonstrate this experimentally in pyrazine It was further found that the excited S_1 state of pyrazine has nonzero radiationless decay channels for both the zero order singlet and triplet states The decay rates for the two channels have been obtained Although not all decays in the ME spectrum could be measured, it was also shown that inclusion of the decays of the remaining states does not much alter the composition of the ME's, nor the decay of the zero order states

ACKNOWLEDGMENTS

[1] B J van der Meer, H T Jonkman, J Kommandeur, W L Meerts, and W A Majewski Chem Phys Lett 92, 565 (1982)
[2] B J van der Meer, Harry T Jonkman, and Jan Kommandeur, Laser Chem 2, 77 (1983)
[3] A Amirav and J Jortner, J Chem Phys 84, 1500 (1986)
[4] P J de Lange, B J van der Meer K E Drabe, J Kommandeur, W L Meerts, and W A Majewski (submitted)
[5] H T Jonkman, K E Drabe, and J Kommandeur, Chem Phys Lett 116, 357 (1985)
[6] P J de Lange, K E Drabe, and J Kommandeur, J Chem Phys 84, 538 (1986)
[7] W Majewski and W L Meerts J Mol Spectrosc 104, 271 (1984)
[8] K F Drabe, J Langelaar, D Bebelaar, and J D W Voorst, Chem Phys 97, 411 (1985)
[9] W Majewski, Opt Commun 45, 201 (1983)
[10] W D Lawrance and A E. W Knight J Phys Chem 89, 917 (1985)
[11] W J Schutten (private communication, 1985)
[12] K Nakamura, J Am Chem Soc 93 3138 (1971)
[13] K K Innes, J P Byrne, and I G Ross, J Mol Spectrosc 12, 125 (1967)

69

HIGH RESOLUTION QUANTUM BEAT SPECTROSCOPY OF THE PERTURBED J'=1 LEVEL OF THE $^1B_{3u}$ STATE OF PYRAZINE

W.M. van Herpen, K.E. Drabe * and W.Leo Meerts

Fysisch Laboratorium, Katholieke Universiteit

Toernooiveld, 6525 ED Nijmegen, The Netherlands

ABSTRACT

An external modulated cw narrow band laser and a collimated molecular beam was used to apply high resolution quantum beat spectroscopy to the molecular eigenstate spectrum of pyrazine. A resolution of 1 MHz was achieved in the near ultraviolet region. A beat pattern was observed from the temporal decay following excitation of a molecular eigenstate in the J'=1, K'=0 manifold. From the inhomogenety of the molecular eigenstate spectrum it is concluded that it is difficult to deconvolute the molecular eigenstates into unperturbed zero order states of pyrazine.

1. INTRODUCTION

The electronic decay of the first excited singlet $^1B_{3u}$ state of pyrazine has, been subject of extensive studies in recent years. The intramolecular dynamics of this molecule are

---

* Present address: Physical Chemical Laboratory, Vrije Universiteit, de Boelelaan 1083, 1081 HV Amsterdam, The Netherlands.

attributed to the limiting case of intermediate level structure (ILS) [1]. Quantum beats were observed, which proved to depend on the rotational state [2,3] and on an applied magnetic field [4]. The temporal decay is biexponential as was first demonstrated by Frad *et al.* [5]. The data are interpreted in terms of an excited singlet (S_1) state $|S>$, connected via intrastate coupling to a number of nearly isoenergetic triplet (T) states $\{|T>\}$. This results in a manifold of mixed states $|n>$, the molecular eigenstates (ME):

$$|n> = C_S|S> + \sum_T C_T|T>, \qquad (1)$$

where the coefficients C_S and $\{C_T\}$ denote the singlet and triplet contents of the ME state. The states $|S>$ and $|T>$ are usually called zero-order states. The resolved ME spectrum of pyrazine was first observed by van der Meer *et al.* [6]. The O_0^0 parallel rovibronic band of this near-symmetric top molecule contains P(J") and R(J") branches with groups of lines belonging to specific J values, separated by empty spectral regions. The K-rotational structure is perturbed due to the S_1-T coupling and a number of ME states are observed within each P(J") or R(J") group of lines. For example the P(1) or R(0) spectra terminate in a single excited state level; (J'=0,K'=0) or (J'=1,K'=0) respectively, and would normally consist of a single spectral line. However, it appeared that the P(1) transition contains at least 36 lines in a 7.5 GHz region [7]. The R(0) spectrum, as depicted in fig. 1, was devided into a series of about 100 spectral lines [8].

It is possible to derive the zero order singlet and triplet state basis and the coupling matrix elements V_{st} from the ME spectrum of the J'=0 levels [9]. Lawrance and Knight [10] presented a mathematical approach with a Green's function method, to derive the unique solution of this deconvolution procedure. The method is limited by the condition that a spectrum can only be deconvoluted if it consists of a single singlet state, with an allowed transition dipole moment to the ground electronic state, which is coupled to a number of dark states (T). Such unique 'doorway state' is found in the P(1) and R(0) spectrum. As input for the deconvolution procedure, the frequencies and relative absorption intensities of the ME spectrum are needed. In a recent experiment we showed that it is incorrect to replace the absorption intensities by the experimentally observed excitation intensities from laser induced fluorescence spectra [7]. From the lifetimes of the ME states it was derived that absorption and excitation intensities are not proportional for the P(1) spectrum. With an accompanying model it was concluded that the zero order triplet states undergo a significant nonradiative decay into unknown dark states (T' or S_0 levels).

Recently several attempts have been made to obtain more specific information about

71

the various coupling mechanisms that play a role in the radiationless decay of pyrazine [11,12]. It would be very helpfull if more detailed information was available about the (J',K') dependence of coupling strength and quantum yield for higher energy ME states of pyrazine. Therefore a deconvolution procedure of several (J',K') levels is a worthwhile effort. In the present paper we show that a carefull interpretation of the spectra is needed. It will be shown for one of the R(0) ME states that spectral lines may very well be inhomogeneous, despite the high resolution resolution achieved. In that case there is no straight forward interpretation of the line intensity and a carefull aproach is in its place in the deconvolution into the zero order situation.

2. EXPERIMENTAL

The experimental apparatus was the same as used in a previous time resolved experiment on the J'=0 levels of pyrazine [7]. A collimated molecular beam was crossed at right angles with a cw single frequency tunable laser. The beam was formed from an expansion of pyrazine vapour, at room temperature, and argon through a 100 μm diameter nozzle at a total backing pressure of 0.5 bar. The rotational temperature is estimated to be about 3 K. Narrow band radiation was obtained from an intracavity frequency doubled ring laser with a 0.5 MHz bandwidth and a typical cw output power of 2 mW [13]. The laser was modulated with an electro-optic modulator in conjugation with a polarizer. This resulted in pulses of single frequency laser radiation with a light on-off ratio of about 150. The repetition rate was 12 kHz and the typical pulsewidth 40 ns. The total undispersed laser induced fluorescence was collected and imaged to a photomultiplier (EMI 9863 QA). A time resolved single photon counting technique was used and pileup was carefully avoided. By accumulated measuring cycles a histogram is obtained of counted photons versus time.

3. RESULTS AND INTERPRETATION

As was already pointed out, a single doorway state is needed in an ME manifold to apply deconvolution into zero order states and to derive the coupling matrix elements [10]. Therefore one has to make a (J',K') assignment of the ME states. In general this may be achieved by labelling specific states in a double resonance experiment. In case of the R(0)
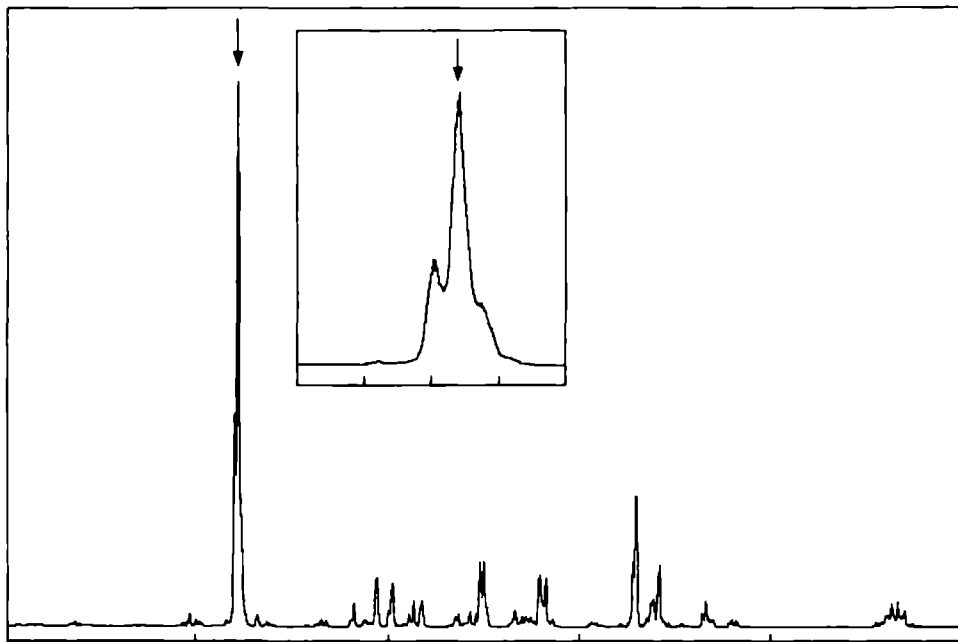
FIG. 1. Molecular eigenstate spectrum of the (J'=1,K'=0) coupled states of pyrazine. The frequency scale is marked in GHz. The indicated line was used in the quantum beat experiment. The insert shows an exploded view of a 200 MHz region containing this transition.

manifold of ME states such assignment is obvious. These transitions start from the (J"=0,K"=0) ground state level and with the selection rules $\Delta J=1, \Delta K=0$ it follows that the unique (J'=1,K'=0) level of the S_1 state is reached. It is therefore allowed to apply the deconvolution procedure. However a more practical problem is encountered in the form of spectral congestion. In fig. 1 the R(0) spectrum is depicted. The experimental linewidth is 12 MHz, due to the residual Doppler effect. Even at such high resolution the ME spectrum is not completely resolved. This is demonstrated for the strongest line of R(0), marked in fig. 1. As the insert shows, this line consists of at least three transitions. They are partly resolved and their frequencies and intensities may be deduced. The two satellite lines are separated about 19 and 15 MHz from the main strongest transition.

The laser was held on top of the middle transition and its radiation was modulated with 40 ns pulses. The detected fluorescence as function of time is shown in fig. 2. A clear beat pattern is observed. The laser pulse is not Fourier limited, but from its width
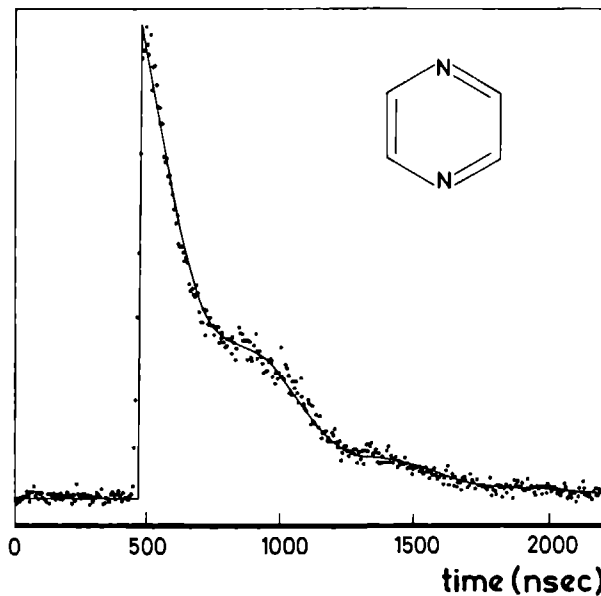
FIG. 2. Decay of the strongest line of the R(0) transition. The dots represent the experimental points, while the drawn curve indicates the theoretical path.

in time domain we estimate that its width in frequency domain is 30 MHz. This means that states within typically 15 MHz of the centre frequency are coherently excited by the laser. The two lines next to the main peak are therefore under weak excitation condition. If only a single state was excited, the temporal decay would be of single exponential form, as observed for all states in P(1) [7]. If more than one state is coherently excited a quantum beat pattern is observed as in fig. 2. From such a beat pattern it is possible to derive the energy splitting of the involved coherently excited levels, as is customary in quantum beat spectroscopy, by Fourier transformation. The Fourier transform of the decay curve of fig. 2 yielded only a single splitting. Thus the beat pattern merely results from two coherently excited levels. In that case the decay is described by:

$$I(t) = I_0 \exp\left[-\frac{t-t_0}{\tau}\right]\left(1+B\cos\left[2\pi\nu_{12}(t-t_0)\right]\right), \qquad (2)$$

where ν_{12} indicates the frequency splitting between the two excited levels. The shape of the laser pulse is taken as a δ-pulse at $t=t_0$. This is a valid approximation if the lifetime

74

of the excited state is much longer than the pulsewidth. We now adopt the constraint that indeed only two levels are involved in the observed decay and fit eq. (2) to the experimental data. The resulting curve is shown in fig 2. It can be seen that the agreement between experimental and calculated data is good. The parameters in eq. 2 have the values: ν_{12}=1.9(1) MHz, B=0.16(2) and τ=395(10) ns. The observed frequency splitting is of course in agreement with the direct Fourier transform, only its accuracy is somewhat higher because of the extra constraint. We conclude that the frequency components are not due to the partially resolved lines in fig. 1, since their splitting is much larger. Therefore the main peak of the considered transition is still not completely resolved. At least two spectral lines are present with considerable excitation intensity. The origin of the two lines is unclear. They may simply result from two accidentally isoenergetic triplet levels or from hyperfine structure. Another possibility is a splitting of a state due to the earth's magnetic field. As will be published elswhere, it proved that the ME spectrum of pyrazine, the R(0) band included, is affected by magnetic fields.

Resuming we come to three main conclusions of this work: (i) It was shown that the obtainable resolution of a cw narrow band laser in combination with a collimated molecular beam can be even further expanded into the range of 1 MHz. (ii) At least one and probably more lines in the high resolution ME spectrum of pyrazine are not completely resolved. (iii) Due to this effect a deconvolution into zero order states and the derivation of coupling strengths as a function of (J',K') becomes more difficult, even at low J values. It is therefore a problem to derive more detailed information concerning the coupling mechanisms, involved in the radiationless decay of pyrazine.

ACKNOWLEDGEMENT

REFERENCES

[1] F. Lahmani, A. Tramer and C. Tric, J. Chem. Phys. 60 (1974) 4431.

[2] B.J. van der Meer, H.T. Jonkman, G. ter Horst and J. Kommandeur, J. Chem. Phys. 76 (1982) 2099.

[3] S. Okajima, H. Saigusa and E.C. Lim, J. Chem. Phys. 76 (1982) 2096.

[4] P.M. Felker, W.R. Lambert and A.H. Zewail, Chem. Phys. Lett. 89 (1982) 309.

[5] A. Frad, F. Lahmani, A. Tramer and C. Tric, J. Chem. Phys. 60 (1974) 4419.

[6] B.J. van der Meer, H.T. Jonkman, J. Kommandeur, W.L. Meerts and W.A. Majewski, Chem. Phys. Lett. 92 (1982) 565.

[7] W.M. van Herpen, W.L. Meerts, K.E. Drabe and J. Kommandeur, J. Chem. Phys. 86 (1987) 4396.

[8] W. Siebrand and W.L. Meerts, to be published.

[9] B.J. van der Meer, H.T. Jonkman and J. Kommandeur, Laser Chem. 2 (1983) 77.

[10] W.D. Lawrance and A.E.W. Knight, J. Phys. Chem. 89 (1985) 917.

[11] A. Amirav, Chem. Phys. 108 (1986) 403.

[12] P.J. de Lange, B.J. van der Meer, K.E. Drabe, J. Kommandeur, W.L. Meerts and W.A. Majewski, J. Chem. Phys. 86 (1987) 4004.

[13] W.A. Majewski, Opt. Comm. 45 (1983) 201.

HIGH RESOLUTION ABSORPTION SPECTRUM
OF THE MOLECULAR EIGENSTATES OF PYRAZINE

W M. van Herpen, P.A.M. Uijt de Haag and W. Leo Meerts

Fysisch Laboratorium, Katholieke Universiteit

Toernooiveld, 6525 ED Nijmegen, The Netherlands

ABSTRACT

The high resolution absorption spectrum of the P,Q and R branches of the $^1B_{3u}$ (0-0) electronic transition of pyrazine was recorded with a bolometer in a supersonic molecular beam. A comparison is made between excitation and absorption intensities of the molecular eigenstate spectrum

1. INTRODUCTION

Together with pyrimidine the pyrazine molecule serves as a prototype of an intermediate case molecule in the theory of intramolecular radiationless transitions [1]. This molecule has received much attention and a large amount of theoretical and experimental data has become available over the years. The development of narrow band lasers, in frequency as well as in time domain, opened the possibility to obtain extensive time-resolved and energy-resolved information. For a recent review see ref. [2] and references therein. The main attention is focussed on the fluorescence decay of the first excited $S_1(^1B_{3u})$ singlet electronic state of pyrazine. It was shown that this decay is rotationally dependent [3] and quantum beats were reported [4,5], which proved to be magnetic field dependent [6,7]. The temporal decay is biexponential i.e. it is characterized by a short- and a long-time

component, as was first demonstrated by Frad et al. [1,8]. This biexponential decay was also shown to depend on the rotational J' quantum number [9]. The described properties of the excited singlet state are attributed to the fact that the intramolecular dynamics in pyrazine is considered a limiting case of intermediate level structure (ILS) [8]. The experimental data are interpreted in terms of an excited singlet state (S_1) level, connected via interstate coupling to a number of nearly isoenergetic triplet (T) levels. This results in a manifold of mixed states, containing singlet and triplet character. The molecular eigenstate (ME) spectrum was first directly observed by van der Meer et al. [10] It was found that the $S_1 \leftarrow S_0 \, O_0^0$ electronic band displays a near symmetric top rotational structure with well resolved P(J") and R(J") branches. These branches consist of groups of lines, characterized by a single J quantum number, well separated by empty regions in between. The K rotational structure is hidden due to the distribution over different molecular eigenstates. The splittings caused by the S_1–T coupling are thus of the same order of magnitude as the K structure. The P(1) transition, terminating in the (J'=0,K'=0) level of the S_1 state, appeared to exist of about 36 lines in a 7.5 GHz region [11] instead of the single line which would be expected in the absence of the state mixing. Attempts have been made to reconstruct the unperturbed, so-called zero-order singlet and triplet states and their coupling matrix elements V_{st} [12,13], in order to obtain more detailed information about the coupling mechanisms involved in the radiationless decay of the MEs. This is only possible in case one 'doorway state' is present, i.e. a state with an allowed transition dipole moment to the ground state, connected to a number of 'dark' states. For this so-called deconvolution procedure the energies and relative absorption intensities of the ME manifold are needed. Such single doorway state is obviously present in the P(1) and R(0) spectra, where an unique S_1 singlet level is excited: (J'=0,K'=0) and (J'=1,K'=0) respectively. That is the main reason that such deconvolution has first only been reported for the P(1) spectrum. Recently Siebrand and Meerts have extended the deconvolution to J'=1-4 states [14]. It was recently shown [11] (chapter 6-a) that it is not correct to approximate the absorption intensities of the MEs by their excitation intensities as was previously assumed. The latter intensities are relatively easy to obtain from high resolution laser induced fluorescence spectra. The ME-absorption spectrum is much harder to obtain. It may be derived from the excitation spectrum if the lifetime of the individual MEs is known [11]. These lifetimes (typically 400 ns) can be obtained by modulation of a cw narrow band laser excitation of the MEs in a collimated molecular beam and monitoring the temporal decay. This was achieved for the strongest lines in the P(1) spectrum.

In recent work, more attention was given to the nature of the coupling mechanisms

involved in the decay. The absolute quantum yield under medium resolution of 1 cm^{-1} was determined of the J' levels [15]. The presence of Coriolis coupling was demonstrated [16] with an assumed K-scrambling at higher J' levels. Also the excistence of 'grass' was predicted [17], a broad background in the ME-spectra of weak lines with a 1.5 GHz linewidth. To test these models, additional data on the ME-spectra is needed. More information is required on the (J',K') dependence of the quantum yield, coupling strength and lifetimes of higher energy MEs. For deconvolution of other P(J") or R(J") manifolds it is neccessary to assign the K' quantum numbers to selective individual doorway states [14]. This may, for example, be achieved by double resonance techniques. Another problem to be solved is the conversion of excitation intensities into absorption intensities. In other words, the quantum yield of individual MEs is needed. We will here approach the latter problem. It will be demonstrated that it is in principle possible to obtain high resolution absorption spectra of the ME-structure of pyrazine. Narrow band laser radiation is used to excite molecules in a molecular beam. The LIF spectrum is determined in the usual way. The molecular beam has to be strongly collimated to resolve the MF-structure. Therefore the direct absorption of radiation from the crossing laser is extremely weak. It is possible to determine the increase in energy, contained in the molecular beam, instead of determination of the decrease of energy in the laser beam. Since the quantum yield of pyrazine rovibronic states is low (in the order of few percent) it is a good approximation to state that nearly all absorbed energy stays in the molecular beam and only a tiny fraction is lost via fluorescence. Such increase in energy can be determined by application of a bolometer to monitor the energy flow in the beam.

2. EXPERIMENTAL

The molecular beam apparatus used in this experiment has been described elsewhere [18]. A bolometer was applied to detect the molecular beam. The supersonic beam is formed from a continuous expansion of pyrazine seeded with helium through a 75 μm diameter nozzle. The sample of pyrazine (Janssen Chimica) with a 99+% purity was kept at room temperature. The backing pressure of helium was in the range 0.25-0.5 bar. Normally, argon seeding results in a much better rotational and vibrational cooling under comparable expansion conditions. However in the present experiments argon could not be applied because it condensates on the cold surface of the bolometer element. The molecular beam is strongly collimated by two conical skimmers of 1.5 mm diameter, in a differential pumping system.

Molecules were excited at 30 cm from the nozzle, by a cw tunable radiation field from a frequency doubled ring dye laser (a modified Spectra Physics 380D). Intracavity frequency doubling was performed with an angle tuned $LiIO_3$ crystal [19]. About 1 mW of single frequency radiation was obtained around 324 nm with a 3 MHz bandwidth. Frequency calibration was performed with a temperature stabilized sealed Fabry-Perot interferometer at the fundamental wave. Part of the output of the laser was sent to this interferometer and frequency markers were recorded simultaneously with a spectrum. The laser beam is mechanically chopped at 90 Hz. The total undispersed laser induced fluorescence (LIF) is collected by two spherical mirrors and imaged to the photocathode of a photomultiplier (EMI 9863 QA).

Approximately 30 cm downstream of the crossing of the laser the molecular beam reaches the bolometer. The doped germanium detector with a size of 1x1 mm (Infrared Laboratories), is mounted on a diamond substrate of 2x5 mm. The element is operated in the region 2.2-4.2 K by pumping a helium bath cryostat. At 4.2 K the noise equivalent power of the bolometer is $4.8x10^{-13}$ $W/Hz^{1/2}$ and the responsivity R is $R=5x10^4$ V/W. The initial response time is 2.5 ms but during the measurements this value slowly increases due to the so-called cryofrost. This effect is caused by the fact that molecules tend to condensate on the cold detector surface. Therefore the source was not heated and a diluted mixture of pyrazine vapour was applied. The pressure in the bolometer compartment of the apparatus was kept at 10^{-7} mbar. Nevertheless cryofrost imposes a limit on the operational time of the bolometer of about 4 hours. External sources of heat radiation were shielded by two screens at 4.2 K and 77 K. Laser stray light does not significantly reach the detector due to spatial filtering and the large distance between laser excitation area and bolometer.

The total beam signal is given by:

$$S_B = R N E,$$ \hfill (1)

where N is the number of particals per second and E the energy of the beam. Apart from the continuous translational and internal energy of the molecules, E contains contributions from the absorption energy. Only the latter one is detected by a phase sensitive detection method. A 1 s RC constant was used.

3. RESULTS

With the described experimental setup we recorded simultaneously laser induced fluorescence spectra (FS) and the bolometer spectra (BS). The first one displays the excitation, while the latter basicly the absorption of the O_0^0 transition in pyrazine. At different backing pressures (0.25-0.5 bar), high resolution spectra were obtained of the J'=0-5 states. As was shown before [10], the LIF data display bunches of lines in a confined spectral area where one or few transitions to a given (J',K') state would be expected. The regions between these groups of lines appear empty with the present sensitivity. Figs. 1-6 display the P(3)-R(3) transitions. Also the Q branch was recorded, depicted in figs. 7,8. The obtained signal to noise ratio in the BS amounts S/N≈10. This is more than two orders of magnitude below the value for the FS. Combined with the fact that the quantum yield of pyrazine is low (ultimately a few percent), this demonstrates the enormous sensitivity of LIF detection. The S/N value obtained for the BS varies due to the changing sensitivity of the detector element caused by cryofrost. The operational temperature was also somewhat different in various measurements. The indicated intensity scale in figs. 1-8 is therefore in arbitrary units.

The observed linewidth in the LIF spectra amounts 25 MHz This value is dominated by the residual Doppler broadening, due to the divergence of the molecular beam. The spatial sensitivity of the colection optics somewhat narrows the detected area of the molecular beam. Therefore the Doppler linewidth is smaller in the FS compared to the BS, where the entire opening angle of the molecular beam is detected. The BS displays a linewidth of 50 MHz.

FIG. 1-8. High resolution spectra of the P,Q and R-branches of the 0-0 electronic transition of pyrazine. The top traces display the bolometer spectra and the bottom traces the laser induced fluorescence spectra. The intensity axis is in arbitrary units. The frequency scale is marked every GHz.

P(3)

P(2)

P(1)

R(1)

83

R(2)

R(3)
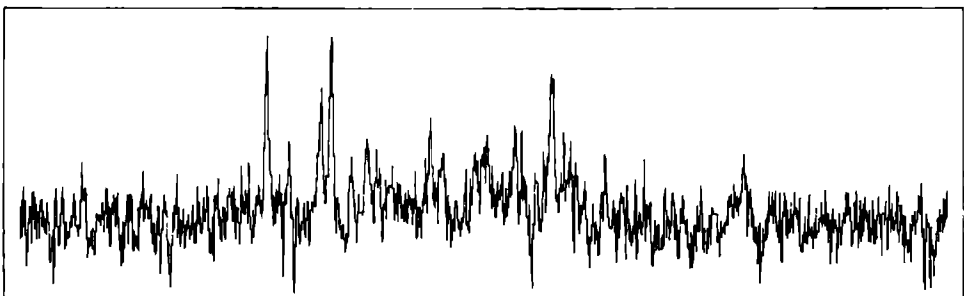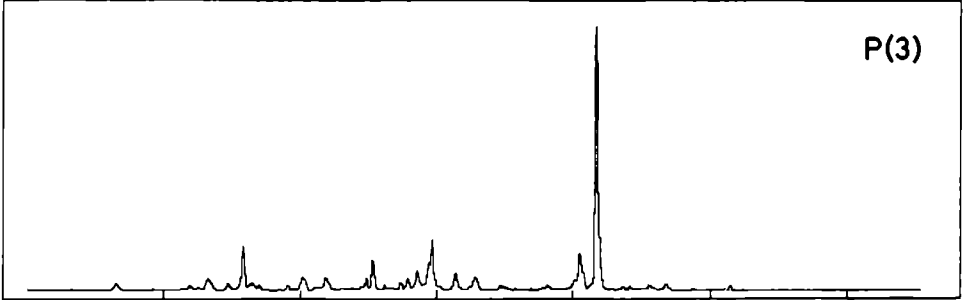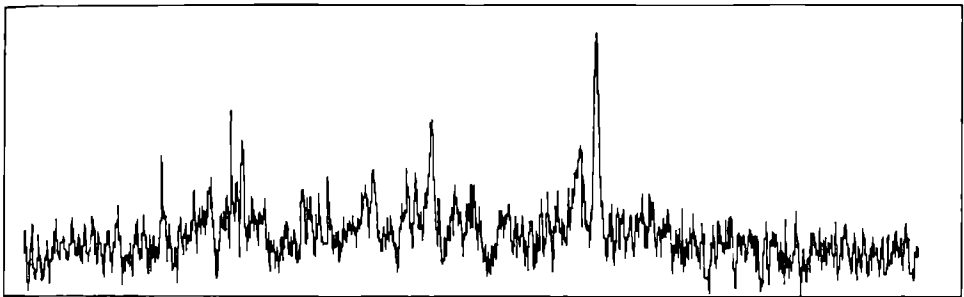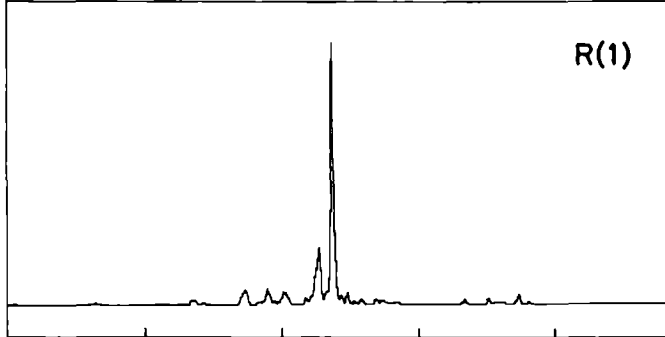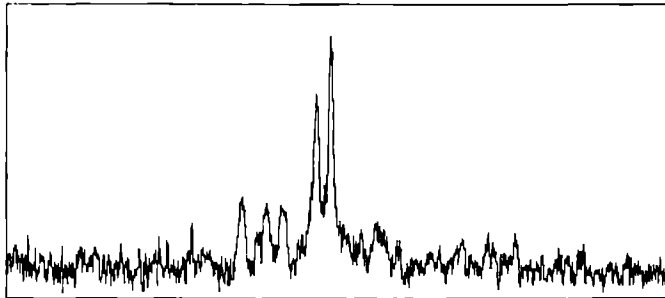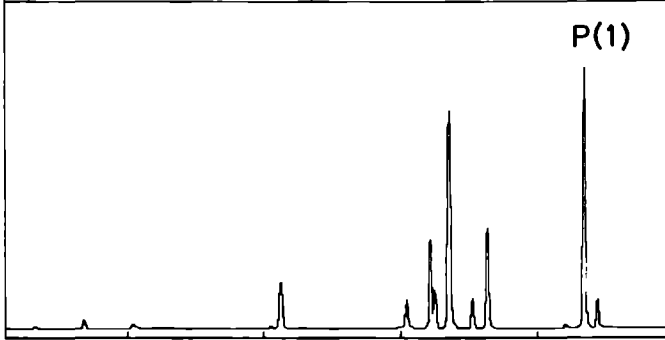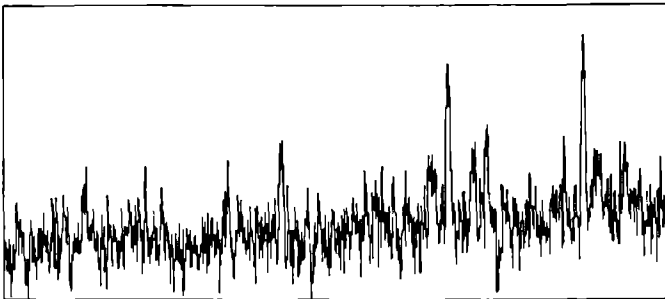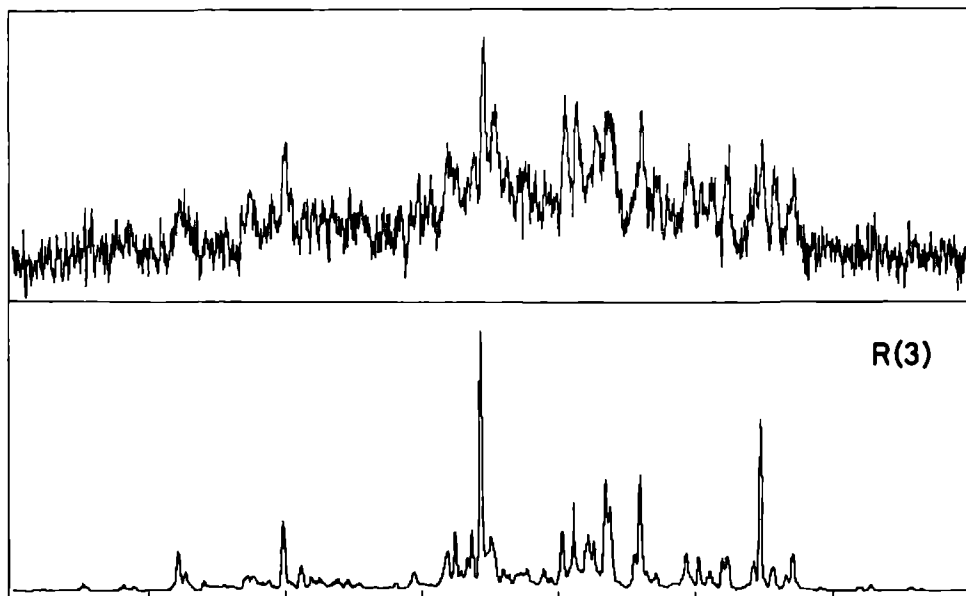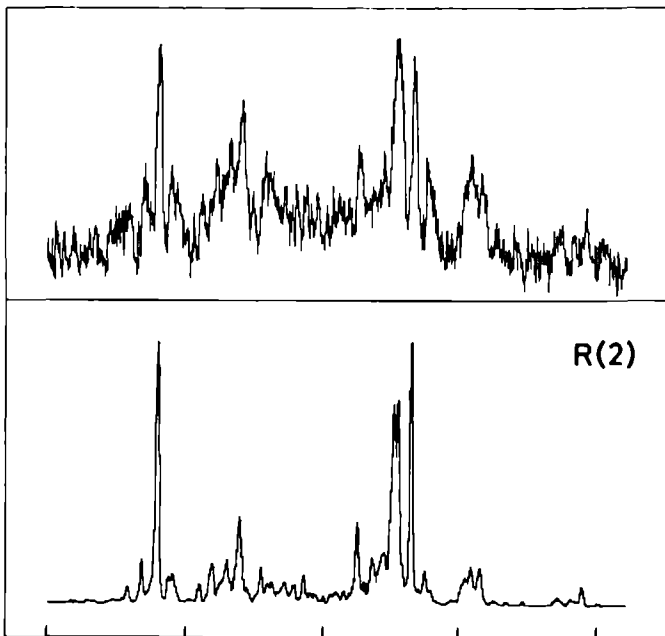
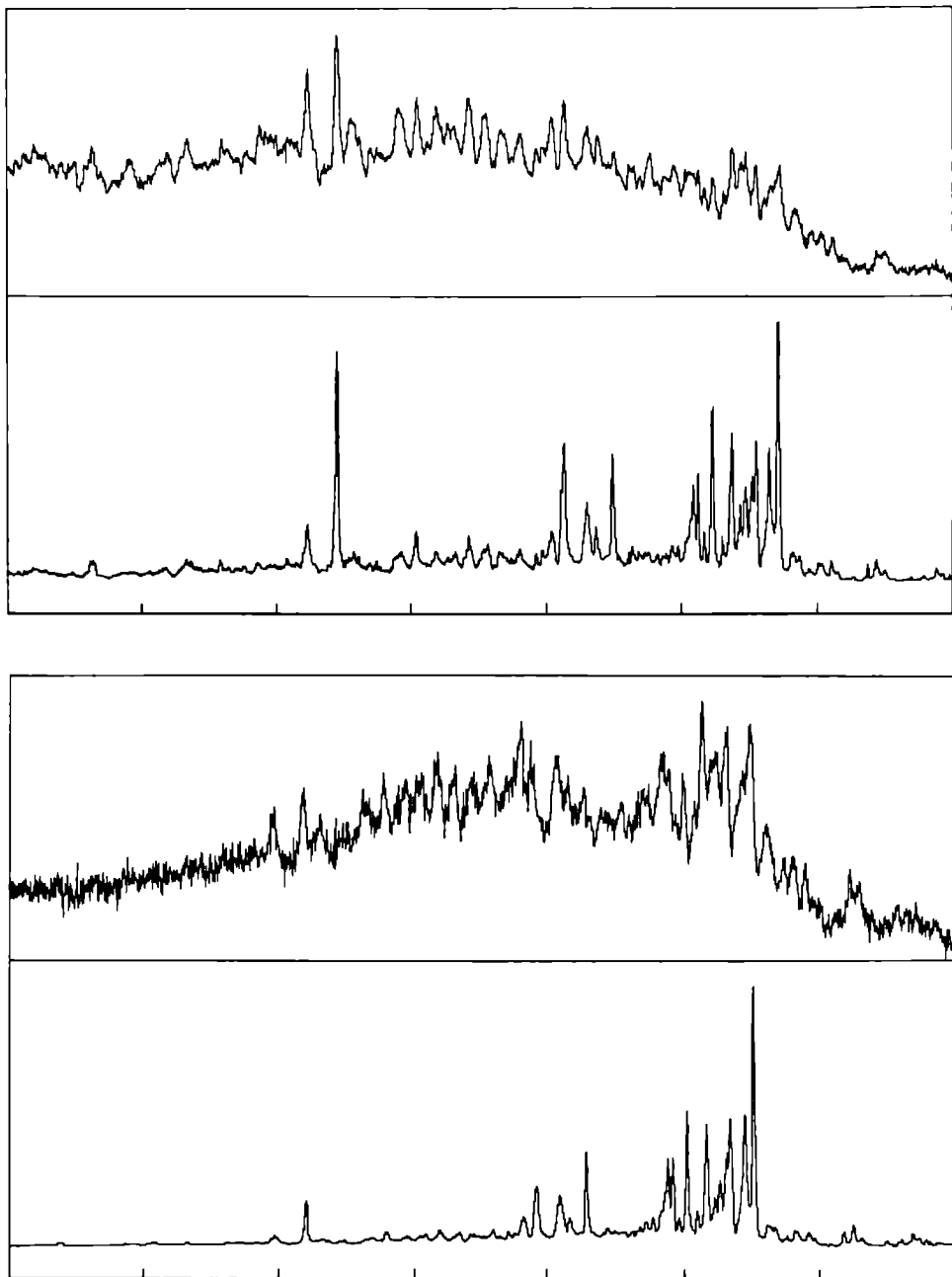FIG. 7-8. The Q branch of the 0-0 transition of pyrazıne, measured with backing pressures of 0.25 (fig. 7, top) and 0.5 bar (fig. 8, bottom).

4. INTERPRETATION AND CONCLUSIONS

Although the signal to noise ratio obtained in the experiment described is limited, a number of qualitative conclusions can be drawn. A more quantitative analysis needs higher quality data, an outline is given in appendix B how this could be obtained. It is shown in appendix A that the bolometer signal essentially displays the ME-absorption spectrum of pyrazine. This molecule satisfies the main limitations; (i) the quantum yield is low [8,20] and (ii) a state independent detection on the bolometer is guaranteed since also the phosphorescence yield is low [8]. The ratio of the line intensities of the FS and BS is equal to the ratio of relative excitation and absorption intensities and denotes the relative quantum yield Y_{me} of a given MΓ-state.

We conclude that it is proven possible to obtain ultra high resolution spectra of pyrazine, in excitation as well as in absorption. As can easily be seen from figs. 1-8, the spectral intensities in the FS and BS are not proportional, which means that absorption and excitation intensities of individual transitions are not proportional. This confirms time resolved data [11](chapter 6-A), of P(1) ME-transitions for which a similar observation was made for J'=0 coupled states. The main result of such observation is that there exists a significant nonradiative decay of the zero-order $^3B_{3u}$ states. The present data show that this conclusion is not limited to P(1) states but, as could obviously be expected, is applicable to all J',K' states. In other words, even with the present S/N ratio it is clear that the quantum yield is not constant for various ME-states. Since no K'-assignment has been made for pyrazine, it is not possible to distinguish a J',K' selective dependence of Y_{me}. For a given J' group of lines all Y_{me}'s are in the same order of magnitude. There are no lines observed, strong in excitation and weak in fluorescence or *vice versa* and it is concluded that Y_{me} is a gradually varying function of excited state energy.

Special attention should be paid to the observed Q-branch. In figs. 7,8 this spectrum is depicted for a 0.25 and 0.5 bar helium backing pressure. The differences are quite striking. It is clear that the intensity distribution in the FS and BS is quite different. For the FS the maximum intensity is reached near the origin of the Q-branch at the high energy side, whereas the BS is much broader, mainly extending to the low frequency side. The FS exhibits sharp ME structure, while the BS has a similar sharp structure but on top of a broad band. The relative intensities in this structure are quite different between both spectra, as was already concluded from P(J") and R(J") transitions. Although there is no complete rotational assignment for the pyrazine molecule, we estimate from comparison with other molecules under similar expansion conditions, that the rotational temperature is about 5 K for a 0.5 bar helium pressure. If this pressure is reduced by a factor of two,

the rotational temperature increases and more J",K" ground state levels are populated The intensity distribution in the Q-branch consequently changes and transitions from high J" levels appear. From fig. 7 it is clear that the low pressure Q-branch is much more extended to the low frequency side and so at this side most spectral lines belong to high J levels. It is concluded that high J' levels appear much weaker in fluorescence than in absorption. An experimental determination of the absolute quantum yield [15] with a resolution of 1 cm^{-1} , showed a dependence of Y=0 124/(2J'+1) for J'=5-22. Since the quantum yield decreases with J', the FS decreases faster than the BS. Although we can not comment on the quantitative dependence of Y, present high resolution data confirm the decrease of Y with increasing J'.

Recently Amirav [20] showed from direct absorption measurements in a jet expansion that the absorption signal stretches out between the various P(J") and R(J") transitions, into areas where no LIF signal is detected. The spectral resolution in this experiment was limited to 2 GHz and therefore no ME-structure was resolved. Amirav attributed [17] this absorption to the excistence of 'grass': a broad continuous background underneath the sharp ME structure. This does not show up in our spectra, neither in absorption, nor in excitation. We performed scans over large frequency regions and did not find evidence for the existence of 'grass' in the excitation spectra of pyrazine. The quantum yield decreases with increasing J', as was concluded from the BS, and therefore the highest sensitivity in the FS is reached between low J'-state transitions. The S/N ratio in the FS amounts 5x10^{-3} in the region of the P(2) transition, where 'grass' was predicted. The computer collection of data allows us to fully exploit this dynamic range. No background underneath the ME-structure was observed in the BS either. One might argue that the S/N raio in the BS is somewhat low to draw this conclusion. However, although the 'grass' was predicted very weak in excitation spectra due to the low quantum yield, it was claimed by Amirav that it would be tremendously enhanced in absorption spectra. We conclude that no experimental evidence was found for the 'grass' in high resolution spectra.

REFERENCES

[1] F. Lahmani, A. Tramer and C. Tric, J. Chem. Phys. 60 (1974) 4431.

[2] J. Kommandeur, W.A. Majewski, W.L. Meerts and D.W. Pratt, to be published in Ann. Rev. Phys. Chem. 38.

[3] G. ter Horst, D.W. Pratt and J. Kommandeur, J. Chem. Phys. 74 (1981) 3616.

[4] B.J. van der Meer, H.T. Jonkman, G. ter Horst and J. Kommandeur, J. Chem. Phys. 76 (1982) 2099.

[5] S. Okajima, H. Saigusa and E.C. Lim, J. Chem. Phys. 76 (1982) 2096.

[6] P.M. Felker, W.R. Lambert and A.H. Zewail, Chem Phys. Lett. 89 (1982) 309.

[7] Y. Matsumoto, L.H. Sprangler and D.W. Pratt, Laser Chem. 2 (1983) 91.

[8] A. Frad, F. Lahmani, A. Tramer and C. Tric, J. Chem. Phys. 60 (1974) 4419.

[9] H. Saigusa and E.C. Lim, Chem. Phys. Lett. 88 (1982) 455.

[10] B.J. van der Meer, H.T. Jonkman, J. Kommandeur, W.L. Meerts and W.A. Majewski, Chem. Phys. Lett. 92, (1982) 565.

[11] W.M. van Herpen, W.L. Meerts, K.E. Drabe and J. Kommandeur, J. Chem. Phys. 86 (1987) 4396.

[12] B.J. van der Meer, H.T. Jonkman and J. Kommandeur, Laser Chem. 2 (1983) 77.

[13] W.D. Lawrance and A.E.W. Knight, J. Phys. Chem. 89 (1985) 917.

[14] W. Siebrand and W.L. Meerts, to be published.

[15] A. Amirav and J. Jortner, J. Chem. Phys. 84 (1986) 1500.

[16] P.J. de Lange, B.J. van der Meer, K.E. Drabe, J. Kommandeur, W.L. Meerts and W.A. Majewski, J. Chem. Phys. 86 (1987) 4004.

[17] A. Amirav, Chem Phys. 108 (1986) 403.

[18] W.A. Majewski and W.L. Meerts, J. Mol. Spectroc. 104 (1984) 271.

[19] W.A. Majewski, Opt. Comm. 45 (1983) 201.

[20] A. Amirav, submitted for publication in J. Chem. Phys. and J. Phys. Chem.

[21] H. Abe, S. Kamei, N. Mikami and M. Ito, Chem. Phys. Lett. 109 (1984) 217.

[22] T. Suzuki, M. Sato, N. Mikami and M. Ito, Chem. Phys. Lett. 127 (1986) 292.

[23] F. v. Moers, T. Hebert and A. Hese, Appl. Phys. B 40 (1986) 67.

[24] M.M. Salour, Opt. Commun. 22 (1977) 202.

[25] J.L. Tomer, L.H. Sprangler, K.W. Holtzclaw and D.W. Pratt, submitted.

APPENDIX A: THEORY OF BOLOMETER DETECTION

It will be shown that a bolometer, inserted in the molecular beam essentially detects a high resolution absorption spectrum in case of molecules with a low quantum yield. We consider a molecule, in our case pyrazine, with a ground state $|g\rangle$ and an excited molecular eigenstate $|u\rangle$. It is assumed that $|u\rangle$ can be reached, starting from $|g\rangle$ with a narrow band laser. The number of molecules in $|g\rangle$ and $|u\rangle$ is denoted as N_1 and N_2 respectively. The laser radiation density per unit volume and frequency interval is given by ρ_L. The excited state exhibits a decay rate Γ consisting of a radiative part Γ_r and a nonradiative contribution Γ_{nr} due to coupling with dark states:

$$\Gamma = \Gamma_r + \Gamma_{nr}. \tag{A-1}$$

Other decay channels like predissociation and ionization are neglected. The rate Γ_r results from the various Einstein coefficients A_{2i} for spontaneous emission to ground state levels $|i\rangle$. The number of molecules in the excited state $|u\rangle$ is given by:

$$N_2 = N_1 \frac{B_{12}\rho_L}{\Gamma} \tag{A-2}$$

with B_{12} the Einstein coefficient for induced absorption. The molecules are excited in a continuous molecular beam by an on-off modulated laser radiation field. The bolometer signal S_B is detected by a phase sensitive method. There are various contributions to this signal. If molecules would disappear from the beam after excitation to $|u\rangle$, a negative signal would be detected on the bolometer. Since we may neglect effects of predissociation and ionisation for pyrazine, we assume that all molecules excited by the laser stay in the beam and reach the bolometer. The lifetime of the excited state is much shorter than the time of flight between excitation area and bolometer (in the order of 300 ns and 300 μs respectively in case of pyrazine). Therefore a number of molecules have decayed to ground state vibrational levels $|i\rangle$ with energy E_i before they are detected. The distribution over states $|i\rangle$ is controlled by the Franck-Condon overlap of $|u\rangle$ and $|i\rangle$. The signal on the bolometer increases due to this radiative decay from $|u\rangle$ with:

$$S_r = N_2 \sum_i \frac{A_{2i}}{\Gamma} E_i. \tag{A-3}$$

The remaining molecules, with absorbed energy E_a , reach the detector. The probability for this proces is Γ_{nr}/Γ. Due to this nonradiative proces the bolometer signal increases as:

$$S_{nr} = N_2 \frac{\Gamma_{nr}}{\Gamma} E_a.$$

(A-4)

Here we have to make an assumption: the energy transfer from the excited state molecule to the bolometer is taken to be state independent. For vibrational energies as in eq. (A-3) the sticking probability and energy transfer will be very nearly state independent but for electronic energies as in eq. (A-4) this is less evident. If the nonradiative process involves coupling with the triplet state, the molecules condensated on the bolometer may partly loose their absorbed energy through phosphorescence, in stead of transfering it to the bolometer. Such processes have been demonstrated in other molecules [21,22]. In principle eq. (A-4) has to be extended with a factor α describing the energy transfer efficiency, and α may be state dependent. In case of pyrazine in its gas phase the phosphorescence yield is low [8]. We therefore assume that $\alpha \approx 1$ and that it is state independent. The state dependence of α is experimentally accessible by detection of the eventual phosphorescence emerging from the detector surface. Such experiments are currently being undertaken in our laboratory.

Combining eqs. (A-3) and (A-4) we find:

$$S_B = \frac{N_2}{\Gamma} \left[\sum_i A_{21} E_i + \Gamma_{nr} E_a \right].$$

(A-5)

The first term in this expression is of order $\Gamma_r \langle E_i \rangle$, where $\langle E_i \rangle$ is the average energy in the ground electronic state of vibrations that contain a significant Franck-Condon overlap with the excited state. Since, in case of pyrazine, $\Gamma_r \ll \Gamma_{nr}$ and $\langle E_i \rangle \ll E_a$, eq. (A-5) is simplified to

$$S_B = N_2 \frac{\Gamma_{nr}}{\Gamma} E_a.$$

(A-6)

The number of excited state molecules N_2 is related to the laser induced fluorescence signal by:

$$S_{LIF} \propto \frac{\Gamma_r}{\Gamma} N_2.$$

(A-7)

90

Here the proportionality constant is determined by geometrical factors like the collection efficiency. The quantum yield Y_{me} of the molecular eigenstate $|u>$ is defined as:

$$Y_{me} = \frac{\Gamma_r}{\Gamma}.$$

(A-8)

Combination of eqs. (A-6) and (A-7) yields:

$$\frac{S_B}{S_{LIF}} \propto \left(\frac{1}{Y_{me}} - 1 \right) E_a;$$

(A-9)

and since $Y_{me} << 1$:

$$\frac{S_{LIF}}{S_B} \propto Y_{me}$$

(A-10)

In this expression S_{LIF} gives the excitation spectrum of the excited state and Y_{me} the relative quantum yield for the ME spectrum. It follows that S_B reflects the absorption spectrum.

APPENDIX B: FUTURE IMPROVEMENT OF EXPERIMENTAL DATA

B-1. EXPERIMENTAL IMPROVEMENTS

In order to draw more quantitatively conclusions from the described experiments, the major problem to be solved is to raise the S/N ratio by at least one or two orders of magnitude. The main improvements is to be expected from a more stable molecular beam, since this presently forms the limiting factor. Points that may be reconsidered are the background pressure, the aerodynamics of the used skimmers and the construction of the source. The latter one can be improved by a more rigid structure; less sensitive for vibrations. As was pointed out in the foregoing, increasing the molecular beam intensity gives rise to more condensation on the cold detector surface and should be avoided. However, adapting the shape of the beam from circular to planar may enlarge the interaction cross section with the laser and therefore enhance the absorption signal. An increase of the laser power will directly be reflected in the obtained signal. With the present setup the uv power is near its maximum value, limited by saturation effects in the dye gain medium. Recently very promising results have been reported with frequency doubling in an external resonator [23]. More than an order of magnitude increase in power should be obtainable. Of course care should be taken to prevent power saturation effects.

B-2. ALTERNATIVE EXPERIMENTAL APPROACHES

Apart from improving the presently followed experimental approach, one has to consider alternative ways to obtain high resolution absorption spectra. The most elegant way would be the direct measurement of absorption. If a molecular beam technique is used, the collimation needed to obtain the required spectral resolution, strongly decreases the path length of the crossing laser. Absorption signals will therefore be extremely small. Extending this path length by application of a slit nozzle will either require an enormous pump capacity of the vacuum apparatus or pulsed operation of the nozzle. Since a narrow band radiation source is needed, an uv laser has to be used in cw operation, to allow frequency stabilization. The resulting application of a pulsed molecular- and a continuous laser beam provides a very inefficient absorption proces. This problem may be overcome by amplification of the cw laser in a high power pulsed amplifier. This so called injection locking method has already been demonstrated [24].

Another, easily accessible, point that needs experimental study is the question whether phosphorescence emerges from excited state of pyrazine. Although the

phosphorescence yield is low [8], phosphorescence spectra of the T_1 vibronic states have recently been obtained [25] in a jet expansion. Sensitized phosphorescence has also been demonstrated in the S_1 state of jet cooled naphtalene [22] and various other molecules [21] with a special technique. The basic idea is that a molecule in the triplet state is trapped on a cold surface, eventually covered with a suitable solid phosphor. Direct phosphorescence or phosphorescence resulting from energy transfer to the phosphor is detected by a space fixed detector. Such phosphorescence excitation spectra with rotational resolution can presumably be obtained for an ultra cold molecule in a molecular beam. Since the space fixed optical detection can be performed very sensitively, it may form an accurate monitor for the absorption signal, even if the phosphorescence yield is low. Such experiments are presently being carried out in the Nijmegen laboratory.

SPECTROSCOPIE EN PHOTODYNAMICA
VAN MOLECULEN
EN VAN DER WAALS COMPLEXEN

Dit proefschrift beschrijft een onderzoek naar de fysische eigenschappen zoals de structuur en de dynamica van de moleculen fluoreen, tetraceen, stilbeen en pyrazine. Tevens werden de eigenschappen bekeken van Van der Waals complexen van enkele van de genoemde moleculen met edelgas atomen. Hiervoor werd gebruik gemaakt van een moleculaire bundel. Deze wordt gevormd uit een supersone expansie in een vacuum tank van een mengsel van het te onderzoeken molecuul met een overmaat aan edelgas atomen. In deze expansie vindt een aanzienlijke reductie plaats van de rotatie- en vibratietemperatuur van de moleculen. Doordat minder toestanden bezet zijn wordt de analyse van waargenomen spectra aanzienlijk vereenvoudigd. In de bundel komen nauwelijks nog botsingen voor en daardoor kunnen ook zwak gebonden moleculen als Van der Waals complexen worden bestudeerd. De moleculen in de bundel worden in een electronisch aangeslagen toestand gebracht door excitatie in het stralingsveld van een kleurstoflaser. De laserstraling in het zichtbare of nabije ultraviolette spectraal gebied kruist de moleculaire bundel onder een loodrechte hoek en de geinduceerde fluorescentie wordt waargenomen.

Op deze wijze werd het rotatie spectrum van fluoreen en het fluoreen-argon complex gemeten. Uit de afgeleide rotatieconstanten werd de positie van het argon atoom bepaald t.o.v. het fluoreen molecuul. Door vergelijking met een isotoop van fluoreen werd nagegaan hoe nauwkeurig de bereikte resultaten zijn. Het blijkt dat deze nauwkeurigheid niet wordt bepaald door de experimentele onzekerheid in de afgeleide rotatieconstanten maar door het feit dat het fluoreen geen volkomen starre structuur heeft.

Een soortgelijke bepaling van de structuur van Van der Waals complexen van tetraceen met edelgas atomen bleek niet mogelijk. Het rotatiespectrum van tetraceen kan worden toegekend maar een storing, die zwak aanwezig is in de spectra van tetraceen, overheerst in de spectra van de complexen. Deze storing wordt toegeschreven aan een toegenomen koppeling van de aangeslagen electronische singlet toestand met andere electronische toestanden.

Ook werden rotatiespectra waargenomen van het trans-stilbeen molecuul. Dit molecuul dient als een prototype in de bestudering van het trans-cis isomerizatie proces, dat optreedt na electronische excitatie. Er kon worden aangetoond, dat naast deze isomerizatie andere intramoleculaire processen een rol spelen, door waargenomen afwijkingen in het rotatie spectrum Deze storing is niet afhankelijk van de vibratieenergie in de aangeslagen toestand tot 1000 cm^{-1}. In het spectrum van het stilbeen-argon Van der Waals complex wordt die storende werking sterk onderdrukt. Hieruit valt af te leiden dat de oorsprong daarvan gezocht moet worden in interne bewegingen van het stilbeen molecuul, die gehinderd woden in het complex.

Er werd ook een studie verricht naar dynamische effecten in de aangeslagen electronische toestand van het pyrazine molecuul. Dit molecuul wordt als een voorbeeld gezien in de bestudering van stralingsloos verval in de limiet van een 'intermediate' geval. De grote hoeveelheid beschikbare experimentele gegevens voor pyrazine worden geïnterpreteerd met behulp van een aangeslagen singlet electronische toestand, die gekoppeld is met triplet vibratie toestanden van gelijke energie. Dit resulteert in gemengde toestanden, aangeduid als moleculaire eigentoestanden. Met behulp van het absorptiespectrum kan een deconvolutie procedure worden uitgevoerd. Daarin worden uit de spectraallijnen behorend bij een enkele gekoppelde singlet toestand de zogenaamde nulde orde singlet en triplet toestanden bepaald en de koppelingsmatrixelementen daartussen Op deze manier kan meer inzicht verkregen worden over de aard van de koppelingen die een rol spelen in het stralingsloos verval van pyrazine. Door de levensduur van een aantal van de moleculaire eigentoestanden te bepalen werd aangetoond dat er een aanzienlijk stralingsloos verval is uit de nulde orde triplet toestanden. Daardoor zijn de experimenteel waargenomen excitatie intensiteiten niet evenredig met de absorptie intensiteiten, zoals eerder werd aangenomen. De deconvolutie procedure werd daardoor enigzins aangepast. De resolutie in de excitatie spectra kan nog verder worden opgevoerd. Door het tijdsafhankelijk gedrag van de fluorescentie na coherente excitatie te bestuderen werden 'quantum beats' waargenomen. De resolutie kan op deze manier worden uitgebreid tot 1 MHz. Een goede indicatie over de aard van de koppelingsmechanismen (b.v. Coriolis interactie) wordt verkregen door de verhouding van stralend en stralingsloos verval te bestuderen als functie van de rotatie quantum getallen. Deze verhouding kan worden bepaald uit de vergelijking van excitatie en absorptie intensiteiten. Voor dit doel werd met een bolometer de geabsorbeerde energie in de moleculaire bundel bepaald. Op deze wijze kunnen simultaan hoge resolutie absorptie en emissie spectra worden waargenomen. Het blijkt dat het stralend verval afneemt met toenemende rotatieenergie.

CURRICULUM VITAE

Op 21 januari 1959 ben ik geboren te Heesch (N.B.). De middelbare school opleiding volgde ik aan het Maasland College te Oss, waar ik in 1977 het diploma Atheneum B behaalde. Daarop volgde de studie natuurkunde aan de Katholieke Universiteit te Nijmegen. Het kandidaatsexamen natuurkunde (N2) werd behaald in april 1981 en in october 1983 volgde het doctoraal examen experimentele natuurkunde. Tijdens mijn afstudeerstage was ik werkzaam op de afdeling Molecuul- en Laserfysica.

Na mijn afstuderen bleef ik als wetenschappelijk medewerker aan deze groep verbonden. Hier heb ik mijn promotieonderzoek verricht, in dienst van de stichting voor Fundamenteel Onderzoek der Materie (F.O.M.) onder leiding van Prof. dr A. Dymanus en Dr. W.L. Meerts. De resultaten van dit onderzoek zijn in dit proefschrift weergegeven.

*

In de vergelijking van fluorescentie- en fosforescentie intensiteiten door Suzuki *et al.* wordt ten onrechte aangenomen dat de fosforescentie opbrengst voor een molecuul steeds 100% is.

T. Suzuki, M. Sato, N. Mikami en M. Ito, Chem. Phys. Lett. 127 (1986) 292.

*

De berekening van de dichtheid van triplet vibrationele toestanden van pyrazine door McDonald *et al.* vertoont een onnodige onnauwkeurigheid ten gevolge van een onjuiste singlet-triplet opsplitsing en sterk benaderde vibratiefrequenties.

D.B. McDonald, G.R. Fleming en S.A. Rice, Chem. Phys. 60 (1981) 335.

*

Het vergt werk om werkloos te zijn. Met het oog op heersende vooroordelen is het jammer dat voor een ambtenaar die inspanning minder is.

*

De door Zewail en medewerkers voorgestelde methode om met tijdsopgeloste polarisatiemetingen rotatieconstanten te bepalen is zeker niet toepasbaar op trans-stilbeen.

P.M. Felker en A.H. Zewail, J. Chem. Phys. 86 (1987) 2461.
J.S. Baskin, P.M. Felker en A.H. Zewail, J. Chem. Phys. 86 (1987) 2483.

*

In de door Suzuki *et al.* gebruikte potentiaal voor de beschrijving van de torsievibratie in trans-stilbeen ontbreekt de wisselwerking tussen het ethyleen frame en de phenyl groepen.

T. Suzuki, N. Mikami en M. Ito, J. Phys. Chem. 90 (1986) 6431.

*

Het niet uitleenbaar stellen van grote delen van een bibliotheek bestand vormt een belemmering van het gebruik. De aanwezigheid van copieermachines vormt daarbij een onvoldoende en tijd-energie- en geldverslindende compensatie.

*

Het door Amirav voorgestelde 'grass' in het spectrum van pyrazine blijft beneden het maaiveld in de hoge resolutie excitatie- en absorptie spectra.

A. Amirav, Chem. Phys. 108 (1986) 403.

*

Onder het snel toenemend aantal bezitters van een personal computer heerst een dwangmatige behoefte zoveel mogelijk software te verzamelen. De toepassingen van een dergelijk bezit raken daarbij op de achtergrond.

*

Bij de bepaling van de rotatietemperatuur van CO in een jet-exspansie door Amrein *et al.* wordt ten onrechte geen rekening gehouden met de beperkte resolutie in het spectrum.

A. Amrein, M. Quack and U. Schmitt, Z. Phys. Chem. 154 (1987) 59.

*

Bij de bepaling van de positie van de Mach disk in een jet-expansie wordt vaak geen rekening gehouden met de invloed van interne vrijheidsgraden van het gas op de flow-snelheid.

D.M. Lubman, C.T. Rettner and R.N. Zare, J. Phys. Chem. 86 (1982) 1129.